Министерство образования и науки Российской Федерации
федеральное государственное автономное образовательное учреждение
высшего образования
**«НАЦИОНАЛЬНЫЙ ИССЛЕДОВАТЕЛЬСКИЙ
ТОМСКИЙ ПОЛИТЕХНИЧЕСКИЙ УНИВЕРСИТЕТ»**

Школа Инженерная школа ядерных технологий
Направление подготовки 14.04.02 Ядерные физика и технологии
Отделение школы (НОЦ) Ядерно-топливного цикла

МАГИСТЕРСКАЯ ДИССЕРТАЦИЯ

Тема работы
Накопительная камера с электростатическим осаждением ионизированных дочерних продуктов распада радона на поверхность полупроводникового детектора

УДК 539.1.074.55:539.163:546.2

Студент

Группа	ФИО	Подпись	Дата
0АМ6И	Мак-Дональд Принс		

Руководитель

Должность	ФИО	Ученая степень, звание	Подпись	Дата
Ассистент ОЯТЦ ИЯШТ	Черепнев Максим Святославович	-		

КОНСУЛЬТАНТЫ:

По разделу «Финансовый менеджмент, ресурсоэффективность и ресурсосбережение»

Должность	ФИО	Ученая степень, звание	Подпись	Дата
Доцент ШИП	Рахимов Т.Р.	к.э.н.		

По разделу «Социальная ответственность»

Должность	ФИО	Ученая степень, звание	Подпись	Дата
Ст. Преподаватель ОЯТЦ	Веригин Д.А.	к.т.н.		

ДОПУСТИТЬ К ЗАЩИТЕ:

Руководитель ООП	ФИО	Ученая степень, звание	Подпись	Дата
ЯППУ	Верхотурова В.В.	к.и.н.		

Томск -2018

Ministry of Education and Science of the Russian Federation
Federal Independent Educational Institution
"NATIONAL RESEARCH TOMSK POLYTECHNIC UNIVERSITY"

School: School of Nuclear Science & Engineering
Direction of training (Specialty): 14.04.02 Nuclear Physics and Technology
Division: Nuclear fuel cycle

MASTER'S THESIS

Topic of the work
A storage chamber with electrostatic deposition of ionized daughter products of the decay of radon on the surface of a semiconductor detector

UDC 621.039.58:621.039.53/.54

Student

Group	Full name	Signature	Date
0АМ6И	Mac-Donald Prince		

Scientific Supervisor

Position	Full name	Academic degree, academic rank	Signature	Date
Assistant Lecturer	Cherepnev Maxim Svyatoslavovich	-		

ADVISORS:

Section "Financial Management, Resource Efficiency and Resource Saving"

Position	Full name	Academic degree, academic rank	Signature	Date
Associate Professor	Rakhimov T.R	PhD Economics		

Section "Social Responsibility"

Position	Full name	Academic degree, academic rank	Signature	Date
Senior Lecturer	Verigin D.A	PhD		

ADMIT TO DEFENSE:

Position	Full name	Academic degree, academic rank	Signature	Date
Nuclear Power Installations Operation	Verchoturova V.V	PhD		

Tomck -2018

School: School of Nuclear Science & Engineering

Direction of training (Specialty): 14.04.02 Nuclear Physics and Technology

Division: Nuclear fuel cycle

APPROVED BY:
Programme Director

_____Verchoturova V.V

(Signature) (Date)

ASSIGNMENT
For the Master's Thesis completion

Master's Thesis
(Master's Thesis)

For Student:

Group	Full name
0АМ6И	Mac-Donald Prince

Topic of the work:

A storage chamber with electrostatic deposition of ionized daughter products of the decay of radon on the surface of a semiconductor detector	
Approved by the order of the head (date, number)	No1882//c at 19.03.2018

Deadline for the completion of Master's Thesis:	04.06.2018

TERMS OF REFERENCE

Initial data for work (*the name of the objective of research design; performance or load; mode of operation (continuous, periodic, cyclic, etc.);type of raw materials or material of the product; requirements for the product, product or process; special requirements to the features of the operation of the object of product in terms of operation safety, environmental impact, energy cost, economic analysis, etc)*	Physical protection system (Nuclear security) Plans for the implementation of nuclear program in Ghana was reviewed and suitable places were analysed for the construction of nuclear power plant. Threats and vulnerability analysis was conducted and based on that, the nuclear facility was designed and categorised. The physical protection system was also designed according to international and local standards (IAEA, DOE, ROSATOM)

List of the issues to be investigated, designed and developed *(analytical review of literary sources in order to elucidate the achievements of world science and technology in the field under consideration, the formulation of the problem of research, design, construction, the content of the procedure of the research, design, construction, discussion of the performed work results, the name of additional sections to be developed; work conclusion).*	Analysis of places to build NPP in Ghana. Description of the hypothetical object (VVER 1000/1200). Threats and vulnerability analysis. Requirements for equipping PPS with engineering and technical equipment within the framework of accounting and control. Designation of nuclear facility and physical protection system in accordance with the requirements of normative documents.
List of graphic material (*with an exact indication of mandatory drawings)*	N/A

Advisors on the sections of the Master's Thesis *(with indication of sections)*

Chapter	**Advisor**
One: Literature Review	Cherepnev Maxim Svyatoslavovich
Two: Methodology	Cherepnev Maxim Svyatoslavovich
Three: Results	Valentina Victorovna Sohoreva
Four: Financial management, resource efficiency and conservation	Timur R. Rakhimov
Five: Social Responsibilities	Verigin D.A.

Date of issuance of the assignment for Master's Disertation completion according to a line schedule	

The task was issued by:

Position	**Full name**	**Academic degree, academic status**	**Signature**	**Date**
Assistant Lecturer	Cherepnev Maxim Svyatoslavovich	-		

The assignment was accepted for execution by the student:

Group	**Full name**	**Signature**	**Date**
0АМ6И	Mac-Donald Prince		

"FINANCIAL MANAGEMENT, RESOURCE EFFICIENCY AND RESOURCE CONSERVATION"

Student:

Group	Name
0АМ6И	Mac-Donald Prince

School	Nuclear Science and Engineering	Division	Nuclear Fuel Cycle
Education Level	Masters	Direction / specialty	Nuclear Physics and Technology

References for "Financial management, resource efficiency and resource conservation":	
1. The cost of research: Logistics, energy, financial, information and human	*According to manual provided*
2. Norms and standards resource consumption	*According to manual provided*
3. used the tax system, tax rates, deductions, discounting and credit	*According to manual provided*

The list of questions for study, design and development:	
1. Evaluation of commercial and innovative potential STI	**Implement** at least 1 option from the list (1-3) below: 1. Potential consumers of research results 2. Analysis of competitive technical solutions from the perspective 3. Technology QUAD 4. SWOT-analysis **Perform** • Evaluation of the project readiness for commercialization • Methods for the commercialization of scientific and technological research
2. Development of the charter of scientific and technical project	• Objectives and outcomes of the project. • The organizational structure of the project. • Identification of possible alternatives
3. Project management planning: the structure and schedule of the budget, risk and procurement organization	• The structure of the work within the framework of scientific research • Determination of the complexity of work • Scheduling scientific research • The budget of the scientific and technical research (STR)
4. Defining resource, financial, economic efficiency	• Integral financial efficiency indicator • Integral resource-efficiency indicator • Integral total efficiency indicator • Comparative project efficiency indicator

List of graphic material
1. *Segmentation of the market* 2. *Estimation of competitiveness of technical solutions* 3. *SWOT Matrix* 4. *Schedule and budget of the project* 5. *Assessment resource, financial and economic efficiency of the project*

Date of issue of assignment	

Assignment given by consultant:

Position	Name	degree	Signature	Date
Associate Professor	Timur R. Rakhimov	PhD Economics		

Assignment received by student for implementation:

Group	Name	Signature	Date
0АМ6И	Mac-Donald Prince		

ASSIGNMENT FOR THE SECTION "SOCIAL RESPONSIBILITY"

For student

Group	Full name
0АМ6И	Mac-Donald Prince

School	Nuclear Science and engineering	**Division**	Nuclear Fuel Cycle
Level of education	Masters	**Direction / specialty**	Nuclear Physics and Technology

Initial data to the section "Social responsibility"	
1. Description of the workplace (working area, technological process, equipment used) for the case of occurrence of:	• Description of the workplace of the engineer who performs calculations on the PC, for the occurrence of: ○ harmful factors of the production environment: an increased level of electromagnetic radiation. ○ Hazardous factors in the production environment: the likelihood of a fire, the likelihood of electric shock.
2. List of legislative and normative documents on the topic	Familiarization with legislative and normative documentation.

List of issues to be investigated, designed and developed:	
1. Analysis of factors of internal social responsibility: *- the principles of the organization corporate culture;* *- the system of labor organization and its security;* *- development of human resources through learning programs and training and development programs.*	• Analysis of identified hazards: ○ increased level of electromagnetic radiation. ○ means of protection.
2. Analysis of external social responsibility factors: *- assistance in environmental protection;* *- interaction with the local community and local authorities;* *- preparedness to participate in crisis situations, etc.*	• Analysis of identified hazards: ○ Electrical safety (including static electricity, protective equipment); ○ Fire and explosion safety (causes, preventive measures, primary fire extinguishing means)
3. Legal and organizational issues of ensuring social responsibility: *- Analysis of legal norms of labor legislation;* *- analysis of special legal and regulatory legislative acts;* *- Analysis of internal regulatory documents and regulations of the organization in the field of research activities.*	• GOST 12.1.038-82 SSBT. electrical safety • PPB 01-03. Fire safety rules in the Russian Federation
List of graphic material:	N/A

Date of issuance of the assignment according to a line schedule	

The task was issued by the Advisor:

Position	Full name	Academic degree, academic status	Signature	Date
Senior Lecturer	Verigin D.A	PhD		

The assignment was accepted for execution by the student:

Group	Full name	Signature	Date
OAM6I	Mac-Donald Prince		

School: School of Nuclear Science and Engineering

Direction of training (Specialty): 14.04.02 Nuclear Physics and Technology

Level of education: Master's Degree

Division of Nuclear Fuel Cycle

Period of completion (fall/spring semester 2017/2018)

Form of presenting the work:

A storage chamber with electrostatic deposition of ionized daughter products of the decay of radon on the surface of a semiconductor detector

(Master's Thesis)

SCHEDULED COURSE ASSESSMENT CALENDAR

for the Master's Thesis completion

Deadline for completion of Master's Thesis:	04.06.2018

Assessment date	Title of section (module) / type of work (research)	Maximum score of the section (module)
09.02.18	Literature Review and Methodology	
04.03.18	Design of nuclear facility and vulnerability analysis	
02.04.18	Design of physical protection system	
01.05.18	Financial management and Social Responsibility	
29.05.18	Compilation of the dissertation (full report)	

Made by:

Position	Full name	Academic degree, academic status	Signature	Date
Assistant Lecturer	Cherepnev Maxim Svyatoslavovich	-		

Agreed:

Position	Full name	Academic degree, academic status	Signature	Date
Nuclear Power Installations operation	Verhoturova V.V	PhD		

Expected learning outcomes

Result code	The result of the training (the graduate should be ready)	Requirements of the FSES HE, criteria and / or stakeholders
professional competencies		
LO1	To apply deep mathematical, natural scientific, socio-economic and professional knowledge for theoretical and experimental research in the field of the use of nuclear science and technology	FSES HE Requirements (PC-1,2, 3, 6, UC-1,3), Criterion 5 RAEE (p 1.1)
LO2	Ability to define, formulate and solve interdisciplinary engineering tasks in the nuclear field using professional knowledge and modern research methods	FSES HE Requirements (PC-2,6,9,10,14 UC-2,3,4, BPC1,2), Criterion 5 RAEE (p 1.2)
LO3	Be able to plan and conduct analytical, simulation and experimental studies in complex and uncertain conditions using modern technologies, and also critically evaluate the results	FSES HE Requirements (PC-4,5,6,9,22 UC-1,2,5,6), Criterion 5 RAEE (p 1.3)
LO4	To use the basic and special approaches, skills and methods for identification, analysis and solution of technical problems in nuclear science and technology	FSES HE Requirements (PC-7,10,11,12,13 UC-1-3,BPC1,3), Criterion 5 RAEE (p 1.4)
LO5	Readiness for the operation of modern physical equipment and instruments, to the mastery of technological processes during the preparation of the production of new materials, instruments, installations and systems	FSES HE Requirements (PC-8,11,14,15, BPC-1), Criterion 5 RAEE (p 1.3)
LO6	The ability to develop multivariate schemes for achieving the set production goals, with the effective use of available technical means	FSES HE Requirements (PC-12,13,14,16, BPC-2), Criterion 5 RAEE (p 1.3)
cultural competencies		
LO7	The ability to use the creative approach to develop new ideas and methods for designing nuclear facilities, as well as modernize and improve the applied technologies of nuclear production	FSES HE Requirements (PC-2,6,9,10,14, UC-1,2,3), Criterion 5 RAEE (p 1.2,2.4,2.5)
basic professional competencies		
LO8	Independently to study and continuously to raise qualification during all period of professional work.	FSES HE Requirements (PC-16,17,21, UC-5,6, BPC-1), Criterion 5 RAEE (p 2.6) coordi-nated with the requirements of the international standard EURACE & FEANI

LO9	Actively own a foreign language at a level that allows you to work in a foreign language environment, develop documentation, present results of professional activity.	FSES HE Requirements (BPC-3, UC-2,4), Criterion 5 RAEE (p 2.2)
LO10	To demonstrate independent thinking, to function effectively in command-oriented tasks and to have a high level of productivity in the professional (sectoral), ethical and social environments, and also to lead the team, form assignments, assign responsibilities and bear responsibility for the results of work	FSES HE Requirements (PC-18,20,21,22,23 UC-1,4, BPC-2), Criterion 5 RAEE (p 1.6,2.3) coordinated with the requirements of the internation-al standard EUR-ACE & FEANI

Abstract

Graduation qualification work contains 124 pages, 19 drawings, 35 graphs, 24 tables, 41 sources and 1 applications.

Key Words: Radon flux density, Thoron flux density, Storage chamber, Semiconductor, Spectrometer, Activity, Decay products, Pulses, Spectrogram, Polonium-216, Polonium-214, Radon-222,

The purpose of this work is the development of electrostatic precipitation chamber designs. Analysis of the measurements made with these structures and selection of the best design option.

In the thesis, the possibility of electrostatic precipitation of the products of decay of radon and thoron from the soil surface is considered, taking into account this possibility, three different designs of accumulating electrostatic chambers have been developed. The analysis of measurements with these structures is made and the best design options are chosen.

A technique has been developed to find the radon and thoron flux density from the soil surface using the obtained spectrometric distribution.

Graduation qualification work was carried out in the text editor Microsoft Word 2010, using the following programs: Mathematica 7, Math Type 5.0, Microsoft Excel 2010, Simnra 7.01, SRIM 2008.

List of abbreviations

PPR – Radon Flux Density

PPT – Thoron Flux Density

ND – Accumulation Chamber

PPD – Semiconductor Detector

Rn – Radon

Ra – Radium

Th – Thorium

U – Uranium

Bq – Becquerel

PC – Personal Computer

ADC – Analog Digital Converter

Ctrl – Control

PgUp – Page UP

PgDn – Page Down

Contents

Introduction.

Interest in the radon problem is caused by the need to evaluate the role of radon in the physics of the surface layer of the atmosphere, its electrical properties, and construction. The processes of exchange of soil air and its constituents with a surface atmosphere lead to the release of soil gases into the surface layer of the atmosphere, including radon, thoron and to the entry of atmospheric gases into the soil.

The zones of strains and contractions arising in the lithosphere lead to a change in the intensity of the gas flows (including radon and thoron) from the earth's interior to the lower boundary of the active layer of the soil. Charged products of the decay of radon in the boundary layer of the atmosphere form the aero electric convective structures, the evolution of which ultimately leads to the formation of clouds, and, in the long run, to climate change. The intensity of gas exchange between the lithosphere and the surface atmosphere is determined by the distribution and regularities of migration of gases, including radon and thoron in the soils, and therefore its surface layer plays the role of the main regulating element in the global radon cycle.

In addition to the processes that lead to a change in the intensity of radon fluxes at the lower boundary of the active soil layer, the factors controlling the rate and direction of the gas exchange between the soil and the surface atmosphere are variations in the temperatures of the surface layer of the soil and the surface layer of the atmosphere, atmospheric pressure, soil moisture, direct solar radiation, wind speed and direction. The combined effects of these factors in a complex manner affect the variations in radon flux density from the underlying surface.

In connection with the increased interest in this problem, problems have arisen associated with the development of methods for measuring radon flux density and thoron flux density, as well as evaluating their reliability. Usually, the thoron flux density measurements are made simultaneously with the measurement of radon flux density using the storage chamber method. The purpose of the storage chamber, which is installed on the surface of the soil for a certain time, is to accumulate gases emitted from the ground. After the accumulation, the measurement process follows.

In the known methods of joint measurement of radon and thoron flux density from the ground surface by alpha radiation, a measuring device (radiometer or detector) is located outside the storage chamber. When transferring accumulated gases from the storage chamber to the measuring device, deterrent aerosol products of decay of radon and thoron filters are used to eliminate their influence on the measurement result. Of the methods currently available for measuring radon flux density and thoron flux density, only one method is known with the location of the measuring device inside the storage using an ionization chamber, which is the widely used radiometer of the radon AlphaGUARD (Genitron Instruments, Germany). However, this method allows the measurement of only the flux density of radon and thoron.

The goal in this research is the development of a storage chamber including a semiconductor alpha detector and an electrostatic precipitation system for positively charged decay products of radon isotopes, to measure the radon and thoron flux density from the soil surface.

Tasks;

1. To develop several variants of experimental samples of storage chambers with different electrostatic precipitation system for positive ions - products of decay of radon and thoron.

2. Carry out a series of tests of the experimental chamber samples. Choose the optimal variant for the design of the storage chamber in terms of registration efficiency and alpha spectrum formed

3. Make a series of measurements of the alpha-radiation spectra with the chosen version of the storage chamber, and the subsequent identification of radionuclides.

4. Development of the methodology for determining the flux density with the selected version of the storage chamber.

1. Methods of Density Measurement of Flow of Radon and Thoron

In this chapter, various methods for measuring the flux density of radon and thoron are considered and classified. Classification of methods for measuring radon flux density and thoron flux density is made by the type of the detector, measured by the parameter, the duration of the measurement, depending on the design features of the storage chamber in which radon and thoron accumulate, and other features. Methods for measuring the flux density are briefly described. An analysis of the advantages and disadvantages of various techniques used to measure the flux density of radon and thoron are considered.

1.1 Classification of methods for measuring the flux density of radon and thoron

All known methods for measuring the flux density of radon and thoron from hard surfaces are divided into:

1. methods for measuring the flux density from the surface of the soil (usually produced in the field), where the required value is measured in units of Bq m^{-2} s^{-1};

2. Laboratory methods for measuring the flux density from a surface or unit of mass of a sample of a porous material (soil or building material), where the sought value is usually expressed in mass units Bq kg^{-1} s^{-1}.

Here we should mention the existence of methods for measuring the flux or density of the radon flux from water surfaces, where the required value is measured in units of Bq s^{-1} (Bq m^{-2} s^{-1}, Bq l^{-1} s^{-1}), which in this context is not considered.

First of all, all methods for measuring the flux density of radon and thoron from the soil surface are divided into:

• **Direct methods of measurement** (accumulation of radon in a chamber installed on the surface of the ground with subsequent or synchronous measurement of accumulated activity)

• **Indirect methods of measurement** (calculation methods based on one of the models of radon transfer in porous media, together with measurements of one of the input parameters of the model (radon activity in soil or atmospheric air, radium or

uranium in the soil) with subsequent recalculation of the measured value in the radon flux density.

Indirect methods include 4 options:

1. Method for calculating the radon flux density based on the diffusion transport model and Fick's law, using measured or reference data on physical and geological characteristics of soils: specific activity of ^{226}Ra (^{238}U), porosity, soil density, emanation and diffusion coefficients of radon [7].

2. The method for calculating the radon flux density from the measured gradient of the volume activity of radon in the soil and the diffusion transport model [8].

3. The method for calculating the radon flux density based on the diffusion-advection model of transport from two values of the volume activity of radon, measured at two depths, differing by a factor of 2 [9].

4. The method of calculating the effective (average over a large territory) the value of the radon flux density using the balance method [8]. The balance method consists in measuring the vertical distribution of radon decay products in the atmosphere during aircraft sounding. During airborne soundings at different heights, the aerosol components of the air were taken to the filter, followed by the measurement of the total alpha activity of the short-lived products. The results of this method were useful in studying a number of problems of atmospheric dynamics. However, this method has many limitations, it is labor-intensive and expensive. A similar method, only at the terrestrial surface and with respect to the estimation of the thoron flux density, was proposed in [4].

The basis of all direct methods for measuring radon flux density is the use of a measuring device (detector, radiometer) and a storage chamber. Depending on their relative location, direct methods have 2 options:

1. The measuring device is located directly inside the storage chamber (or combined with the storage chamber;

2. The measuring device is located outside the storage chamber.

According to the design features of the storage chamber, all methods are divided into static (the camera is closed during accumulation) and dynamic ("ajar" camera), for measuring the "unperturbed" flow. The most common is the static method, in which the storage chamber is closed for a certain time of accumulation of radon, then it is ventilated before the start of a new measurement. According to the method of accumulation, there are methods with accumulation of radon:

• In air (volume) within storage chamber (about 70% of published scientific works are devoted to this method);

• On activated carbon located inside the storage chamber (~ 30% of the work).

The method with accumulation of radon on activated carbon is used in combination with the following methods of measuring accumulated activity:

1. Gamma spectrometric method using scintillation, usually NaI (Tl), or germanium semiconductor detector;

2. Radiometric method: gamma or beta radiometer, alpha / beta counter based on liquid scintillator.

The method with the accumulation of radon in the air inside the storage chamber, which is often called the "storage chamber" method, is also used in combination with known methods of measuring accumulated activity (in percentages of published scientific works where this method is used):

1. scintillation (~ 35%);

2. Semiconductor (also in combination with electrostatic precipitation of charged products of decay of radon) (~ 15%);

3. ionization (ionization chambers, gas-discharge counters, electret detectors) (~ 30%);

4. track (track solid-state detectors) (~ 20%).

By the duration of one measurement, methods of measuring the flux density, by analogy with the methods of measuring radon OA, can be divided into:

• **Integral** (duration of one measurement from several days to a month). Example: a static method using track detectors;

• **Quasi-integrated** (from one to several days). Example: dynamic method using electret detectors; static method using coal absorbers;

• **Instant** (from tens of minutes to several hours). Example: a static method using scintillation, semiconductor detectors, an ionization chamber, gas-discharge counters; One dynamic method is also known in combination with a scintillation (ZnS) counter [10].

All developed methods of measuring the flux density can be classified, depending on the purposes of applying their results:

• **For single measurements**. Purpose: assessment of the radon hazard of territories in radioecology, construction, geo ecology. The basic requirement for the device is: light weight → mobile; cheap → mass measurements;

• **For continuous** (continuous) measurements. Purpose: monitoring, scientific research. The main requirement is an automated storage chamber in combination with one of the instant methods, which will allow obtaining time series of data with a high sampling frequency.

The latest and most important classification of methods for measured isotopes of radon:

1. Methods for measuring radon flux density:

• In which the contribution of thoron to the measurement result is neglected;

• In which thoron is separated, using various technical methods and techniques: aging until complete decay of thoron [11], delaying volumes [12], delaying filters [13], etc.

2. Methods for simultaneous measurement of the radon and thoron flux densities [5, 6], in which either pulse analyzers or various technical and theoretical methods are used to separate the signals. Method for measuring the flux density of thoron [4].

1.2 Brief description of methods for measuring the flux density

1.2.1 Method of a static (closed) storage chamber

The essence of the static storage chamber method is that the radon flux from the ground increases the concentration of radon in the storage chamber (NC) exposed

on the site under investigation. Based on the geometric dimensions of the storage chamber, the exposure time and the accumulated activity of radon, it is possible to estimate the radon flux density from the surface of the soil.

In the general case, the radon flux density, Bq m^{-2} s^{-1}, in this method is calculated from expression

$$q = \frac{A(t) \cdot V}{S \cdot t} ,$$ (1.1)

Where $A(t)$– is the volumetric activity of radon in the air of the storage chamber, measured in time, t, Bq m^{-3};

    S – surface area of the base of the storage chamber m^2;

    t – Radon accumulation time, s;

    V – volume of the storage chamber m^3.

    Taking into account the radioactive decay, the radon flux density is calculated from the formula (1.2), which is obtained by solving the equation for the balance of radon activity inside the storage chamber, taking into account the intensity of incoming radon into the chamber and its radioactive decay, with the initial condition that the background activity inside the storage chamber is zero

$$q = \frac{V \lambda A(t)}{S(1 - e^{-\lambda t})} ,$$ (1.2)

    In the event that the initial (background) radon activity inside the ND is not zero, the solution of the balance equation gives the following expression for the radon flux density

$$q = \frac{V \lambda (A(t) - A_0 e^{-\lambda t})}{S(1 - e^{-\lambda t})} ,$$ (1.3)

Where A_0 – is the radon volume activity measured at the initial time Bq m^{-3}; $A(t)$ – the final volume activity of radon, measured at the time t, Bqm^{-3};

    λ – Radon decay constant, s^{-1}.

1.2.2 Measurement of accumulated activity by scintillation method

A distinctive feature of this method is the measurement of the accumulated radon and thoron activity from the alpha-radiation produced by the scintillation detector (or Lucas cell) operating in counting mode. Divide radon and thoron using the counting mode of measurement is possible only if special techniques and means are used the usual scheme of measuring radon flux density:

1. the accumulation of radon inside the storage chamber;

2. transfer of radon into the measuring device through a filter that detects the products of the decay of radon and thoron;

3. the subsequent exposure for 3 hours to establish an equilibrium between radon and two alpha-emitting products of its decay (not used in all methods);

4. Measurement of accumulated radon activity. Conversion of the measured activity into the value of the radon flux density is carried out according to the formulas (1.1-1.3).

In [1], a somewhat different scheme was used, the activity of the radon emerging from the surface was measured with a PAL-1 scintillation alpha radiometer at the initial moment and after the accumulation time, which, depending on the type of soil, was 15 to 60 min. Recalculation in the value of radon flux density was carried out by the formula (1.3). In [15, 11,14, 15], the measurement of accumulated radon activity was carried out with a scintillation detector ZnS (Ag), then the radon flux density was calculated from formula (1.1).

In [15], an increase in the sensitivity of the method was achieved using an electric field, under the action of which positively charged decay products were collected on a thin aluminized Mylar mounted in front of the detector.

1.2.3 Measurement of accumulated activity by the semiconductor method

To measure the radon flux density by a semiconductor method in combination with the method of a storage chamber, commercially available instruments are commonly used: radon radiometers based on a semiconductor alpha detector that operate in the spectrometry mode. This makes it possible to separate the signals from

radon, thoron, and alpha-emitting decay products, and simultaneously measure the flux density of radon and thoron.

In Russia, mainly, radiometers of the PPA type are used, which are equipped with a sampling kit POU-04, which contains one or two storage chambers for measuring radon flux density, as well as an appropriate methodology. Calculation of the value of the radon flux density is carried out according to the formula (1.1), slightly modified by taking into account additional volumes: the measuring chamber; connecting tubes; sampler.

Radium and thoron radiometers RTM1688-2, RTM2100 from German firm SARAD GmbH, equipped with PPDs and the corresponding instruction for measuring radon flux density, as well as radiometers RAD7, which are used for simultaneous measurement of radon and thoron flux density [16], are used mainly abroad.

1.2.4 Measurement of accumulated activity by the ionization method

Measurement of radon flux density using the ionization method was carried out in [6, 12, 17, 18]. Radon radiometer type AlphaGUARD, connected cyclically with storage chamber, or located inside the storage chamber [18], measured the linear increase in radon activity by the secondary characteristic - the created ionization density. Usually, 10-minute measurement intervals and a total accumulation time of 60 minutes or more are used. Then, from the slope of the linear accumulation function OA of the radon,

$$q = \alpha \cdot \frac{V}{S} \ , \tag{1.4}$$

Where the coefficient α, Bq m^{-3} s^{-1}, is determined from the equation.

$A(t) = \alpha t$

Using the slope angle of the linear function of radon accumulation allows, in this method, to cut off the contribution of thoron to the measurement result. In [12], a retentate volume of 1.5 l, installed between the storage chamber and the ionization chamber, was used to separate the thoron. The gas leaving the ground surface inside

the storage chamber was pumped through the containment volume at a rate of 0.5 l / min.

The disadvantage of the method of measuring by the AlphaGUARD radiometer, according to the results of [24], is that it takes a certain time to restore the background level inside the ionization chamber after measuring large radon concentrations. Despite this drawback, AlphaGUARD devices are actively used in radon flux density measurements, moreover, they are successfully combined with automated storage chamber [12, 18] to obtain long time series of data on radon flux density.

1.2.5 Measurement of accumulated activity by track method

The track method is used, mostly in the laboratory, to measure the radon flux density from a unit area or mass of a sample of a porous material. The sample and the track detector (LR-115 or CR-39) are placed inside the storage chamber, the chamber is sealed and held for a long time from 1 to 3 months. Then the accumulated activity is determined from the track density. This method was used in [19-21]. The value of the radon flux density, Bq m^{-2} s^{-1}, is obtained from the expression [19]

$$q = \frac{AV\lambda}{S} \Big/ \left(T + 1/\lambda(e^{-\lambda T} - 1)\right),$$ (1.5)

where A is the integral value of the radon OA measured by the track detector inside the storage chamber, Bq/sm^{-3}; - the time of exposure of the sample inside the closed storage chamber, s

1.2.6 Measuring the activity of radon accumulated on activated carbon

Historically, the method of accumulating radon activity on activated carbon was created first. In 1906, Rutherford proposed the use of activated carbon for the adsorption of radioactive emanations [22], and the following year activated carbon was used to collect radon, followed by measuring the accumulated activity on an electroscope.

Later, activated carbon began to be used in measurements of radon flux density and thoron flux density from the surface of the earth or a sample of porous material. The radon activity accumulated on the carbon absorbers is measured using a scintillation or semiconductor [23] gamma spectrometer. Liquid scintillators are also used for this purpose [14, 24]. For example, in [24], a counting system based on the liquid scintillator Tri-Carb 3100TR was used to measure the alpha and beta activity of radon and its decay products, then the measured pulse count rate was recalculated into activity using a conversion factor (imp / s) / Bq.

In Russia, for the accumulation of radon using a set of equipment "Camera" [2]. In work [2], the measurement of the radon activity accumulated in the coal of the storage chamber-32 was performed by the RGG-20P1 radiometer in gamma radiation and the RGB-20P1 radiometer by beta radiation, then the value of the RVP is calculated by the formula

$$q = \frac{\lambda A}{nfS(1-e^{-\lambda t})} \,,$$

(1.6)

Where A is the total activity of radon in the coal quantity of storage chamber-32 installed on the site under investigation, Bq; f- Correction factor, rel. units; - the working surface area of storage chamber-32, m^2; - Radon accumulation time, sec.

The activity of the decay products of radon by the scintillation (NaI) gamma spectrometer was measured in [30], and the value of the radon flux density was calculated from expression

$$q = \frac{\lambda^2 \cdot t_3 \cdot e^{\lambda t_2}}{(1-e^{-\lambda t_1})(1-e^{-\lambda t_3})} \cdot \frac{C}{f_{eff} \cdot f_{ads} \cdot S_{NaI}} \,,$$

(1.7)

where C is the number of pulses registered by the detector in time t_3;

t_1 - exposure time of activated carbon (s); t_2 - the time elapsed from the end of the exposure before the start of the measurement (s);

f_{eff} – Detector detection efficiency, imp. Bq^{-1}; f_{ads} – radon adsorption efficiency, rel. units*;*

S_{nal} – sensitive surface of the detector, m^2.

1.2.7 Dynamic chamber method

Another version of the storage chamber method is embodied in integrated monitors, which are a dynamic storage chamber with an electret detector located inside (a charged Teflon disk). Radon enters the chamber through a filter that retards the decay products of radon and thoron, and exits through the valves, hence a semi-equilibrium concentration is established inside the chamber. In advanced electret monitors, a diffusion filter is installed between the chamber and the surface of the sample. A chamber with a pre-charged electret is placed on the surface of the ground for several hours or days. The rate of discharge characterizes the radon flux density. After exposure, the voltage drop due to radon is measured by a standard meter. For determining background discharge rate (V / h) due to gamma radiation from the porous material is placed between the sample and the chamber aluminum foil.

1.2.8 Advantages and disadvantages of different methods

Below are the results of comparison of various methods for measuring radon flux density from the earth's surface. Advantages and disadvantages of static and dynamic methods were elaborated and reasoned in [25], where a general method of a storage chamber for measuring the flow (flux density) of any gases emerging from the earth's surface is considered.

Advantages of the static method:

• Equipment and procedure is much simpler and cheaper, which allows for simultaneous mass surveys (for example, the method of accumulation of radon on activated carbon is considered the cheapest);

• In combination with instantaneous methods of measuring accumulated activity, it is possible to measure temporal variations in the value of radon flux density during a day;

• A simple recalculation into the value of the radon flux density.

The disadvantage of the static method is that when the radon concentration inside the storage chamber increases, the concentration gradient and, accordingly, the radon flux

from the ground decrease. With an increase in the radon concentration within the storage chamber to 25% or more, the calculated flux density can be underestimated. Therefore, the exposure time should be selected depending on the characteristics of the subject area, which can significantly complicate the entire procedure.

The advantage of the dynamic method is that there is no background concentration in the chamber.

Disadvantages of the dynamic method:

• More complicated procedure and expensive equipment, which limits the possibility of conducting mass surveys;

• Under certain conditions, radon and thoron can enter (from the atmosphere) into the interior of the oil well, which cannot be controlled, or can be taken into account by introducing a correction factor, since this process has not been thoroughly investigated;

• It is not possible to measure temporal variations during the day.

A comparison of the direct and indirect methods of measuring radon flux density has been made in many works [4, 7, 26], as a result, the main shortcomings and advantages of indirect methods can be briefly summarized.

Disadvantages of indirect methods:

• A method based only on the diffusion model (option 1) gives an underestimated value of the radon flux density;

• The method based on the diffusion-advection model (variant 3) gives good results only in the case of a relatively homogeneous geological structure [9].

The main advantage of the indirect method (option 3) is the ability to restore the dynamics of the radon flux density based on the results of the earlier monitoring of radon OA in soil air, as, for example, in [3].

Here we should also mention the shortage of the direct method of the storage chamber, which was discovered in [1], that during the storm wind this method did not yield reliable results.

2. Semiconductor Alpha-Spectrometry

This chapter provides information on semiconductor alpha detectors (PPDs). Their types, properties, characteristics and capabilities. The possibility of electrostatic deposition in the storage electrostatic chamber of the decay products of radon and thoron is considered

2.1 Semiconductor alpha-radiation detectors

Semiconductor detectors (PDDs) are widely used as particle number counters and as particle energy analyzers (spectrometers) with high resolution. The principle of their operation is based on the fact that when passing through the counter of the ionizing particle, the charges formed in the counter material collect on the electrodes, i.e. in the first approximation, the semiconductor detector can be regarded as an ionization chamber with a solid dielectric between the electrodes.

However, the processes of generation and transport of charge carriers in a semiconductor and the mechanism of carrier recombination are of a different nature than analogous processes in a gas. The formation of one pair of charge carriers in a semiconductor counter requires ~ 10 times less energy than in gases. The energy used in the scintillator to generate one photoelectron in a system consisting of a scintillator and a photomultiplier is ~ 300 eV, i.e. in ~ 100 times more than in a semiconductor detector. An increase in the number of charge carriers and, consequently, a decrease in the relative fluctuation of the magnitude of the signal is one of the reasons for the much higher resolution of the semiconductor in comparison with ionization and scintillation detectors.

The sensitive volume of semiconductors can reach hundreds of cubic centimeters. At a large density of matter (at $\sim 10^3$ times higher than the density of gases), not only heavy particles with energy of tens of MeV, but also electrons with energy up to 2 MeV can be decelerated completely. The efficiency of γ-radiation detection in some types of semiconductors is comparable with the efficiency of large-scale scintillation detectors. At the same time, semiconductors can be made with a very

small gap between the electrodes, and one of the electrodes is made very thin. Such a detector is used to measure specific energy losses.

In addition, for semiconductor, a short time signal front is provided that provides a time resolution of the order of several nanoseconds, and a linear dependence of the signal amplitude on the energy absorbed in the sensitive volume of the detector. Finally, an important feature of semiconductor counters is their small size. This greatly expanded the possibilities of using such detectors not only in the field of physical experiment, but also in technology - in process control devices and in medicine.

2.2 The main types of semiconductor alpha-radiation detectors

The good parameters of semiconductor detectors, the realization of which became possible after the creation of low-noise and highly stable electronic equipment and the development of special cooling and evacuation systems, make it possible to widely apply them in almost all areas of nuclear physics.

According to the methods of formation of transitions, semiconductors are subdivided into surface-barrier, p-i-n-type diffusion detectors, also called drift detectors, and very pure germanium detectors-HPGe detectors.

In a surface-barrier detector, an n-p transition is formed by oxygenation of the n-silicon surface, followed by depositing a thin gold layer on the surface p-layer thus formed. The thickness of the working region of such detectors does not exceed 0.2÷0.5 mm, therefore they are used mainly for detection and spectrometry of heavy particles at an energy resolution of 1 keV. The thickness d of the sensitive area depends on the bias voltage:

$$d = 5{,}3 \cdot 10^{-5} \left(\rho V \right)^{1/2} cm,$$
(2.1)

Where ρ is the resistivity in ohms,

V is the bias voltage in volts.

To increase the thickness of this region, which is necessary for measuring the energy of long-range particles, it is possible to increase the bias voltage. But increasing

the voltage on the detector results in an increase in noise. These detectors can work at room temperature without special cooling Figure 2.1
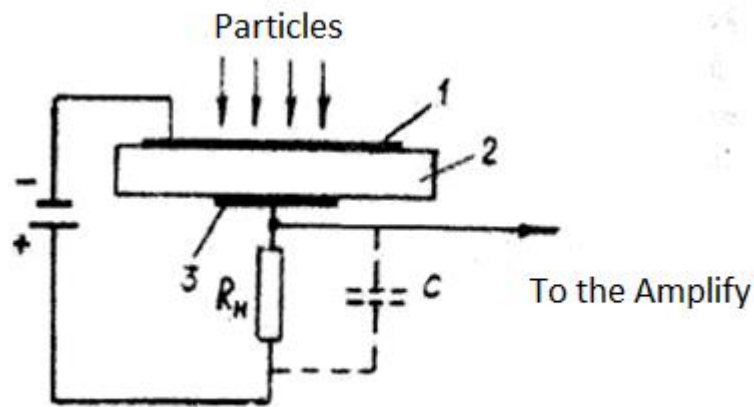

Figure 2.1 Scheme of inclusion of a surface-barrier semiconductor detector:

1-thin layer of gold, 2 plates of silicon of n-type, 3-layer of nickel

In diffusion detectors, the transition is obtained by compensating for the impurity p-conductivity of silicon by diffusion of donor atoms (usually phosphorus) into it. According to their characteristics and application, they are close to surface-barrier detectors and also operate at room temperature.

The detectors with a p-i-n-junction (more precisely n^+-p-p^+, the sign + signifies strong doping) obtained by the drift of lithium ions have a particularly large volume of the sensitive region. Lithium ions, due to their small dimensions, diffuse easily into silicon and germanium, not at the lattice sites, but in the interstices. The diffusion coefficient lithium to germanium, for example, is 10^7 times greater than that of conventional donors.

The surface of the p-semiconductor is sputtered with lithium, which, when heated to a temperature of about 400 ° C, diffuses to a depth of about 0.1 mm, forming a thin high-doped n^+ layer. Then a voltage (plus to the n-layer) is applied to this p-n junction, under the action of which the controlled diffusion of lithium ions in the p-semiconductor occurs until the number of lithium ions becomes exactly equal to the number of acceptor atoms (this is usually boron). The opposite surface is doped with

boron atoms with an energy of ~10 keV, resulting in a thin p^+ layer with high conductivity. Surface p^+ - and n^+ -layers serve as electrodes. Between them is a sensitive region of up to 1 cm of a fully compensated semiconductor, the resistivity of which is equal to the resistance of a pure crystal. Silicon detectors can work without cooling, while the energy equivalent of noise is several tens of keV.

Detectors with p-i-n-junction from extremely pure germanium. The technology of manufacturing HPGe detectors is similar to the technology of manufacturing Li-drift detectors, excluding the stage of drift of Li into the interior of the p-crystal. Here, not lithium-compensated germanium is located between the surface n^+ and p^+ -layers-electrodes, but very pure germanium with an impurity concentration of about 10^{10} cm^3. With such a concentration of impurities, upon cooling to the temperature of liquid nitrogen, the resistance of the semiconductor increases to such an extent that it becomes possible to create a semiconductor with a thickness of the sensitive region of about 1 cm. The structure of such a detector is shown in Fig 4.5

The maximum admissible concentration of impurity atoms in germanium, at which it is still possible to produce semiconductor without compensation, is $3*10^{10}$ cm$^-$^{3}. HPGe -detectors are characterized by exceptionally low level of leakage currents (about 10-11 A) and high resolution.

Unlike silicon semiconductor detectors, germanium detectors must be operated at a low temperature. This is due to the fact that the width of the forbidden band of germanium is noticeably smaller than that of silicon (0.66 eV for germanium and 1.09 eV for silicon). In connection with this, the probability of thermal generation of minority charge carriers in germanium is much higher, and at room temperature the leakage currents are unacceptably high. One of the significant advantages of HPGe detectors over similar diffusion-drift Ge (Li) detectors is the possibility of storing them at room temperature in the period between measurements, although during operation they must also be cooled to the temperature of liquid nitrogen. Ge (Li) detectors have the same high energy resolution as the HPGe detectors, but they should always be in a cryostat with liquid nitrogen - even a short-term increase in the temperature of the Ge

(Li) detector to room temperature, caused, for example, by late filling the cryostat with liquid nitrogen, disables the detector.

2.3 Transitions in semiconductors

To make a semiconductor single crystal with insufficiently high resistivity to fabricate a semiconductor, the properties of the transition region between two regions of a semiconductor with different types of conductivity are used. There are different ways to create a transition. As an example, consider the properties of a pn-type transition in a silicon semiconductor.

A layer of a substance containing phosphorus or arsenic is deposited on the surface of a silicon plate with hole conductivity and the lowest possible concentration of acceptor impurity. The plate is kept at a high temperature. As a result of thermal diffusion of donor atoms into the main crystal, a thin n-layer with high conductivity is formed on its surface, in which the concentration of donors is much higher than the concentration of acceptors. Figure 2.2a shows the location of impurity charge carriers in the n- and p-layers.

In addition to the carriers shown, in both layers there are own pairs of "electron-hole" carriers created by thermal transitions through the forbidden zone. But since the probability of recombination increases with the presence of impurities, the concentration of these carriers is small. In addition, it must be remembered that the donor and acceptor centers (circled) are fixed in the crystal lattice and cannot move, i.e. are not free charge carriers. In the absence of an external electric field, conduction electrons supplied by donors (for example, phosphorus) will mainly be in the n-region (Fig. 2.2a), since electrons are attracted by the positive space charge of the donor ions.

Holes supplied by acceptors (for example, boron atoms) are mainly in the p-region, since they are attracted by negatively charged acceptor ions. However, at the interface between the p- and n-layers, due to diffusion, the electrons and holes will be mixed, i.e. holes will go into the n-region, leaving behind a negative charge, uncompensated by the acceptor, and electrons, going into the p-region, create a positive charge of donor ions at the boundary of the n-region.

a)

б)

⊕ - donor center   ⊖ - acceptor centre

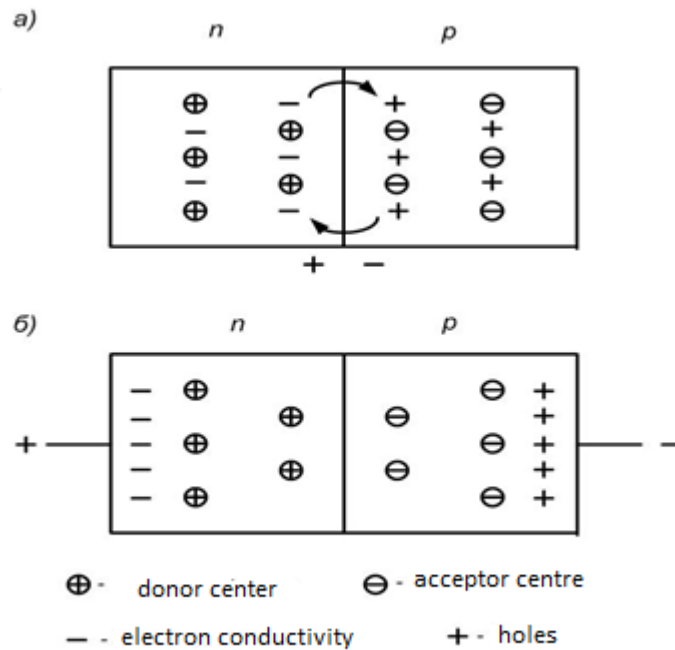— - electron conductivity   + - holes

Figure 2.2 Location of impurity charge carriers:

a - without an external electric field, b - in an external electric field

Holes supplied by acceptors (for example, boron atoms) are mainly in the p-region, since they are attracted by negatively charged acceptor ions. However, at the interface between the p- and n-layers, due to diffusion, the electrons and holes will be mixed, i.e. holes will go into the n-region, leaving behind a negative charge, uncompensated by the acceptor, and electrons, going into the p-region, create a positive charge of donor ions at the boundary of the n-region.

Thus, due to diffusion at the boundary of the pn layer, a double electrostatic layer is formed whose electric field stops further diffusion of electrons and holes through the boundary of the layer. At the interface, a region is formed, depleted of free charge carriers, in which there is an electric field and in the absence of an external voltage source.

But due to the small width of this region ($<10^{-4}$ cm), it cannot be used to detect charged particles. The sensitive region of the detector can be increased by applying an external electric field to the crystal, such that the effect of the double electrostatic layer is further enhanced. For this, a negative voltage is applied to the p-region, so that charge carriers-holes are pulled to the negative electrode, and electrons from the n-layer to

another (positive) electrode. The resulting picture of the distribution of charge carriers in this case is shown in Fig.2.2b. As a result, a comparatively extended transition region (a depleted region) is formed inside the crystal, in which there are no charge carriers-electrons and holes. In this region there are only the atoms of the initial semiconductor, the ions of acceptors and donors, which form a double electrostatic layer. It is this region of the semiconductor that is the working or sensitive region of the detector.

2.4 The formation of carriers under the action of ionizing radiation

During the passage of the ionizing particle, there are fast electrons, which in the cascade process of impact ionization knock out electrons from different energy zones, including the deepest ones. This process continues until the electron energy becomes less than the threshold energy - about 1.5 E.g. The creation of electron-hole pairs in a cascade process that lasts during the deceleration time of the primary charged particle ($\sim 10^{-12}$ s) is shown in Fig. 2.3 a.

Then, as a result of a different type of interaction of electrons with the crystal lattice, the electrons descend to the bottom of the conduction band, and the holes rise to the upper edge of the valence band; the velocity distribution of the nonequilibrium carriers created by the particle becomes thermal-equilibrium (Fig. 2.3b).
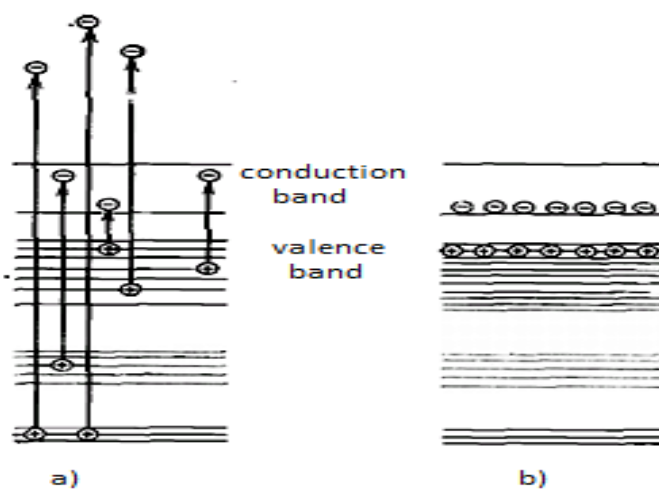

Figure 2.3 Energy diagram of the formation of electron-hole pairs

This stage also ends within a time of the order of 10-12 s, i.e. generation and deceleration of carriers to thermal velocities terminate practically together with the deceleration of the primary particle.

The average energy ω necessary to create one electron-hole pair is approximately three times the width of the forbidden band Eg, which is the minimum energy necessary for the formation of a pair. One of the reasons for the increase in ω is that the secondary electrons, reaching threshold energy, can later lose it only on interactions with the lattice. In addition, in the process of slowing down to thermal velocities, the electrons interact with the lattice, exciting the oscillations mainly in the optical range, whereby the remaining excess energy is spent.

2.5 Characteristics of a semiconductor spectrometer

Fluctuations in the output signal of the PPD at registration of monoenergetic particles, whose range completely fits in the sensitive volume of the detector, depends on the processes occurring both in the detector itself and in the electronic path. The causes of these fluctuations are:

1. fluctuations in the number of produced pairs of carriers;

2. fluctuations in the number of collected carriers;

3. thermal noise;

4. fluctuations of leakage currents;

5. noise of the preamplifier.

The amplitude distribution of the pulses can be described with sufficient accuracy by the Gaussian distribution with dispersion $\sigma^2 = \sum_i \sigma_i^2$, where each source of scatter of signal amplitudes corresponds to its partial standard deviation σ_i. In practice, the width of the distribution at half-height is taken as the measure of the spread of the pulse amplitudes, which in the case of the Gaussian distribution is equal to 2,36 σ. Often the standard deviation of the number of collected carrier pairs σ or σ_i expressed in energy units, assuming it is equal to the energy of the particle are

expressed in energy units, assuming it is equal to the energy of the particle, forming a signal equal to the standard deviation. In this case, the standard deviation in energy units is $\omega \cdot \sigma$.

Fluctuations in the number of formed carrier pairs. They are due to the statistical nature of the energy distribution between the ionization process and competing processes. Average number of pairs formed $N = E / \omega$, where E – particle energy. If the fraction of the energy going to ionization is small and the formation of pairs obeys Poisson's statistics for independent events, then the variance of the number of pairs N is

$$\sigma^2 = N = E/\omega ,$$
(2.2)

However, in semiconductor, an appreciable part (~30%) of the particle energy is used to form carriers, and therefore the process is not described by the Poisson distribution. The deviation from this distribution is taken into account by the Fano factor, which is equal to the ratio of the observed variance to the variance for Poisson statistics. If all the energy of the particle was spent only on the formation of carriers, i.e. equality would take place $\omega = E_g$, then the Fano factor would be zero. Scintillation counters require 400 to 1000 eV for the formation of one photoelectron when the scintillation light falls onto the photocathode. Therefore $F = 1$. taking into account the Fano factor in energy units

$$\sigma = \omega\sqrt{FE/\omega} \quad u \quad \frac{\sigma}{E} = \sqrt{F\omega/E} ,$$
(2.3)

For silicon and germanium, depending on the quality lies in the interval 0.05-0.15. For a silicon detector with $\omega = 3.7 eV$ c with E = 1MeV, we obtain: $\sigma = \sqrt{0.1 * 10^6 * 3 \cdot 7} \sim 0 \cdot 5 keV$, $\Delta E = 2 \cdot 36\sigma \sim 1 \cdot 2 keV$ and the relative resolution Relation $\Delta E / E \sim 0 \cdot 15\%$ (4.2) determines the fundamental limit of the energy resolution of the PPD

Fluctuations in the number of collected carriers are due to the fact that during the collection of charge carriers as a result of their recombination and temporary capture by traps, they may not reach the electrodes. These fluctuations can be

neglected if the carrier acquisition time is much shorter than their mean lifetime before recombination and capture. An additional contribution to the fluctuations is made by the uneven distribution of the traps in the volume of the detector. This is especially important for semiconductor gamma-ray spectrometers, which have a large volume of the sensitive region.

Thermal noise is caused by fluctuations in the rate of thermal motion of the carriers, leading to an inhomogeneous distribution of carriers in the semiconductor. At room temperature thermal noise in units of keV:

$$\sigma \approx (1,2 \text{ ; } 1,5)\sqrt{C},$$

(2.4)

where c is the capacity of the transition.

Fluctuations of leakage currents. The conductivity of the transition region to which the bias voltage is applied is different from zero. Therefore, a current flow through the junction, which is commonly called the leakage current. Fluctuations in the number of charge carriers in this region that occur during thermal generation lead to current fluctuations. In addition, because of the different concentration of electrons and holes in the n- and p-regions, a diffusion current arises through the junction. The latter is approximately two orders of magnitude smaller than the generation current.

In addition to volumetric leakage currents along the side surfaces of the crystal, surface leakage currents flow, depending on the quality of the PPD fabrication.

Thermal noise and leakage currents, therefore, and the energy resolution of the detector depend very much on temperature.

The noise of the preamplifier is mainly determined by the head (first) cascade, for the construction of which the field effect transistors are usually used. To reduce noise, the preamplifier is often mounted together with the detector, cooled and evacuated. Despite these measures, noise contributes significantly to the energy resolution in the spectrometry of x-ray radiation with energy of several keV.

In modern semiconductor detectors, the spectrometric path has a linear characteristic, i.e. the channel number is proportional to the amplitude of the signal at its input and, correspondingly, to the value of the charge at the output of the detector.

Thus, the relationship between the channel number and the energy can be assumed to be linear. In this case, one can apply such a characteristic as the price of the channel, expressed in energy units, for example, keV / channel. In this case, the price of the channel, and, consequently, the range of energies of the detected radiation, are determined by the characteristics of the detector and the amplification factor of the main amplifier.
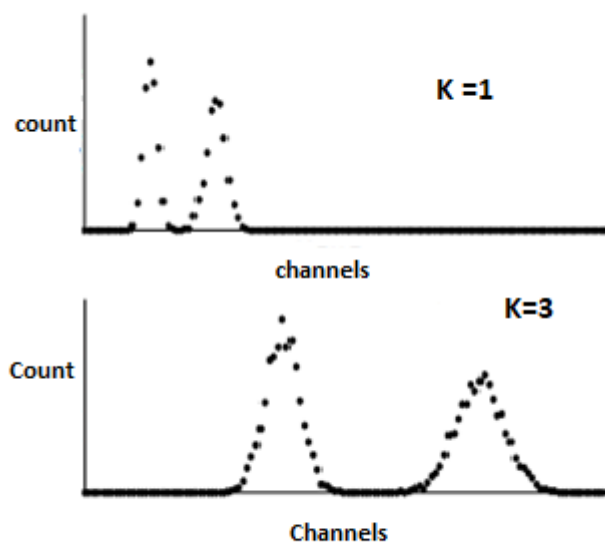

Figure 2.4 Amplitude distribution of two lines at different amplification factors. K is the gain

In Fig. 2.4 shows the amplitude distributions of the two energy lines, with the lower distribution recorded at a gain factor 3 times greater than the upper one. From this figure it can be seen that the positions of peak peaks are shifted in proportion to the increase in the gain, which corresponds to a threefold decrease in the price of the channel; The width of the peaks, expressed by the number of channels, also increases proportionally.

We especially draw attention to the fact that the PSIV can characterize the resolution of the spectrometer only if it is expressed by energy units, but not by the number of channels. This is what Figure 4.2 shows. The width of the peaks in the histograms depends on the gain, but the relative resolution of the spectrometer does not depend on it but is determined by the technical data of the detector and the

spectrometric channel. Above we assumed that there is a linear dependence between the energy absorbed by the detector and the position of the peak maximum in the channels. In reality, this is not always the case.

First, the A / D converter (ADC) can process analog signals only in a limited range. In particular, there is a threshold below which the amplitudes of the input pulses in the channel number are not transformed. This leads to the fact that the calibration line must be represented, at least

measure, by the function $E = G0 + G1p$, where G0 and G1 are constants. Consequently, the calibration can be performed if the energies of not less than two lines are known.

Secondly, the amplitudes of the signals at the output of the amplifier are proportional to the energy only approximately and the amplitude characteristic differs from the straight line. The contribution to the nonlinearity introduced by the HPGe detector is small and the deviation of the amplitude characteristic from the line is mainly determined by analog circuits of electronic equipment (preamplifier, main amplifier, ADC). The quality of the spectrometer is estimated by two values:
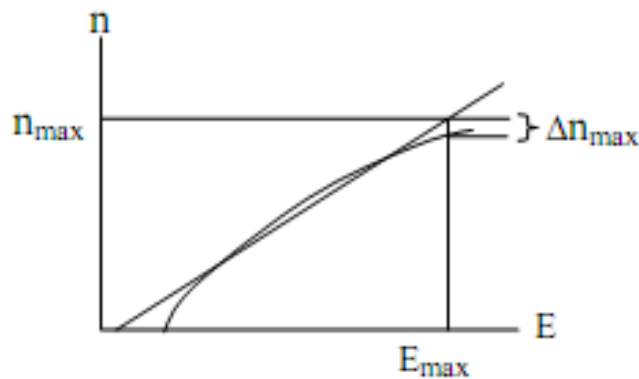
Figure 2.5 Amplitude characteristic of the spectrometer

1. Integral nonlinearity: $l = \Delta n / n$ where Δn_{max} is the maximum deviation of the real curve from the ideal curve, n_{max} is the maximum channel number;

2. Differential nonlinearity - $\delta = (\Delta U_{Ki} - \Delta U_{Ksr.}) / \Delta U_{Ksr}$, where ΔU_{Ki} is the channel width with the number i, $\Delta U_{Ksr.}$ - average channel width; The channel width is the amplitude range corresponding to one channel

2.6 Heavy charged particle spectrometry

Heavy charged particles - α-particles with energy up to several tens of MeV, fission fragments (kinetic energy of the order of hundreds of MeV) - are most often objects of spectrometry using surface-barrier semiconductor detectors. For these short-range particles, as a rule, condition

$$R < d, \qquad (2.5)$$

where R is the range of the particle in the detector material, d is the thickness of the sensitive region.

In the spectrometers of short-range particles, silicon surface-barrier detectors are usually used. Alpha-spectrometers with such detectors allow obtaining a high energy resolution (of the order of several keV) and revealing details of the fine structure of α-spectra. Condition (2.5) ensures a high linearity of the energy calibration curve for α-spectrometers. Semiconductor thin detectors are convenient for measuring specific ionization losses. They are often used in the identification of particles in the composition of (ΔE-E) telescopes as ΔE-counters.

2.7 Substantiation of the possibility of electrostatic precipitation of products of decay of radon and thoron.

As a result of the decomposition of ^{222}Rn, ^{218}Po and ^{214}Po are formed in Fig. 2.6 have a positive charge (up to +7). The results of [28, 29] have shown that 88% of the ^{218}Po, ^{216}Po, ^{214}Pb and ^{210}Po atoms at the end of their path due to the recoil energy, after the emission of the alpha particle during decay of the radon and thoron nuclei, are positively charged and the remaining 12% are neutral.

This fact allows us to talk about the possibility of using the electrostatic precipitation method to collect ^{218}Po, ^{216}Po, ^{214}Pb ^{210}Po atoms on a semiconductor alpha detector with their subsequent recording. The characteristics of radon, thoron, and all their decay products are given in Table 2.1. Later, when analyzing the spectral distributions obtained experimentally with the help of different constructions of storage chambers, we use this table to identify the peaks belonging to the products of the decay of radon and thoron.

The electrostatic precipitation technique for the determination of radon flux density is used in many devices, for example, in a radon radiometer PPA-01M-03.

As a result of studying the design of the radon radiometer PPA-01M-03, it was found out that a positive voltage of 2000 V is applied to the body of the storage chamber to electrostatically precipitate positive radionuclides on the semiconductor detector located inside the cylindrical body of the radiometer. The volume of the body intended for electrostatic precipitation of radionuclides is approximately 1 liter.
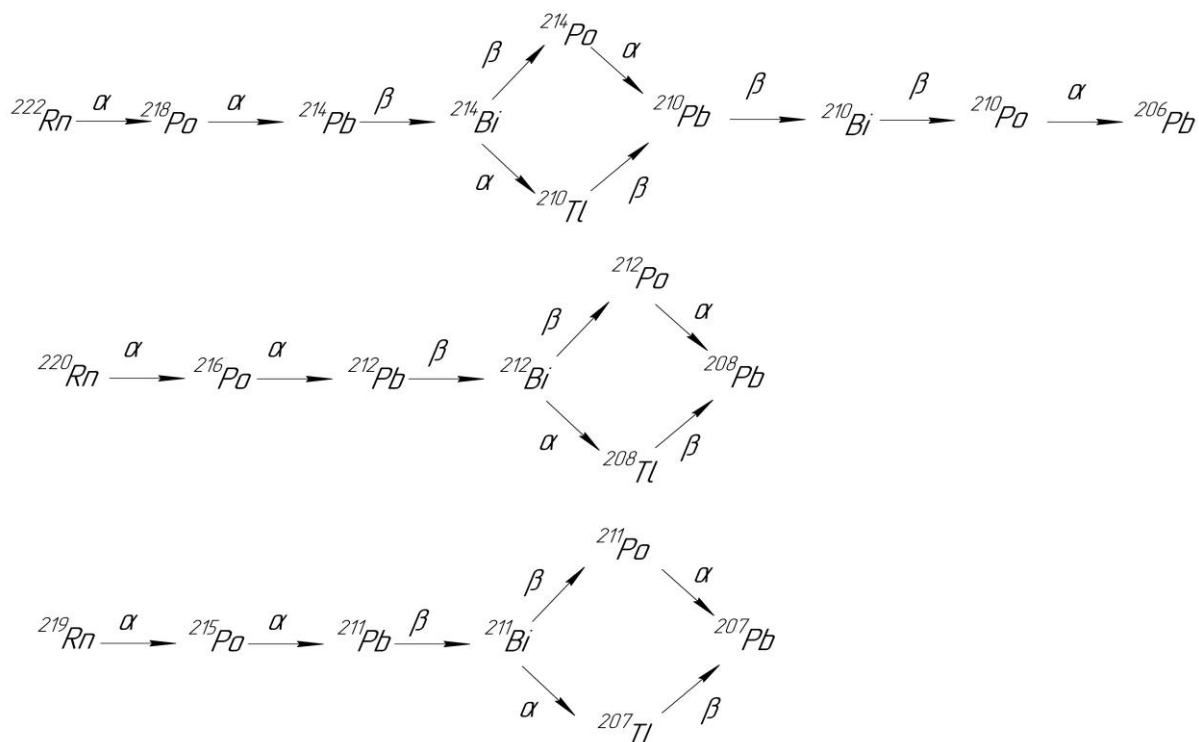
Figure 2.6 The decay chain of radon isotopes

Table 2.1 Characteristics of radon, thoron and their decay products

Element	The half-life $T_{1/2}$ / the decay constant λ	Kind of radiation	The radiation energy, MeV	Emission yield per decay	The radiation intensity *, MeV / decay.
Radon ^{222}Rn	3,823 days / $2,10 \cdot 10^{-6}\,\text{s}^{-1}$	α	5,490	0,999	5,585

Radium A (Ra A) ^{218}Po	3,05 min. / $3,79 \cdot 10^{-3}$ s^{-1}	α	6,003	1	6,115
Radium B (RaB) ^{214}Pb	26,8 min. / $4,31 \cdot 10^{-4}$ s^{-1}	β γ $\sum \gamma$	1,024(max) 0,295 0,352	1,663 0,192 0,371 1,025	0,291 0,249
Radium C (RaC) ^{214}Bi	19,9 min. / $5,86 \cdot 10^{-4}$ s^{-1}	β γ $\sum \gamma$	3,270(max) 0,609 1,120 1,765	0,987 0,461 0,150 0,159 1,289	0,648 1,459
Radium C' (RaC') ^{214}Po	$1,64 \cdot 10^{-4}$ s / $4,23 \cdot 10^{3}$ s^{-1}	α	7,687	1	7,834
Thoron ^{220}Rn	55,6 c / $1,25 \cdot 10^{-2}$ s^{-1}	α	6,288	0,999	6,398
Thorium A (ThA) ^{216}Po	0,15 s / 4,78 s^{-1}	α	6,779	1	6,907
Thorium B (ThB) ^{212}Pb	10,64 hrs. / $1,81 \cdot 10^{-5}$ s^{-1}	β γ $\sum \gamma$	0,573(max) 0,075 0,077 0,239	1,775 0,107 0,179 0,446 0,993	0,104 0,148
Thorium C (ThC) ^{212}Bi	60,55 min. / $1,91 \cdot 10^{-4}$ s^{-1}	α β $\sum \gamma$	6,051 2,246(max)	0,359 1,057 0,283	2,214 0,461 0,185

Thorium C' (ThC') ^{212}Po	$3{,}05 \cdot 10^{-7}$ s / $2{,}32 \cdot 10^{6}$ s^{-1}	α	8,785	1	8,956
Thorium C" (ThC") ^{208}Tl	3,07 min. / $3{,}79 \cdot 10^{-3}$ s^{-1}	β	1,795(max)	0,994	0,559
		γ	0,511	0,216	
			0,583	0,858	
			0,860	0,120	
			2,615	0,998	
		$\sum \gamma$		2,280	3,359

3. The Diagram of the Experiment on Measurement of the Density of Radon and Thoron Fluids

This chapter contains a diagram of the experiment with various designs of storage electrostatic chambers. Description of the structures and schematic drawings of the storage chambers themselves. Also, is a list of devices for their purpose and technical characteristics of the electrostatic chambers used during the experiment with various designs, for example: the alpha spectrometer and high voltage blocks used to create a high voltage on the electrodes of the chamber

3.1. Experimental scheme

In Figure 3.1 shows the scheme of the experiment to measure the density of radon and thoron fluxes from the surface of various types of soil.
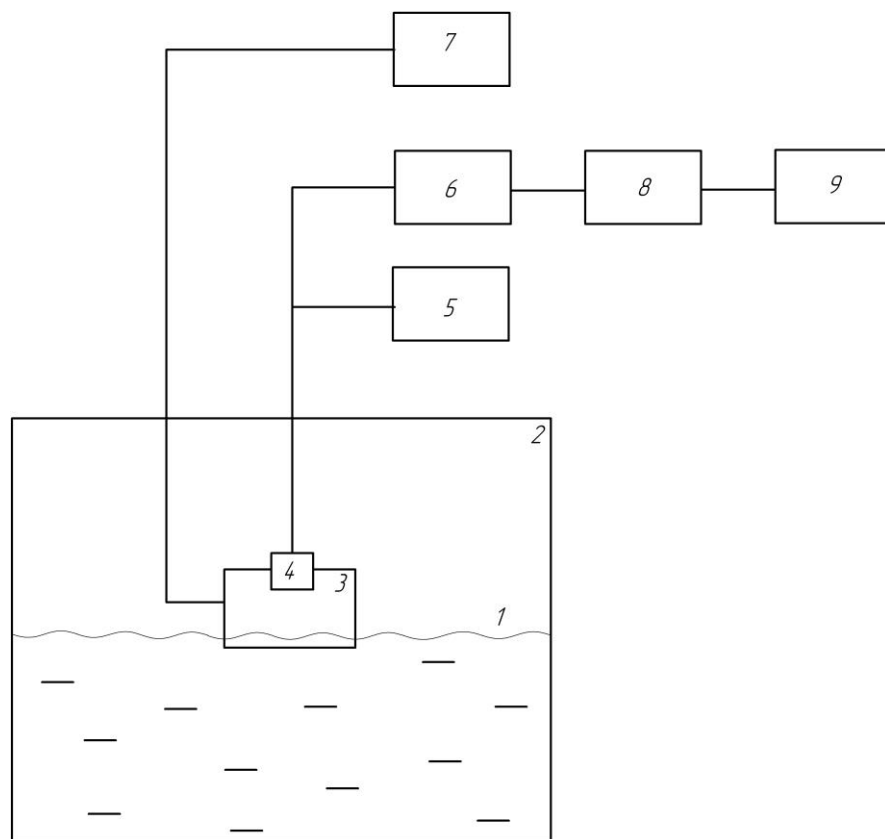
Figure 3.1 Experimental scheme

1 - a line of a surface of a ground; 2 - 100 liter barrel of sand imitating the sandy surface of the earth; 3 - accumulation chamber with electrostatic precipitation; 4-PDD

(semiconductor detector); 5 - power supply unit PPD; 6 - the amplifier of the signal fed from the PPD to the ADC; 7 - blocks of high positive and negative voltage supplied to the ND; 8 - analog digital converter of ADC; 9 - PC personal computer;

Figure 3.2 shows a photograph of the entire measuring system, with the exception of a cask with sand and a container with earth.
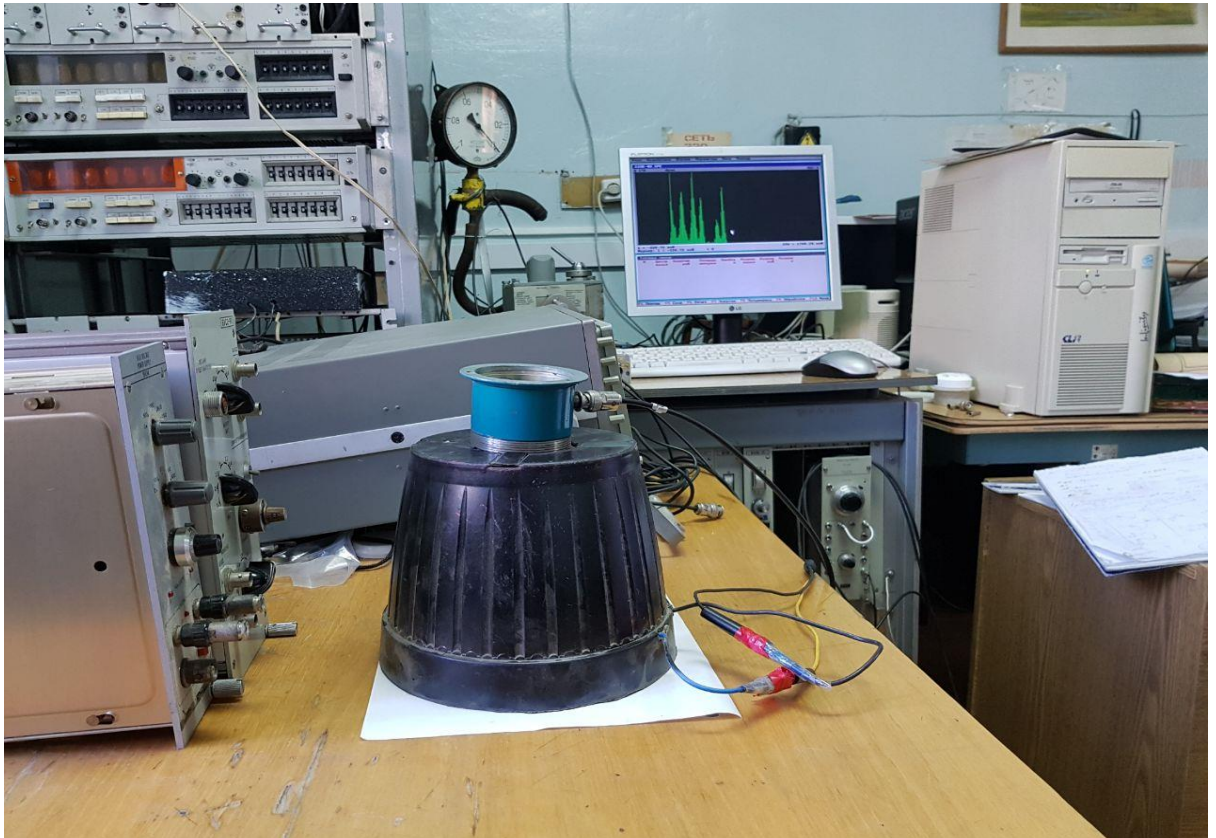

Figure 3.2 Photo of the measuring complex.

In addition to the sand in the accumulation barrel, measurements were also made from the ground containing an increased amount of radium - 226 and thorium - 232. The accumulation chamber, as in the case of sand, was placed in a container with earth. Spectrometric analysis of the radionuclide composition of sand and earth was carried out using a low-background gamma spectrometer. The results are shown in Tables 3.1 and 3.2

Table 3.1. Radionuclide analysis of sand.

Radionuclide	The activity of Bq	Specific activity Bq / kg
K^{40}	324,7	216,5
Ra^{226}	34,82	23,21
Th^{232}	20,82	13,88

Table 3.2. Radionuclide analysis of the earth.

Radionuclide	The activity of Bq	Specific activity Bq / kg
K^{40}	834,7	596,2
Ra^{226}	43,01	30,72
Th^{232}	69,08	49,34

For the measurements, the MKS-01A alpha-spectrometer "Multirad-AC" with a semiconductor detector (4) was used, which was installed inside the storage chamber (3). The semiconductor detector and the spectrometer were connected by a cable. The spectrometer (6) was used to supply the supply voltage to the PPD and amplify the signal coming from it with the PPD. The signal amplification field was transmitted by the spectrometer to an analog-to-digital converter 4K-CATSPP (7), which converts pulsed streams into a digital code. The resulting signal is sent to the computer and displayed on the monitor as a spectrum using a special application (ACP-control v1.1). Power supplies (7) BNV-30-01 and MHV 12-2.0k 1000P were used for supplying the storage electrostatic chamber with high voltage DC voltage of various signs.

3.2 Purpose and technical characteristics of the MKS-01A alpha-spectrometer "Multirad-AS"

1. Measurement of the energy spectra of alpha-emitting radionuclides.

2. Measurement of the activity of alpha-emitting radionuclides in thin-layer (spectrometric) counting samples.

Below are technical characteristics of the alpha-spectrometer MKS-01A "Multirad-AS". Table 3.3. Table 3.3. Technical characteristics of the alpha-spectrometer MKS-01A "Multirad-AS"

Type of detector	Silicon ion-implanted
Detector parameters:	
input deactivated window with a thickness of the "dead" layer	not more than 0.15 μm;
sensitive area	450 mm^2;
background in the interval $3 \div 9$ MeV	no more 0.9 imp / hour $\cdot$ cm^2 for a detector of 450 mm^2;
thickness of the sensitive layer	200 μm;
energy resolution (PSVV) on the line of 5.1567 MeV	not more than 40 keV;
body diameter	32 mm.
Counting sample	thin-layered
Diameter	34 mm
Cooking method	electrolytic deposition
The pumping time of the working chamber to a residual pressure of 0.4 mm Hg	not more than 10 min
Automatically maintained range of operating pressure in the measuring chamber	$0,4 \div 2,0$ mm of mercury.
Energy range	$2 \div 9$ MeV
Background, not more than	100 imp/day
Lower limit of activity measurements	0.1 Bq
Dimensions:	
Spectrometer	370×300×190 мм
The pump	315×120×240 мм
Weight:	
Spectrometer	11 kg
The pump	9.6 kg

Alpha-spectrometer MKS-01A "Multirad-AS" was manufactured by NPP "Doza". SPE "Doza" was founded in 1991 by employees of the VNIIFTRI, the leading organization in the field of metrology of ionizing radiation. The photograph of the used MKS-01A alpha-spectrometer "Multirad-AC" is shown in Fig. 3.3.

Fig. 3.3 Photograph of the alpha-spectrometer MKS-01A "Multirad-AC".

3.3 Purpose and technical characteristics of ADC (4K-CATSPP)

4K-CATSPP - 3-input accumulating spectrometric ADC of a successive approximation with leveling on 4K. The total load is up to 400,000 pulses per second. It is designed to convert high-intensity pulse streams into digital code. The technical characteristics of the ADC are given in Table 3.4.

This analog-to-digital converter is made as a PCI card which is necessary for working with it to be placed in the appropriate connector on the motherboard of the personal computer. Below in Figure3.4, a photo of this board is shown.

Table 3.4. Specifications of ADC (4K-CATSPP)

Conversion Type	Sequential approximation with leveling
Number of simultaneously connected sensors	3
Amplitude of measured pulses of positive polarity	от 40 mV to 4,0 Vw
Duration of the leading edge of the input pulse not less than no more	0.4 μs 10,0 μs

Capacity of the memory channel for each input	2^{32}
Number of digits of conversion for each input	12 (4096) or 10 (1024)
Integral nonlinearity	0,1%
Differential nonlinearity	1,5%
The maximum integral load on three inputs (one of them)	400000 imp/sec
Temporary instability (for 8 hours of operation)	1,0 кан
Type of tire	PCI

The ADC (4K-SATSPP) was manufactured by Parsec LLC. "Parsek" since 1992 has been working steadily in the Russian market, specializing in the production of spectrometric analog-to-digital converters of its own design.

Figure 3.4 Photo of ADC (4K-CACHPP)

3.4 Purpose and technical characteristics of BNV-30-01

BNV-30-01- is designed to supply constant, stabilized, high voltage of various signs to the photomultiplier (photoelectric multiplier).

BNV-30-01 provides a constant stabilized voltage of various signs from 0 to 4 kilovolts and current from 0 to 50 microamps. The food BNV-30-01 is produced from 24V. A photograph of the high-voltage power supply unit itself can be seen in Figure 3.5

Figure 3.5 Photo BNV-30-01

3.5 Purpose Specifications MHV 12-2.0k 1000P

MHV 12-2.0k 1000P - high-voltage unit, designed to supply a constant, stabilized, positive voltage sign. The MHV unit is a highly integrated 12V voltage converter in 2kV.

At the output of the high voltage unit MHV 12-2.0k 1000P we get I_{out} = 100 mA, U_{out} = + 2000V. The input voltage required to operate a high-voltage power supply MHV 12-2.0k 1000P is equal to U input = 12V. In the circuit in Fig. 3.6, there is a 5 kΩ sub-line resistance. Also, the circuit of the high-voltage power unit contains a filtering capacity of 4700 pF at the outlet and a filter capacity of 47μF at the input. When the SW1 switch is closed, an input voltage of 12V is applied to the unit.
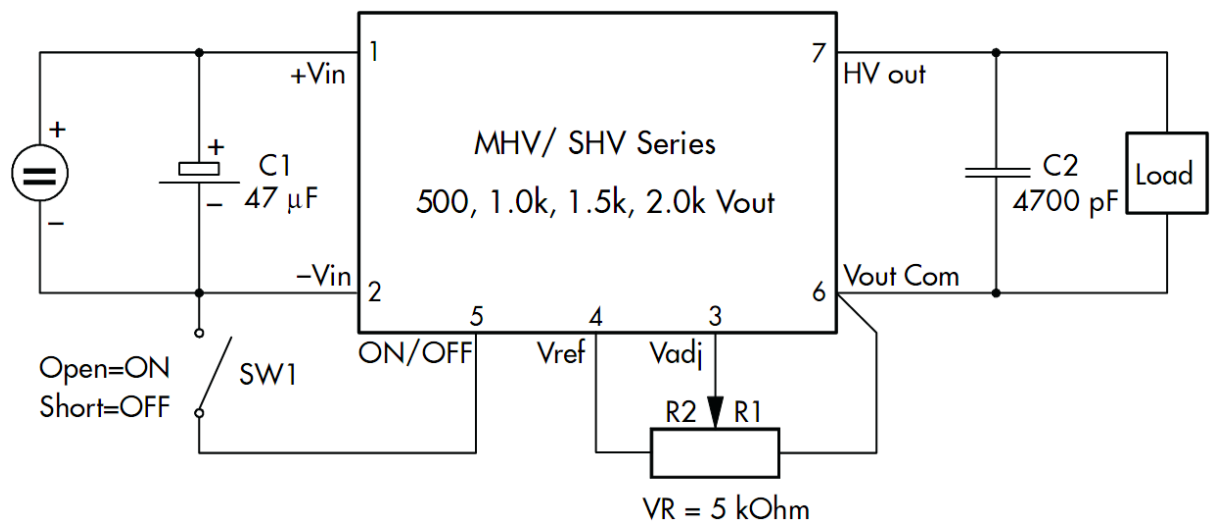
Figure 3.6 Schematic diagram of the power supply MHV 12-2.0k 1000P

3.6 Description of the program ACP-control v1.1

The program ACP-control v1.1 allowed to display the processed ADC spectrum and did not require the installation of the device driver. Therefore, after installing the board in the computer on a system request, you need to refuse to install the driver. In this case, the system will designate the card as an unknown PCI device, and allocate the necessary resources to it.

After entering the program, the menu in Fig. 3.7:

Window.

New - opens a new window for the spectrum image for the next by the number of the input. A new window is also opened by double-clicking on the "Window of the main menu.

Cascade - installs several open windows one by one in the program field.

Arrange icons - organizes icons and windows in the program field.

Close all - close all windows of the program.

Exit is the normal exit from the program, all spectrum parameters of the spectrum are saved in a file with the extension .cfg.

File - working with files:

Read spectrum - opens a file from the proposed list with a ".txt" extension of the text format.

"Hot" keys - Ctrl + O.

Save spectrum - saves the current spectrum to a text file (with the extension ".txt") file. Hotkey F2.

Time Ctrl + T - set the exposure time of the spectrum set in a strictly defined format:

Ddd-day (24 hours);

Hh: mm: ss, where:

hh- hours;

mm- minutes;

ss - seconds.

Start - the beginning of the spectrum set, while the time counter is reset and started.

"Hot" keys - Ctrl + S.

Stop - stop dialing the spectrum.

"Hot" keys - Ctrl + E.

Clear - zeroing the array of dialed data.

"Hot" keys - Ctrl + Del.

Spectrum image window:

The "Integral" board - at the top in the center of the spectrum image window shows the number of dialed pulses between the markers.

Scoreboard "Set" - in the upper left corner of the spectrum image window displays the time of dialing the spectrum from start to stop or until the current moment, there is also a dial indicator.

The "Marker" tab - in the upper right corner of the spectrum image window displays the marker coordinates and the number of dialed pulses in the time channels corresponding to the markers.

The button "Points / Histogram" - in the lower left corner allows you to switch the mode of the spectrum image from points to the histogram and vice versa.

Actions that can be performed in the spectrum image window:

1. Fixing the left (right) calibration peak selected by markers - double-clicking the left (right) mouse button on the chart field between the markers.

2. Changing the coordinates of the marker:

Method 1. Move the cursor to the desired marker, press the left mouse button and, while holding it, "drag" the marker to the desired value.

Note: The invisible 1st (2nd) marker should be searched on the left (right) border of the spectrum image field.

Method 2. Clicking the left (right) mouse button on the "marker" field decreases (increases) the marker's coordinates by one.

Method 3. With the help of hot keys of the keyboard Ctrl + End the 1st marker is shifted to 1 channel to the right, Ctrl + Home-to the left; Ctrl + PgUp- 1/8 part of the visible range of the spectrum to the right, Ctrl + PgDn- to the left. For the 2nd marker is similar, but instead of Ctrl press Alt.

3. The scale of the spectrum image can be changed by clicking the left key (but not far away) from the vertical axis, while the scale increases if you click above the assumed center of the vertical axis, and decreases if you click below the middle of the vertical axis.

"Hot" buttons: Shift + PgUp and Shift + PgDn, respectively.

4. The horizontal scale can be changed by clicking the left mouse button under the horizontal axis. The scale increases if you click to the right of the intended center of the axis and decreases if you click to the left.
"Hot" buttons: PgUp and PgDn respectively.

5. Shift the spectrum image window by clicking the right mouse button under the horizontal axis. Shift to the right - if you click to the right of the intended center of the axis. Shift left - if you click to the left of the intended center of the axis.
"Hot" buttons: End and Home, respectively.

6. Spectra can be represented by dots or histograms. Switching Click the left mouse button on the button in the lower left corner.
"Hot" button: Enter.

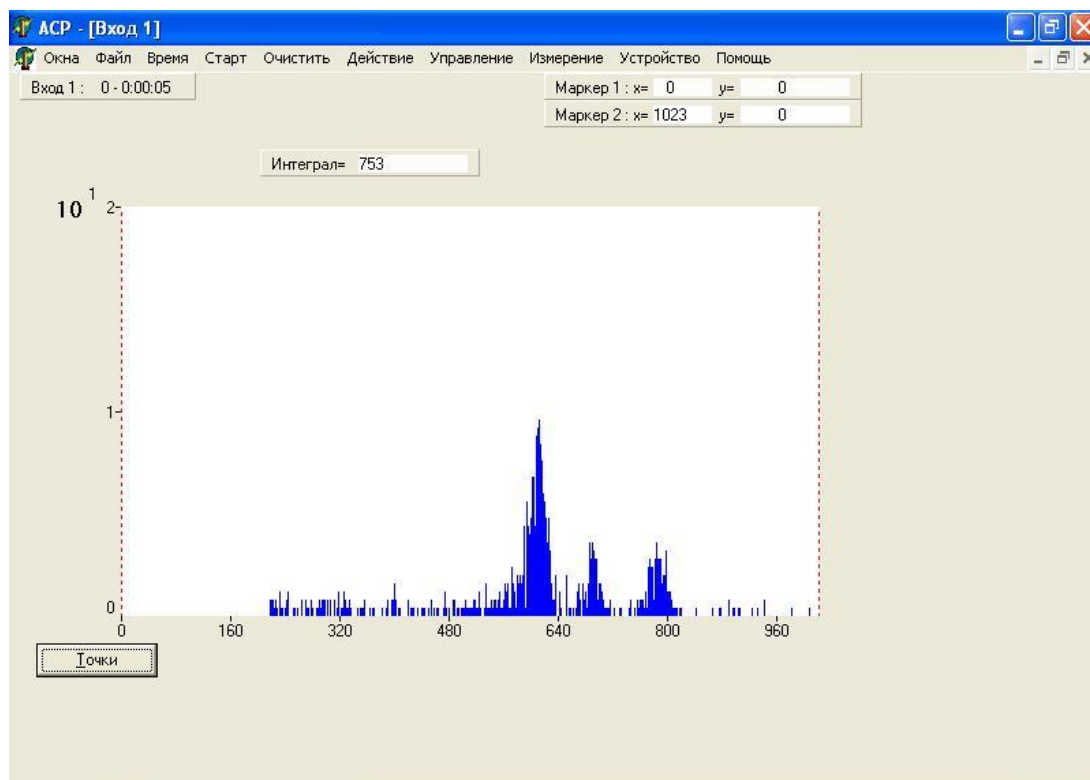7. Disable the help window by pressing the "hot" button-Ins or from the "Help" option of the main menu

Figure 3.7 The working window of ACP-control v1.1

3.7 Description of all constructions of storage electrostatic chambers

In Fig. 3.8 are diagrams of the storage electrostatic chambers used in the experiment. For each design, a brief description of the physical principles of the action of electrostatic precipitation is given.

The design of the accumulating electrostatic chamber No. 1 (Figure 3.8a) is characterized by the accelerating focusing potential of collecting PPR ions of radon on the surface of the detector. Here, there is no provision for equalizing the radionuclide concentration by volume.

The construction of the storage electrostatic chamber No. 2 (Figure 3.8b) is hemispherical with the detector placed on the generator body and with the limitation of the effective collecting volume limited by the grid 3 positively charged with respect to the detector, but with a potential much smaller than the focusing one.
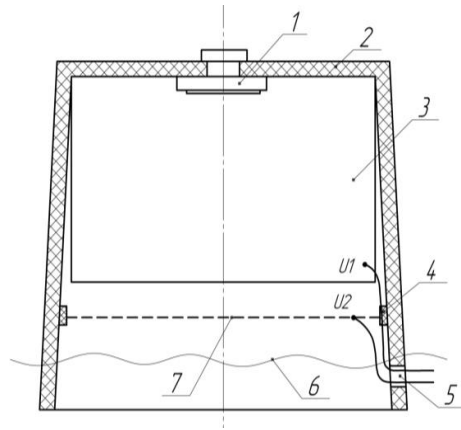
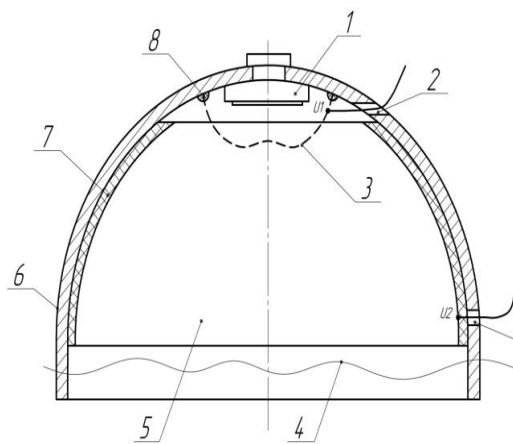Figure 3.8a Scheme of electrostatic storage chamber No.1

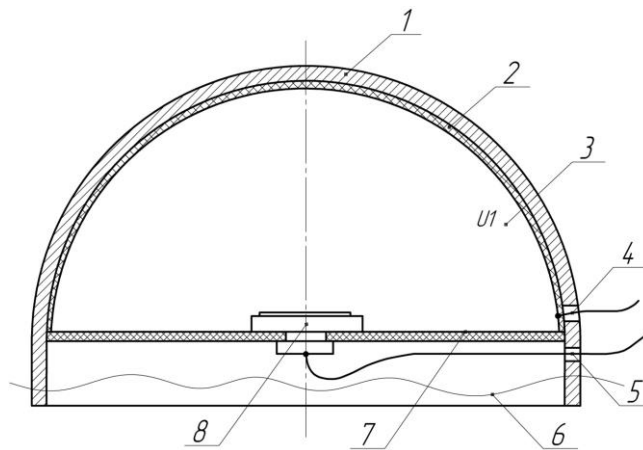Figure 3.8b Scheme of electrostatic storage chamber No.2

Figure 3.8c Diagram of electrostatic storage chamber No. 3

3.8 Description of the construction of the electrostatic storage chamber No.1

A schematic diagram of the construction of the accumulation chamber No.1 is shown in Fig. 3.8a This design is intended for the electrostatic precipitation of positively charged radionuclides formed in the air inside the storage chamber (ND) on a semiconductor detector (1).
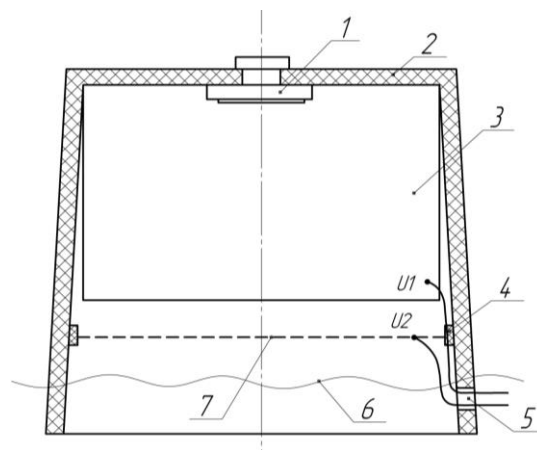

Figure 3.8a Diagram of electrostatic storage chamber No. 1

1 - PDD (semiconductor detector), 2 - housing made of plastic, 3 - metal cylinder with a potential U1 directed to it, 4 - rubber seal, 5 - output from the housing of the structure for high voltage wires, 6 - a line of a surface ground, 7 - a metal fine grid on which the potential U2 moves.

Radioactive gases emitted from the ground inside the storage chamber pass through the aluminum mesh (7). Inside the chamber, there is a decay of radioactive gases such as radon or thoron and the accumulation of products of their decay, most of which when formed are ions. The applied voltage U1 and U2 to the metal cylinder (3) and the metal grid (7) is constant, stabilized and positive.

Positively ionized decay products of radioactive gases in the active zone of the storage chamber are attracted to the PPD window and recorded. Since the PPD is completely grounded and negative bias voltage is applied to it, it is negatively charged with respect to the active zone of the ND. As a result, an electric field arises between the active zone (grid and cylinder) under the positive voltage and the PPD under the negative voltage, the lines of force of which direct the positively ionized decay products to the detection window of the PPD.

Since the grid has a positive potential, only neutral particles pass through it, such as radon and thoron atoms. Positively charged decay products formed in the space between the grid and the ground cannot pass through the grid.

Therefore, to increase statistics, the grid is located as close as possible to the surface of the soil. The volume of this design is 1.8 liters.

3.9 Description of the construction of the electrostatic storage chamber No. 2

A schematic diagram of the construction of the storage chamber is shown in Figure 3.8b This design is intended for electrostatic deposition on a semiconductor detector (1).
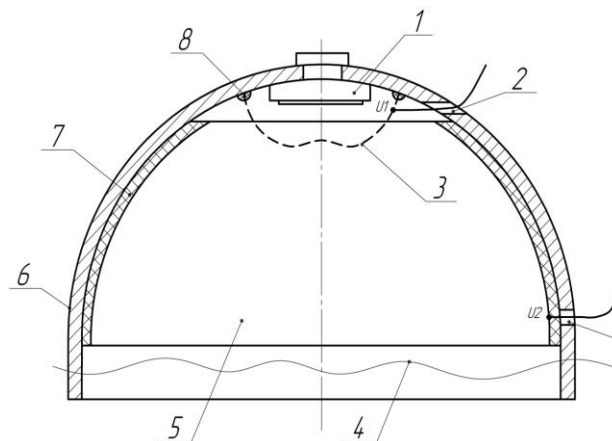

Figure 3.8b Scheme of electrostatic storage chamber 2

1 - PDD (semiconductor detector), 2 - pins from the housing for high voltage wires, 3 - fine metal grid with a potential U1 directed to it, 4 - ground surface line, 5 - metal hemisphere to which the potential U2 is applied, 6 - housing made of liquid plastic two-component, cold curing, 7.8 - rubber seals to better fit the metal parts of the structure to the body.

The principle of operation of this design is similar to design No. 1, however, the volume has been significantly reduced from 1.8 to 1 liter.

The active zone of the storage chamber is a metal truncated hemisphere (5) and a metal grid (3). A high constant positive stabilized voltage U2 and U1, respectively, is fed to the metal truncated hemisphere (5) and the metal mesh (3).

Positively ionized decay products of radioactive gases in the active zone of the storage chamber are attracted to the PPD window and recorded. Since the PPD is completely grounded and negative bias voltage is applied to it, it is negatively charged with respect to the active zone of the ND. As a result, an electric field arises between the active zone (grid (3) and hemisphere (5)) under positive voltage and PPD under negative voltage, the lines of force of which direct the positively ionized decay products to the detection window of the PPD.

3.10 Description of the construction of the electrostatic storage chamber No. 3

A schematic diagram of the construction of the storage chamber is shown in Figure 3.8c When leaving the earth's surface, the radioactive gases get inside the storage chamber.
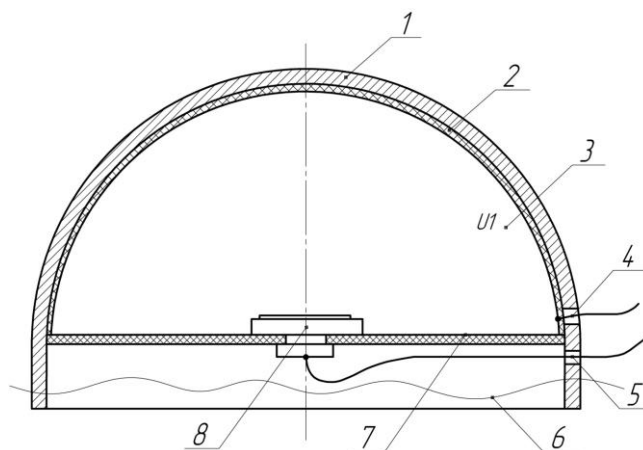
Figure 3.8c Diagram of electrostatic storage chamber No. 3

1 - body made of high-strength carbon fiber reinforced plastic, 2 - rubber seals for better fit of the metal parts of the structure to the housing, 3 - metal hemisphere for which the potential U1 is applied, 4 - lead from the housing for high voltage wires, 5 - signal with PPD, 6 - ground surface line, 7 - rod holder of PPD, 8 - PDD (semiconductor detector).

The active zone of the storage chamber is the metal hemisphere (2). It receives a high constant positive stabilized voltage $U1 = + 3kV$.

Radioactive gases emitted from the ground inside the storage chamber immediately

enter the active zone. Where there is a decay of radioactive gases such as radon or thoron and the accumulation of products of their decay, most of which when formed are positive ions.

Positively ionized decay products of radioactive gases in the active zone of the storage chamber are attracted to the PPD window and recorded. Since the PAP is completely grounded and negative bias voltage is applied to it, it is negatively charged with respect to the active zone of the ND. As a result, an electric field arises between the active zone and the PPD, the lines of force of which direct the positively ionized decay products to the detection window of the PPD.

3.11 Measurement of the Energy Spectrum of Alpha - Radiation with Different Constructions of Accumulating Electrostatic Chambers

Preliminary developed three variants of storage chambers (ND) of various geometry, design of electrodes and methods of supplying voltage. The chapter describes the results of measurements of the density of radon and thoron fluxes from the soil surface produced with three ND designs. The soil for the study was chosen in 2 types: sand with low radium and thorium content, and loamy soil, called further, earth, with a high content of radium and thorium. As a result, according to the measurement results, the best ND variants were selected, which make it possible to obtain an alpha spectrum with a good energy resolution, and also increasing the statics due to the application of the electrodeposition of the PPD by a factor of 2 compared to a simple chamber without electrodeposition.

3.12 Calibration of a semiconductor detector

The spectrometer was calibrated using the Ra^{226} alpha radiation source, the characteristics of which are described in Table 4.1. The spectrum of Ra^{226} is shown in Figures 4.1 and 4.2. The calibration curve is shown in Figure 4.3. When processing the spectrum data (descriptions of the peak of the spectrum by the linear dependence (Table 4.2) of the alpha-radiation energy E on the channel number K, we obtain the gauge equation:

$$E \text{ (KeV)} = 9{,}193*K + 1479{,}4$$

Table 4.1 Technical characteristics of the source Ra^{226}

Isotope	Period half-life, years	Energy α-transition, keV	Radionu clides	Exit, % on disintegr ation	External radiation, p / s	Own half-width line source, keV
Ra^{226} +products disintegrat ion	1617	4599 4782 5490 6002 7687	Ra^{226} Ra^{226} Rn^{222} Po^{218} Po^{214}	5,55 94,45 100 100 100	$1{,}9 \cdot 10^4$	≤20

Table 4.2. The channel table is the energy used for the calibration.

Range of channels under consideration	Maximum value pulses in a given range of channels	The channel number corresponding to the maximum value pulses	Energy, keV	Radionuclide
300 to 380	1328	361	4784,4	Ra^{226}
380 to 460	1845	430	5489,5	Rn^{222}
460 to 550	1660	498	6002,4	Po^{218}
550 to 750	2133	674	7686,9	Po^{214}
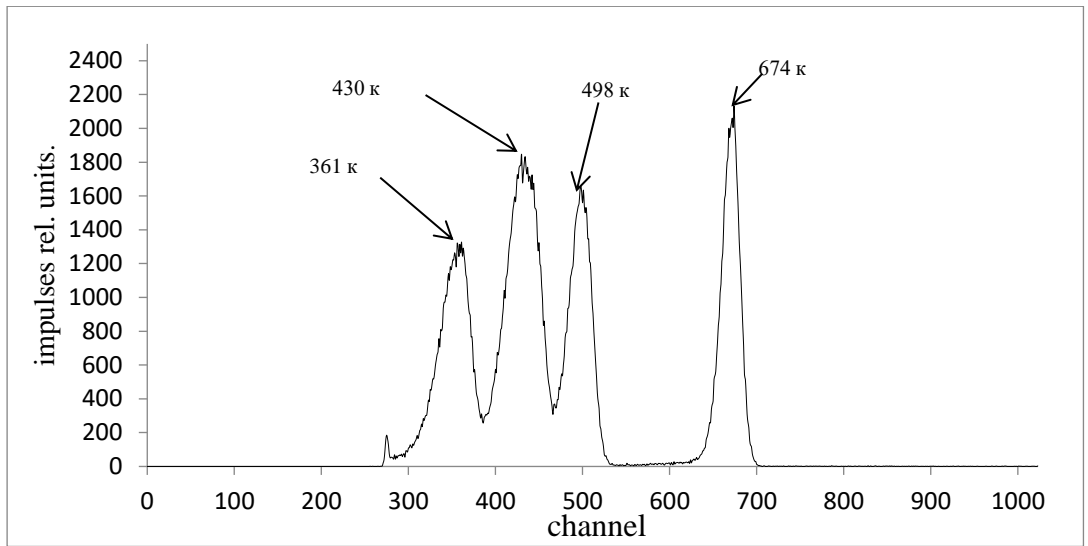
Figure 3.9 Calibration spectrum: Pulses - Channels.
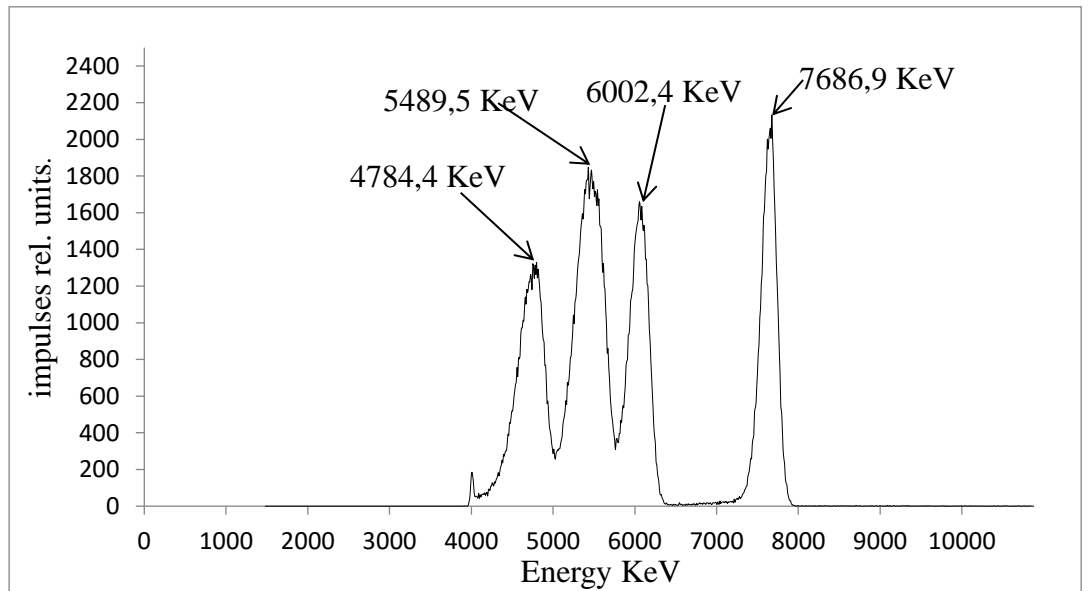
Figure 3.10 Calibration spectrum: Pulses - Energy.

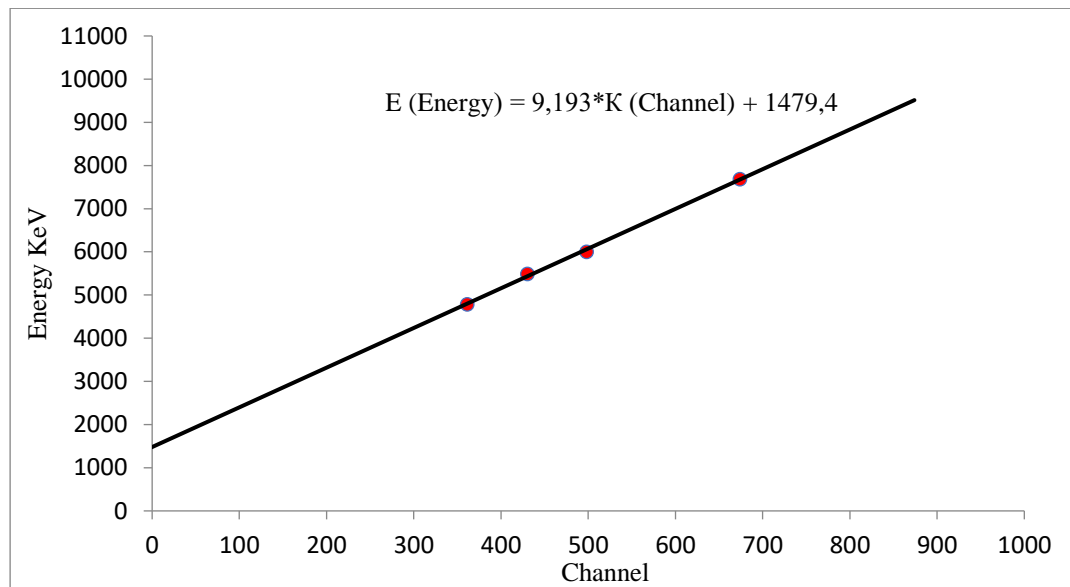$$E \text{ (Energy)} = 9{,}193*K \text{ (Channel)} + 1479{,}4$$

Figure 3.11 Calibration curve: Energy - Channel.

3.13 The results of measurements with a storage electrostatic chamber No. 1

A series of measurements of PPR and PPT was carried out with the help of ND, installed by an open base on the surface of sand and earth, filled up in a cylindrical container. The voltage applied to the active zone of the storage chamber, when measured, is U1 = U2 = + 2 kV. A voltage-free measurement was made to evaluate the effect of the applied voltage on the electrodes of the chamber. Each measurement was carried out for two hours.

Figures 4.4-4.6 show the spectra obtained during the measurement. The spectral distribution obtained in the absence of voltage is shown in Figure 3.12 The spectrum obtained when a voltage of +2 kV is applied to the active part of the storage chamber (grid and cylinder) is shown in Figure 3.13 and Figure 3.14 combines the spectral distributions obtained in the absence of voltage and applied voltage + 2 kV to visually evaluate the increased counting rate and increase the statistics in the spectral maxima for the same time interval. The temporal dynamics of the counting rate of pulses from the surface of sand, both from the surface of sand and from the surface of sand, both in the presence of voltage and its absence at the electrodes of the ND, is shown in Figure 3.15 in different colors.

Each of the figures shows the sum of the pulses registered in all channels during the entire time of the experiment $\sum_i(N_i) \frac{pulses}{2 \text{ hours}}$.
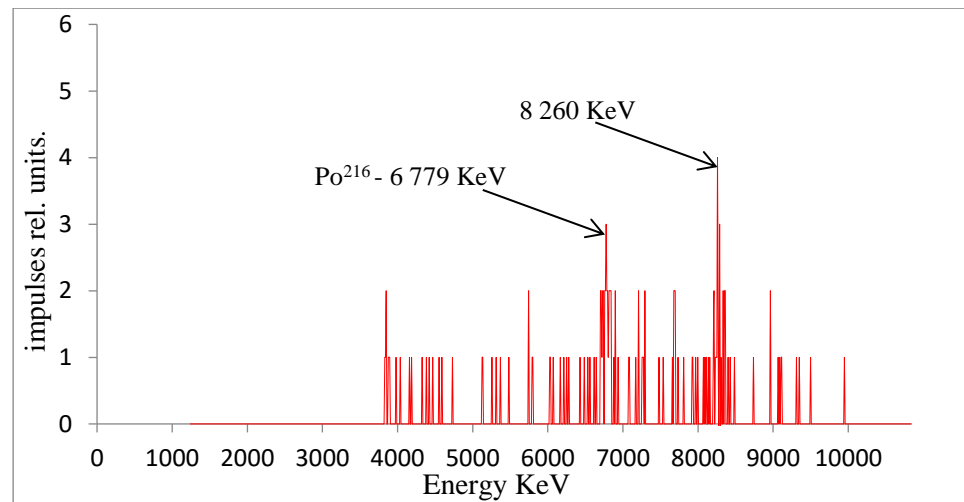
Figure 3.12 The spectrum of sand, taken in the absence of voltage

When analyzing the spectral distributions obtained with the help of accumulating electrostatic chambers of different design, the peaks of the decay products of radon and thoron are of the greatest interest. The spectrum of sand Figure 3.12 shot in the absence of voltage on the electrodes NK has two peaks with energies of 6,779 and 8260 keV. The maximum, with an energy of 6,779 keV, corresponds to Po^{216}, the area below it is equal to 12 pulses, the peak amplitude is 3 pulses.

In Figure 3.13 The spectrum of sand taken at a voltage on electrodes NK + 2kV is shown, which, like the previous spectrum in Figure 3.14, has several weakly expressed maxima with energies: 4421 keV, 6,779 keV, 7687 keV, 8222 keV. The maxima with an energy of 6,779 keV and 7687 keV belong to Po^{216} and Po^{214}, respectively. The area under the highs: Po^{216} - 27 imp. at an amplitude of 4 pulses, Po^{214} - 21 pulses. at an amplitude of 4 pulses.
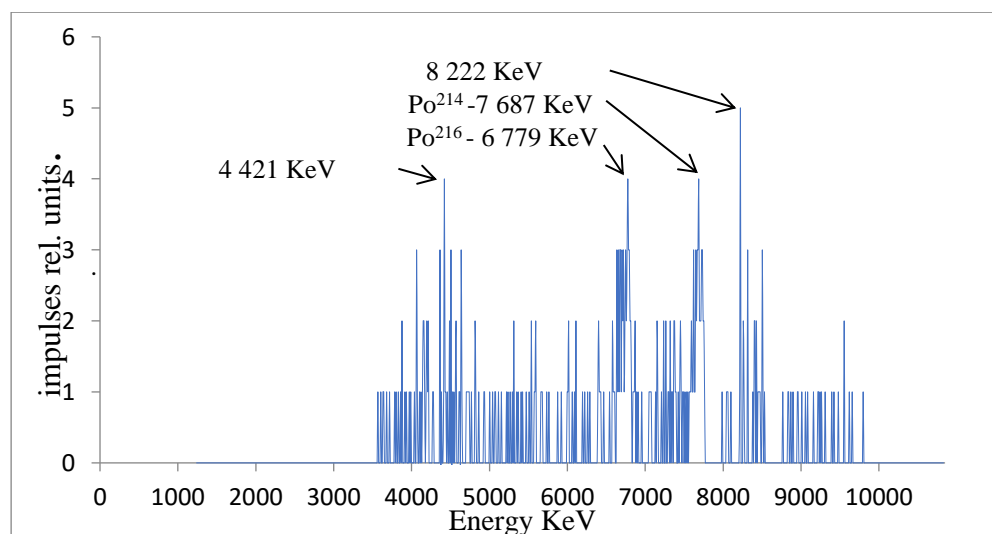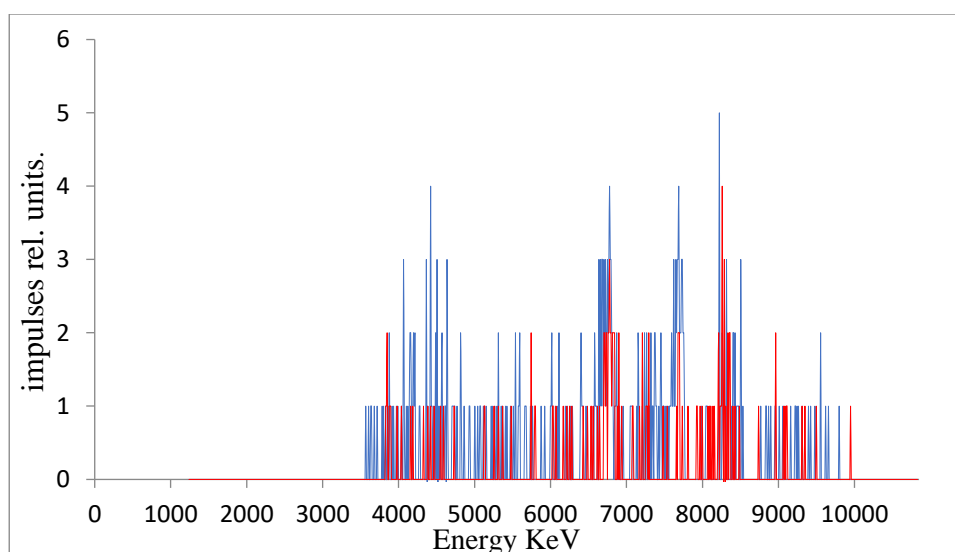

Figure 3.14 Combining the two previous spectra of sand: in the absence of voltage - red, the presence of voltage – blue

An increase in the number of recorded pulses in Figure 3.14 and the counting rate in Figure 3.14 when voltage is applied to the active zone of the ND. When the voltage was applied, 295 were registered, and in the absence of 118 pulses. As a result, due to electrostatic precipitation, the statistics was increased by 2.5, which confirms the efficiency of this design of the electrostatic storage chamber.

When the voltage was applied to the active zone of the ND, the very shape of the spectrum also changed (Figure 3.14), the spectrum became clearer. The Po^{216} and Po^{214} peaks are well identified. Also, several new spectral distribution maxima appeared in the intervals from 3800 to 4900 keV and 7000 to 8000 keV.
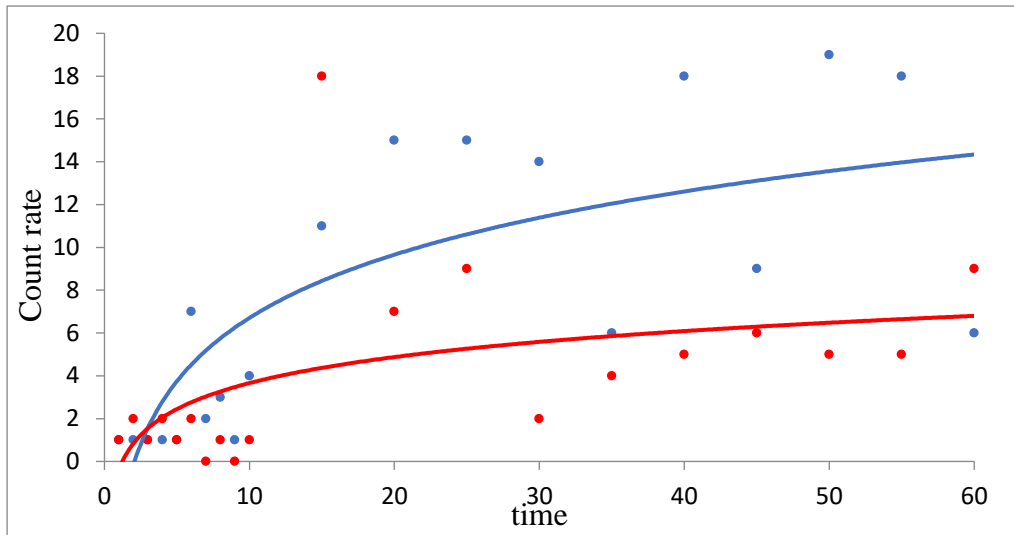
Figure 3.15 Dependence of the growth of counting rate on time when measuring sand: in the absence of voltage - red, the presence of voltage - blue.

Figures 3.16 - 3.18 show the spectral distributions obtained during measurements with ground. The dynamics of the change in the counting rate as a function of time when measuring the earth, both in the presence of voltage and its absence on the electrodes of the ND, is shown in Figure 3.19.

The spectral distribution obtained in the absence of voltage is shown in Figure 3.16. When a voltage of + 2 kV is applied, the spectrum is shown in Figure 3.17 Figure 3.18 combines the spectral distributions obtained both in the absence of voltage and in its presence.
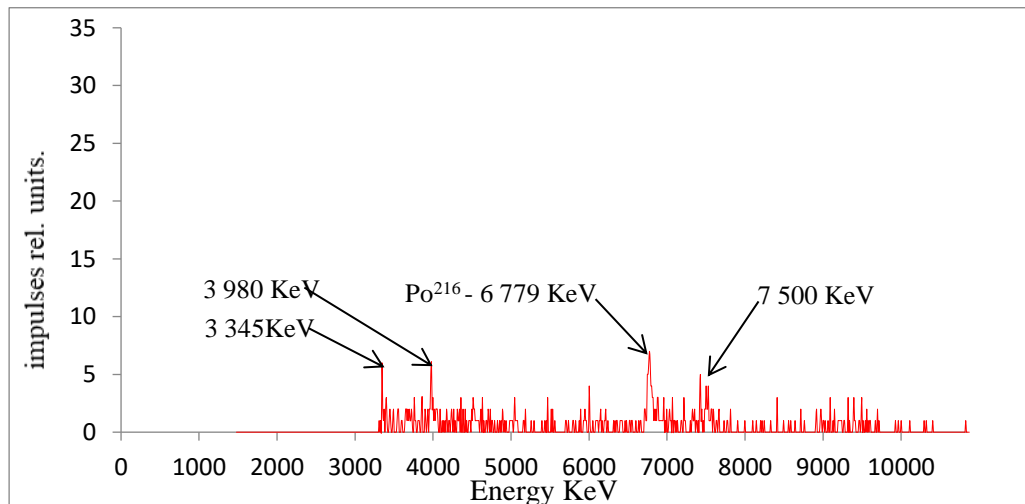
Figure 3.16 The spectrum of the earth taken in the absence of voltage.

The spectrum of the earth (Figure 3.16), obtained in the absence of voltage on the NK electrodes, has several weakly expressed maxima with energies: 3345 keV, 3980 keV, 6779 keV, 7500 keV. The maximum having an energy of 6,779 keV belongs to Po216, respectively. The area under the Pe^{216} peak is 46 pulses. at an amplitude of 6 pulses.
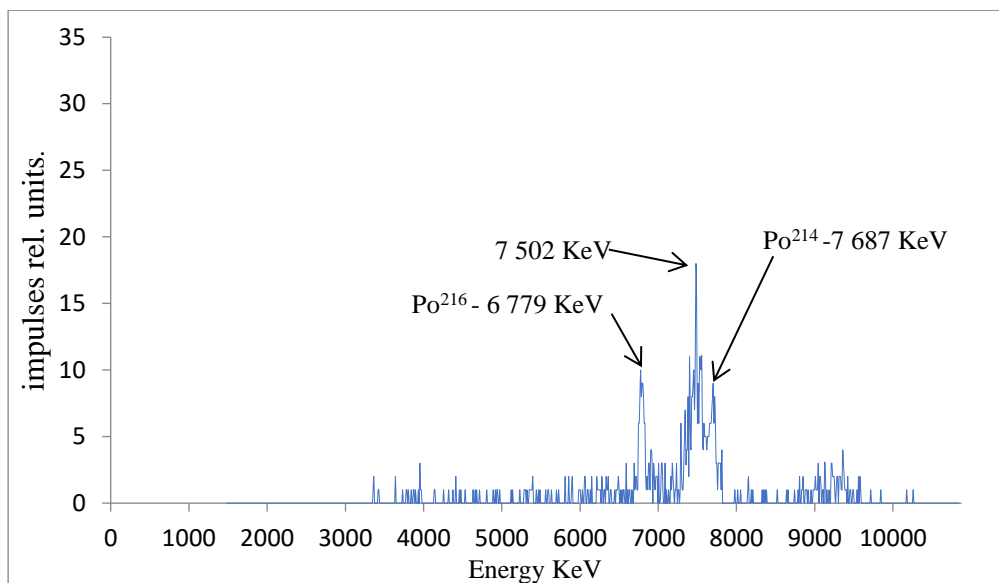
Figure 3.17 The spectrum of the earth taken at a voltage equal to U1 = U2 = + 2kV.

Several maxima with energies: 6779 keV, 7502 keV, 7687 keV are located on the spectral distribution of the earth (Fig. 4.9), obtained with a voltage on the electrodes NK + 2kV. The maxima with energies of 6779 keV, 7687 keV belong to Po^{216} and Po^{214}, respectively. The area under the peaks of the identified radionuclides for Po^{216} was 97 impulses, Po^{214}- 89 imp. Amplitudes of the maxima: Po^{216} - 10 imp. , Po^{214} - 18 imp.
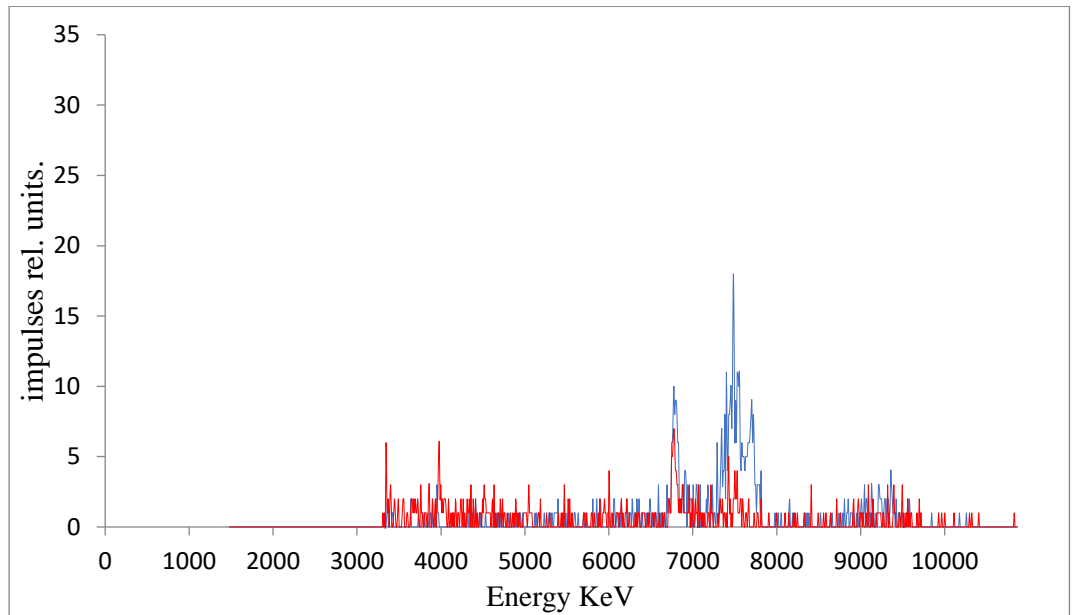
Figure 3.18 The combination of two ground spectra in the absence of voltage is red, the presence of voltage is blue.

The number of recorded pulses in Figure 3.18 and the counting rate in Figure 3.19 when applying voltage to the active zone of the ND. In the absence of voltage, 332 are recorded, and in the presence of 598 pulses. 1.8 times more pulses are recorded when the voltage is applied to the active zone of the ND.

As in the measurement of sand, the shape of the spectrum in Fig. 3.18, when the voltage was applied, the existing radionuclide maxima increased the statistics and thereby defined themselves even more clearly, and new ones also appeared.

Figure 3.19 combines two graphs in one coordinate plane showing the change in counting rate when the voltage is applied to the active zone of the ND and without it.
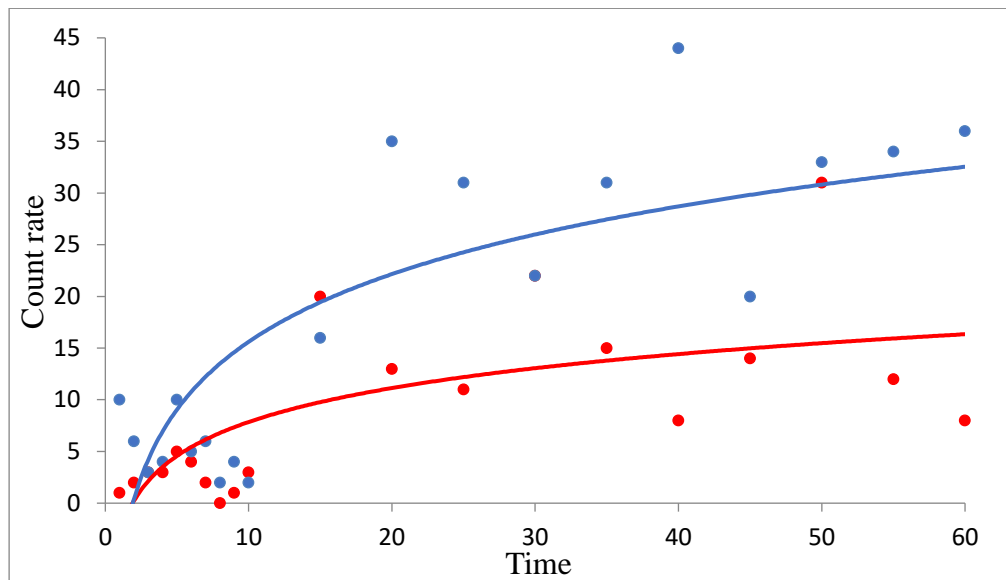
Figure 3.19 Dependence of the increase in counting rate on time when measuring ground in the absence of voltage - red, the presence of voltage - blue.

When measuring sand, the number of pulses recorded in the spectrum during the entire measurement period with applied voltage on the active zone of the ND increased by 2.5 times, and when the earth was measured 1.8 times. On average, the number of recorded pulses increases almost two-fold ($\approx$2 times). As in the measurement of sand and earth, the shape of the spectrum changed when the voltage was applied to the active zone of the ND.

3.14 The results of measurements with a storage electrostatic chamber No. 2

Two measurements were made with the voltage on the active zone of the ND: the voltage for these measurements was changed as follows: 1st measurement U1 = + 3kV, U2 = 0kV Fig. 4.26; The 2nd measurement is U1,2 = + 3kV Fig. 4.27. A measurement was also made in the absence of voltage Fig. 4.25 for the evaluation of the effect of the applied potential on the electrodes of the chamber on the final result (the number of recorded pulses and the shape of the spectrum). Each of these measurements was carried out for two hours.

$$\sum_i N_i = 112 \frac{\text{pulses}}{2 \text{ hours}}$$

Po^{216} - 6 779 KeV
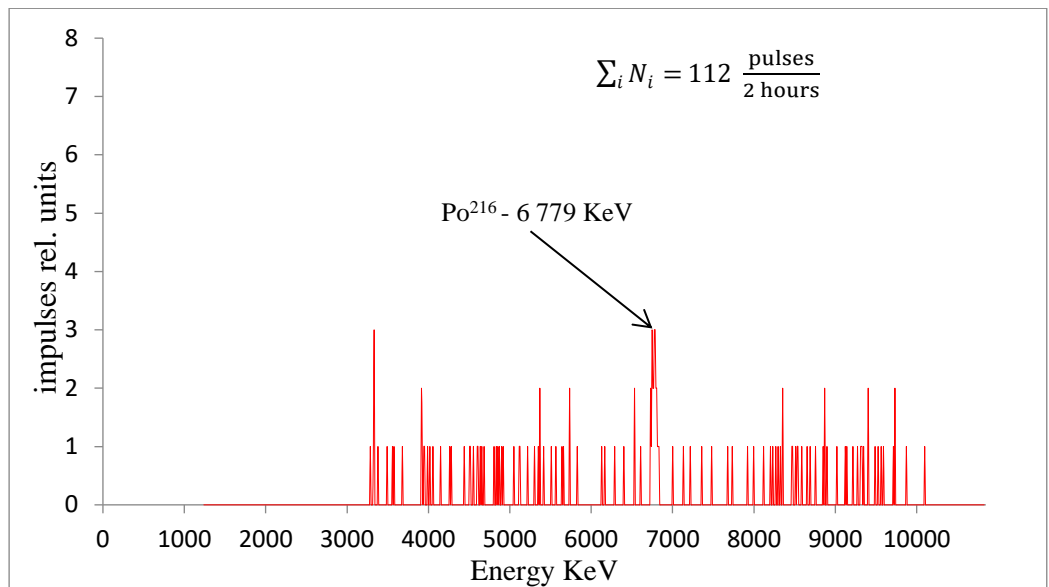
Figure 3.20 Spectrum of sand, taken in the absence of tension.

On the spectrum of sand removed without voltage Figure 3.20 we distinguish the maximum with energies: 6779 keV. The area under this maximum is 23 op. at an amplitude of 3 pulses, and it corresponds to the radionuclide Po216. The remaining maxima have too little statistics for identification.

Po^{214} - 7 687 KeV
Po^{216} - 6 779 KeV
8 194 кэВ
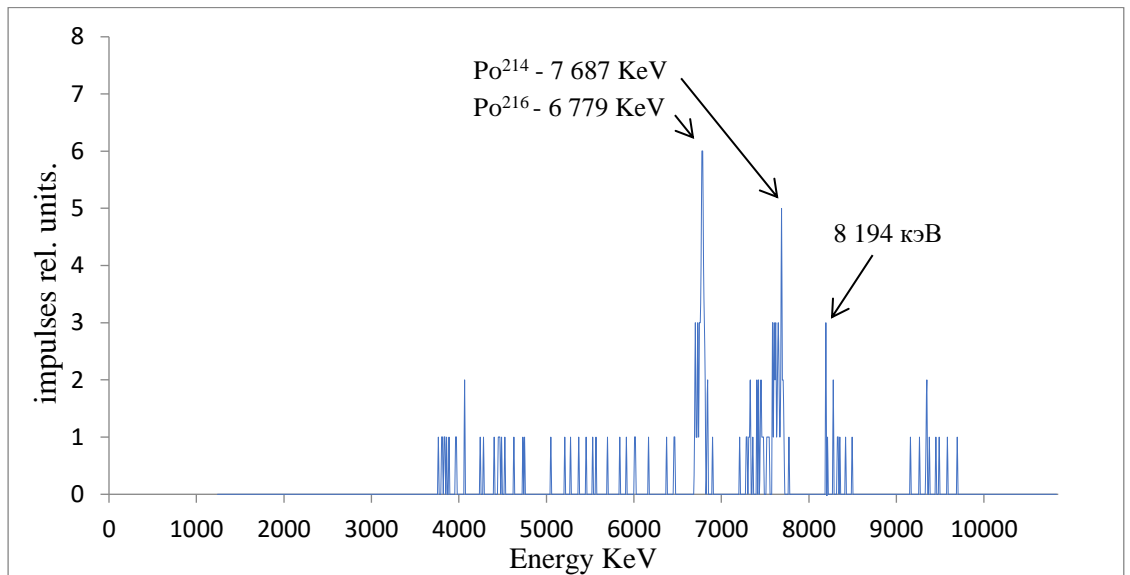
Figure 3.21 The spectrum of sand, taken at a voltage equal to U1 = + 3kV, U2 = 0V.

Figure 3.21 shows a spectrum of sand, taken with a voltage U1 = + 3kV, U2 = 0kV on the electrodes of the ND. Three maxima with energies of 6779 keV, 7687 keV,

and 8194 keV are distinguishable on this spectrum. The maxima with energies: 6779 keV, 7 687 keV correspond to Po^{216} and Po^{214}, respectively. Area under the highs: Po^{216} - 22 imp. At an amplitude of 6 pulses, Po^{214} - 16 pulses. at an amplitude of 5 pulses.
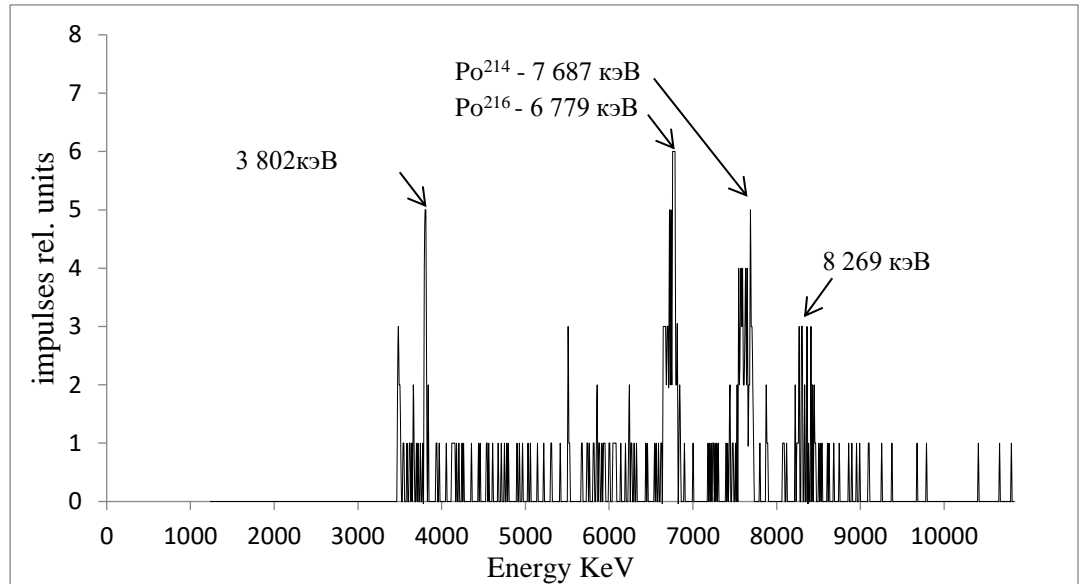
Figure 3.22 Spectrum of sand, taken at a voltage equal to U1,2 = + 3kV.

On the spectrum of sand removed with a voltage U1,2 = + 3kV Fig. 4.27 four maxima with energies of 3802 keV, 6779 keV, 7584 keV, and 8269 keV are distinguishable on the ND electrodes. The maxima with energies: 6779 keV, 7 687 keV correspond to Po^{216} and Po^{214}, respectively. The area under the maxima of Po^{216}, Po^{214} is 29 pulses. at an amplitude of 6 pulses and 17 pulses. at an amplitude of 5 pulses. Figure 3.23 combines the spectral distributions obtained in the absence of voltage and applied voltage equal to U1,2 = + 3kV for estimating the increase in accumulated statistics for the same time interval.
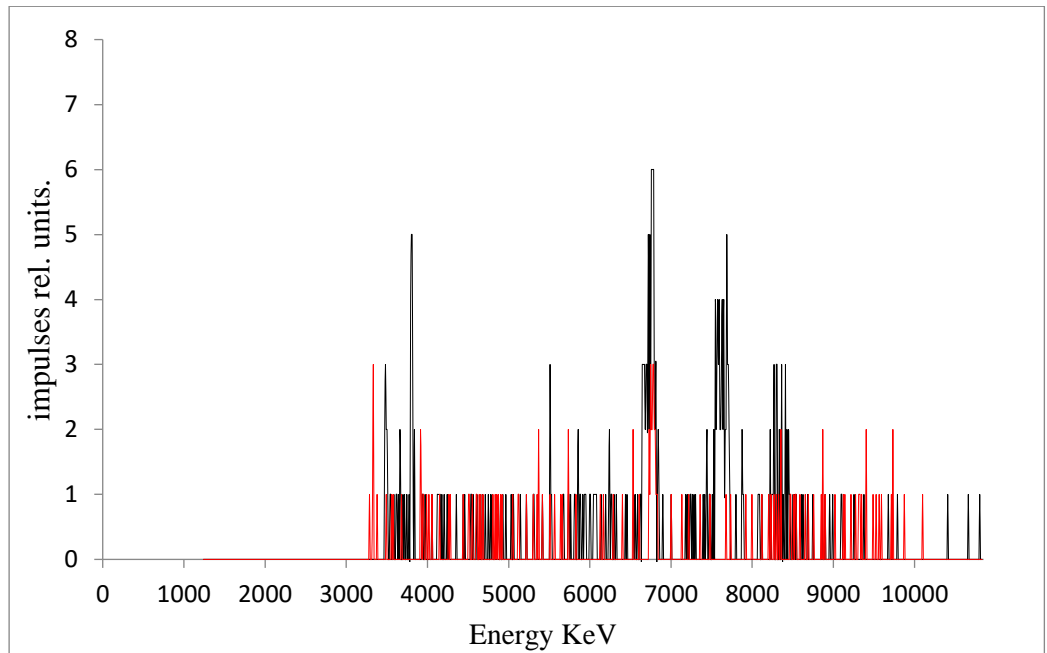
Figure 3.23 The combination of two spectra of sand: at a voltage equal to
U1,2 = + 3kV and equal to zero.

Figure 3.24 is similar to Figure 3.23. It combines the spectral distributions
obtained in the absence of voltage and applied voltage equal to U1 = 0kV, U2 = + 3kV.
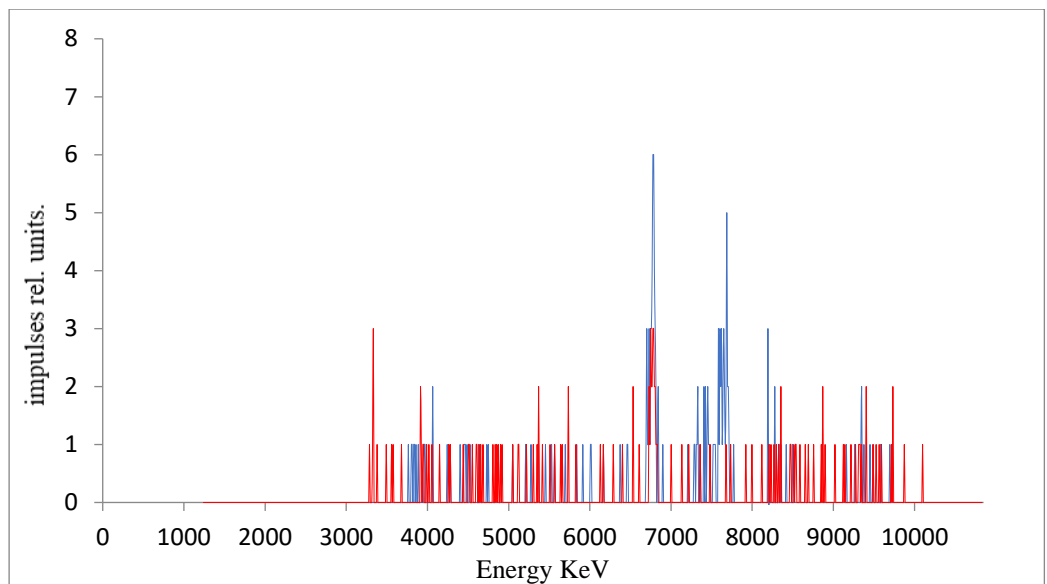
Figure 3.24 The combination of two spectra of sand: with a voltage equal to
U1 = + 3kV, U2 = 0V and equal to zero.

Applying the voltage U1 = + 3kV, U2 = 0V, the number of all registered PDU
pulses does not increase. Without voltage, only 112 pulses were registered, and with

voltage even less than 104. However, the shape of the spectrum itself has changed. The peaks of the decay products of radioactive gases and other radionuclides have become more isolated at the background level, that is, the number of recorded pulses directly at the maximum of radionuclides has increased. Such a maximum, for example, is Po^{216} with an energy of 6,779 keV.

Also, several new peaks appeared, such as Po^{214} on the spectral distribution of which, without applying voltage to the ND electrodes, was not observed. When the voltage is applied, the counting speed differs slightly from Fig. 3.25 from the same characteristic only of the voltage obtained without application. In the interval from 10 to 30 minutes there is an abrupt increase in counting speed, after which it goes to saturation. The counting rate obtained without application of the voltage begins to increase just at the moment when the count rate obtained by the voltage starts to go out to saturation.

By feeding the voltage $U1,2 = + 3$ kV to the active zone of the ND, an increase in the number of recorded pulses occurs when measuring sand. Fig. 4.28 and the counting rate in Fig. 3.23. 2.3 times more pulses are recorded when the voltage is applied according to the scheme $U1,2 = + 3$ kV. This, as well as the fact that the shape of the spectrum itself in Fig. 3.22: the peaks of the decay products of radioactive gases and other radionuclides have become more distinguished at the background level, indicating the effectiveness of this design of the electrostatic storage chamber. When the voltage is applied, 251 are registered, and in the absence of 112 pulses. In this case there was an increase in the counting rate in Fig. 3.26.

Figure 3.25 Dependence of counting speed increase on time when measuring sand: in the absence of voltage - red, presence of voltage U1 = + 3kV, U2 = 0 kV - blue.

Figure 3.26 Dependence of the increase in counting rate on time when measuring sand: in the absence of voltage - red, the presence of voltage U1,2 = + 3kV - black.

Also, three similar measurements were made with the earth. The spectra obtained in the absence of voltage are shown in Figure 3.27 at a voltage U1 = + 3 kV, U2 = 0kV Figure 4.33, and for voltage U1.2 = + 3kV Figure 4.34.
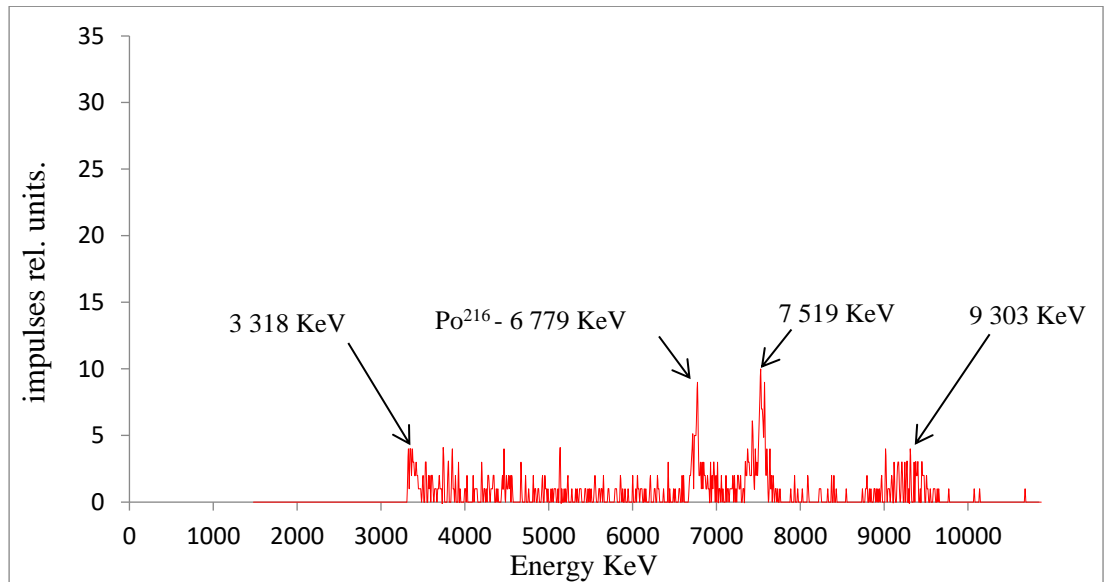
Figure 3.27 The spectrum of the earth, taken in the absence of tension.

On the spectrum of sand removed without tension Fig. 3.27 four maxima with energies of 3318 keV, 6779 keV, 7519 keV, 9303 keV are distinguishable on the ND electrodes. A maximum with an energy of 6779 keV, an amplitude of 7 pulses with an area below it 39 pulses. belongs to Po^{216}.
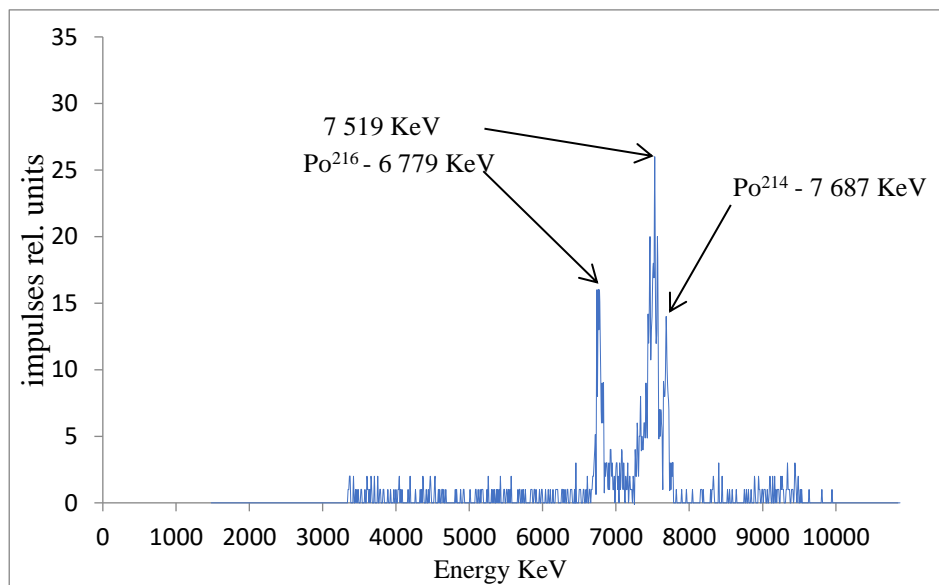
Figure 3.28 The spectrum of the earth, taken at a voltage equal to U1 = + 3kV, U2 = 0kV.

On the spectrum of sand removed at a voltage equal to U1 = + 3kV, U2 = 0kV Fig. 3.28 three maxima with energies of 6779 keV, 7519 keV, and 7687 keV are distinguishable on the ND electrodes. Po^{216} and Po^{214} belong to maxima with energies of 6779 keV, 7687 keV with an area below them 107 pulses. amplitude of 16 pulses and 61 impulses. amplitude of 14 pulses respectively.
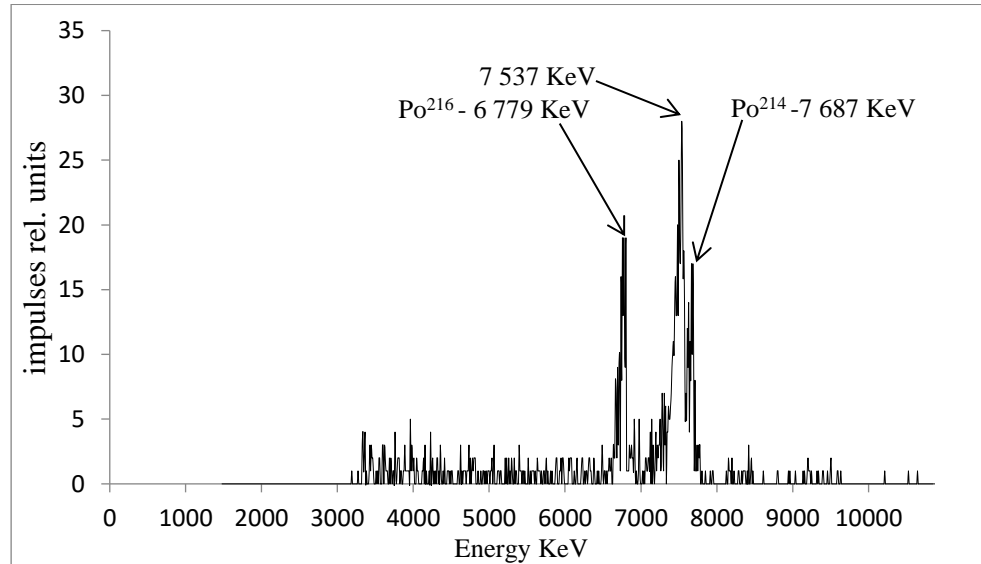
Figure 3.29 The spectrum of the earth, taken at a voltage equal to U1,2 = + 3kV.

On the spectrum of sand removed at a voltage equal to U1,2 = + 3kV Fig. 3.29 three maxima with energies of 6779 keV, 7537 keV, and 7687 keV are distinguishable on the ND electrodes. Po^{216} and Po^{214} belong to maxima with energies of 6779 keV and 7687 keV with an area of 121 imps below it. amplitude of 19 pulses and 76 impulses. amplitude of 17 pulses respectively.
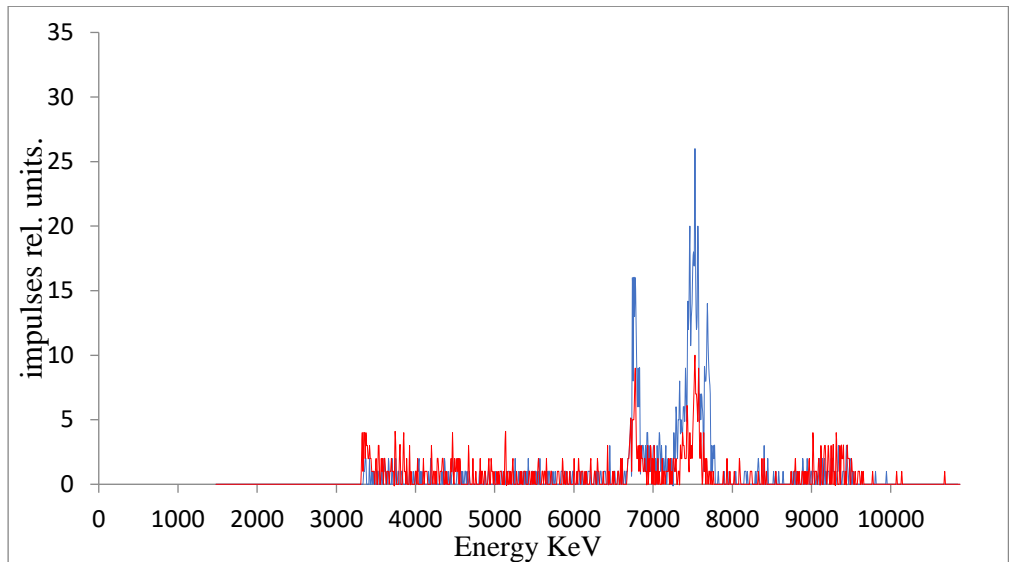
Figure 3.30 The combination of two ground spectra: with a voltage equal to U1 = + 2kV, U2 = 0V and equal to zero U1,2 = 0.

When the voltage U1 = + 3kV, U2 = 0kV is applied to the active zone of the ND, 780 pulses are recorded with ground, with no voltage of 559 pulses. With such a voltage feeding scheme, the number of pulses increased by a factor of 1.4. With voltage U1,2 = + 3kV, also measuring the ground recorded 1038 pulses. The number of pulses increased 1.8 times. Also, in both voltage options, the number of pulses recorded in the Po^{216} peak increased and the Po^{214} peak appeared.
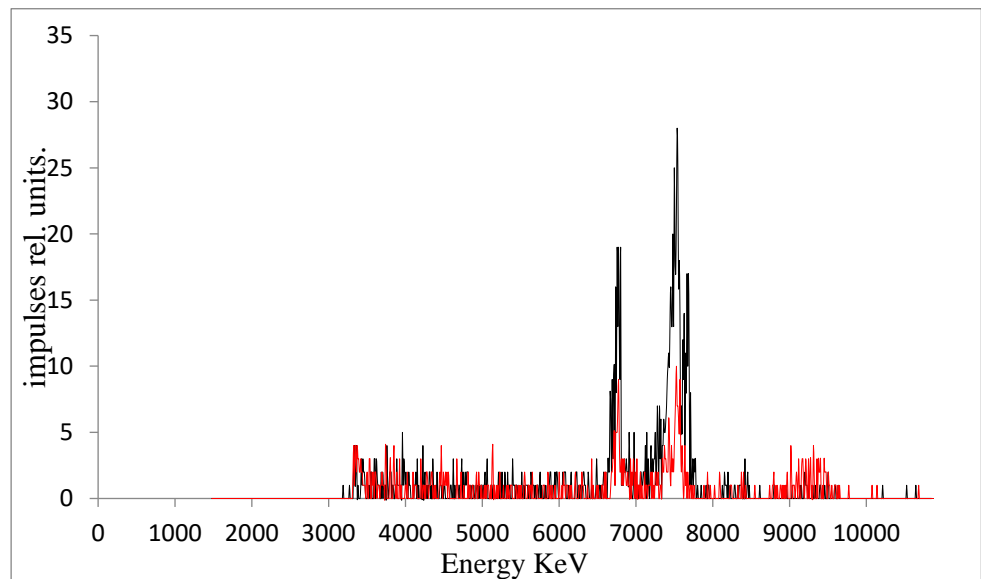
Figure 3.31 The combination of two ground spectra: with a voltage equal to U1,2 = + 3kV and equal to zero.

In each of Figures 3.32 and 3.33 two graphs are combined in one coordinate plane showing the change in counting rate when voltage is applied to the active zone of the PPD and without it.

Figure 3.32 combines the graph illustrating the change in counting rate without applied voltage and with the applied voltage U1 = + 3kV, U2 = 0kV. Figure 4.38 is similar to Figure 4.37 The only difference is that the applied voltage U1,2 = + 3kV.
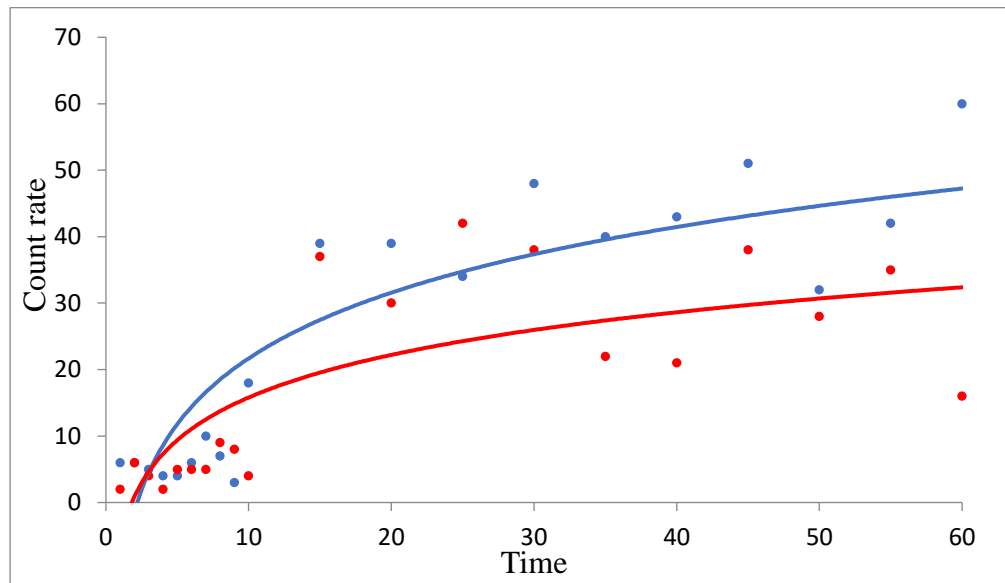
Figure 3.32 Dependence of the counting rate increase on time when measuring ground: in the absence of voltage - red, the presence of voltage U1 = + 3kV, U2 = 0 kV - blue.
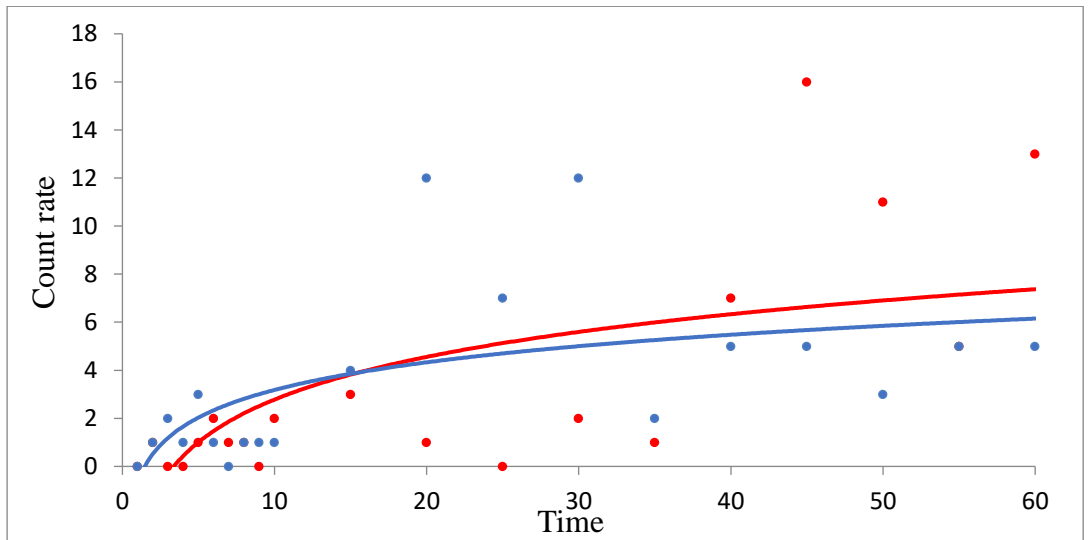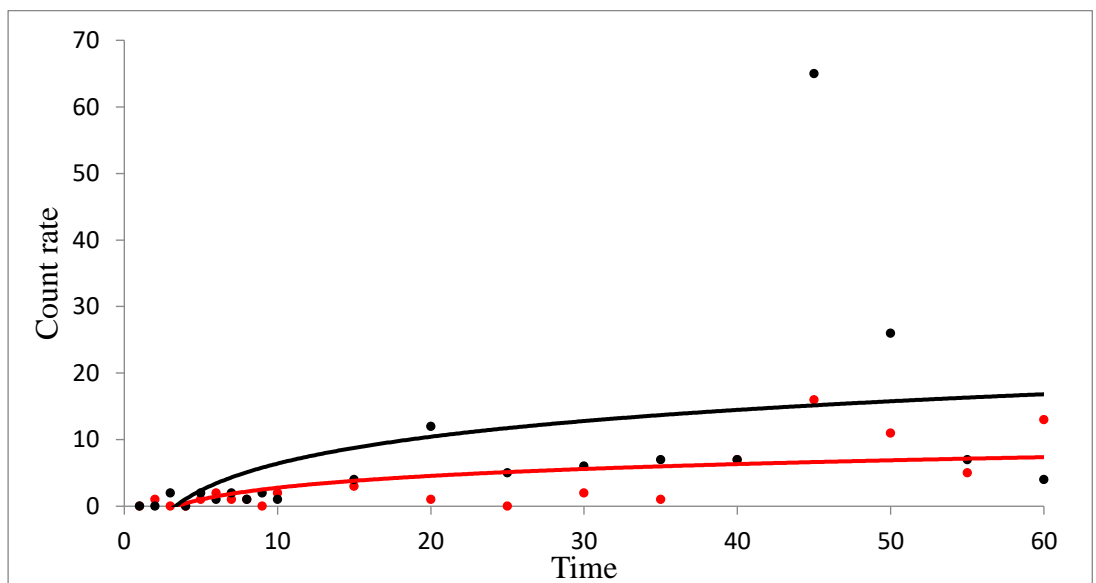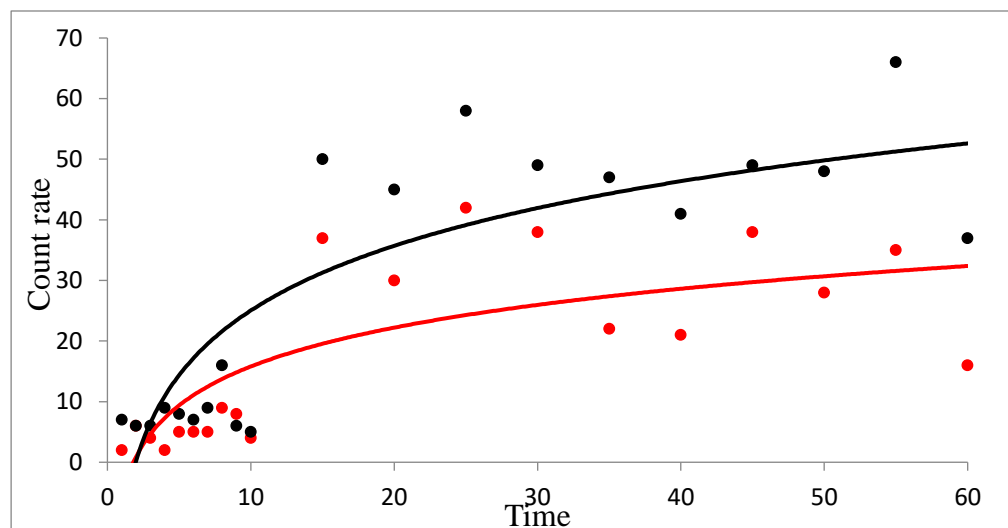
Figure 3.33 Dependence of counting speed increase on time when measuring ground: in the absence of voltage - red, presence of voltage U1,2 = + 3kV - black.

3.15 The results of measurements with a storage electrostatic chamber No.3

Spectrometric and counting measurements of sand and earth were carried out at a voltage applied to the active zone of the storage chamber equal to: 1) $U1 = 0$ kV; 2) $U1 = + 3$kV.

Figures 3.34 – 3.36 show the spectra obtained when measuring sand in a storage drum.

The dynamics of the change in the counting rate as a function of time when measuring sand, both in the presence of voltage and its absence at the electrodes of the ND, is shown in Figure 3.37.

The spectral distribution of alpha radiation in an experiment with sand, obtained in the absence of voltage, is shown in Fig. 3.34. When the voltage in $U1 = +$ 3 kV is applied to the active part of the storage chamber, the spectral distribution shown in Fig. 3.35 is obtained. Figure 3.36 combines the spectral distributions obtained in the absence of voltage and its application.
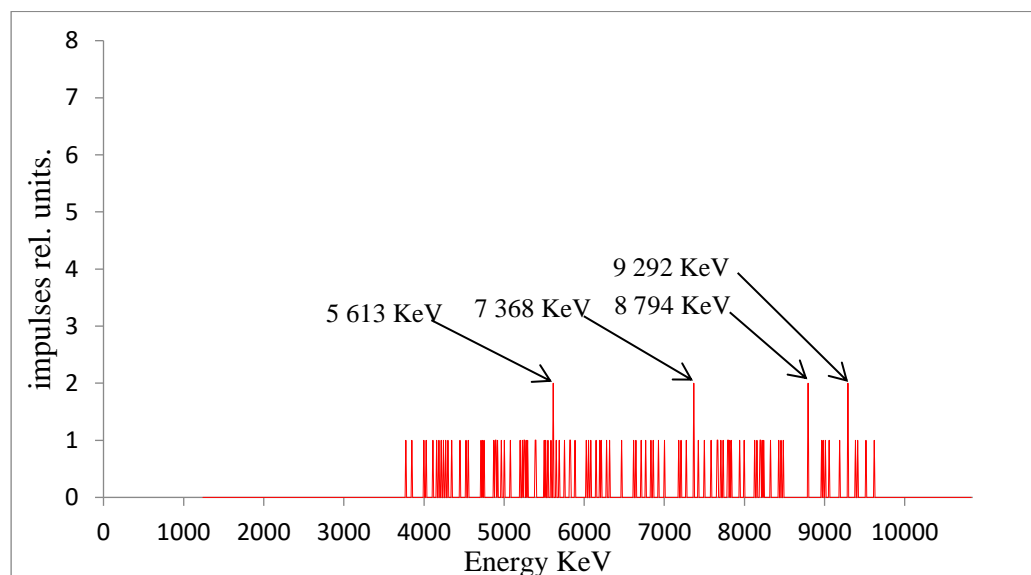
Figure 3.34 Spectrum of sand, taken in the absence of tension.

On the spectrum of sand removed from the absence of tension Fig. 3.34 it is possible to distinguish, 4 maxima with energies: 5613 keV, 7368 keV, 8794 keV, 9292 keV. In each of these maxima there are two pulses. An accurate estimate of the radionuclide composition cannot be given due to small statistics at the maxima.
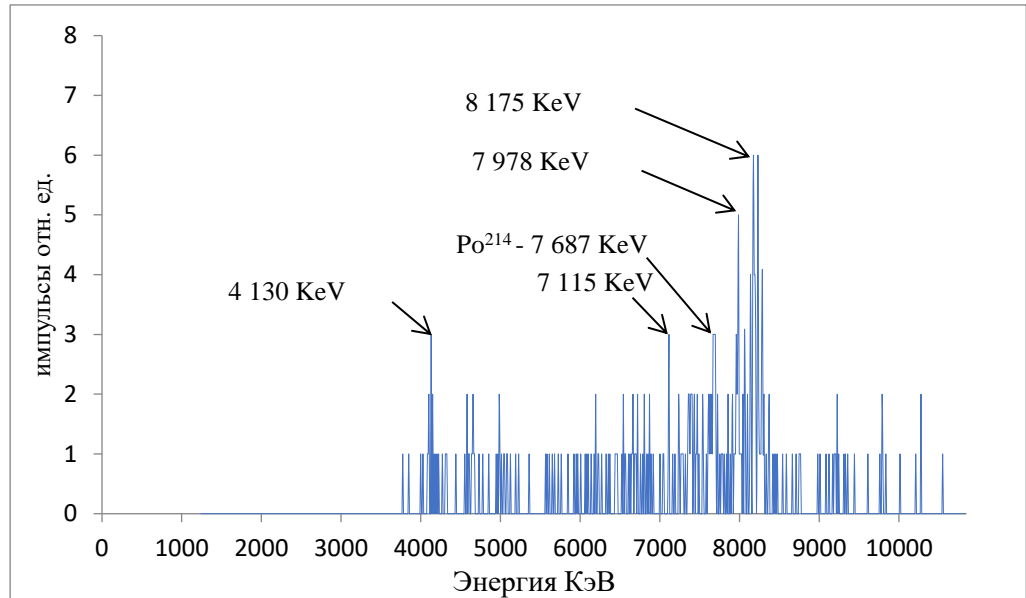
Figure 3.35 The spectrum of sand, taken at a voltage equal to U1 = + 3 kV.

On the spectrum of sand removed with a voltage of +3 kV Fig. 3.35 it is possible to distinguish, 5 maxima with energies: 4130 keV, 7115 keV, 7687 keV, 7978 keV, 8175 keV. The maximum with an energy of 7 687 keV corresponds to Po^{214}. The area below it is 14 imp. at an amplitude of 3 pulses.
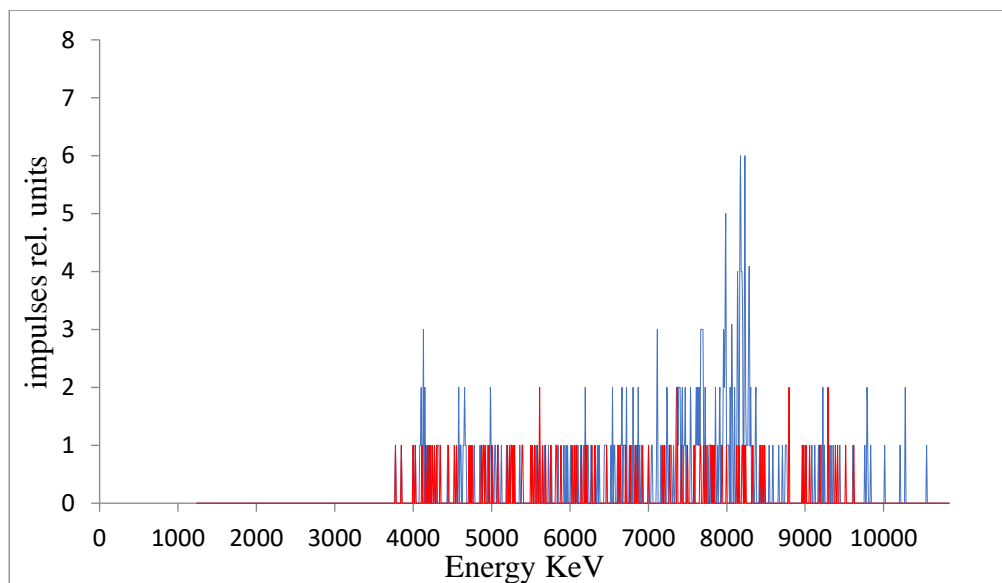
Figure 3.36 Combining the two previous spectra of sand: in the absence of voltage - red, the presence of voltage equal to - blue.

The number of recorded pulses in the spectral distribution of Fig. 3.36 and the counting rate in Fig. 3.37 increases when the voltage is applied to the ND electrodes. 2.9 times more pulses are recorded when the voltage is applied to the active zone of the ND. In the absence of voltage, only 103 were recorded, and 287 pulses were registered when it was applied to the ND electrodes.

Figure 3.37 combines two graphs in one coordinate plane showing the change in counting rate when a voltage of +3 kV is applied to the active zone of the PPD and without it. From this graph it is seen that there is an increase in the counting rate when the voltage is applied + 3 kV. According to this graph, an increase in counting speed occurs twice when measuring sand.
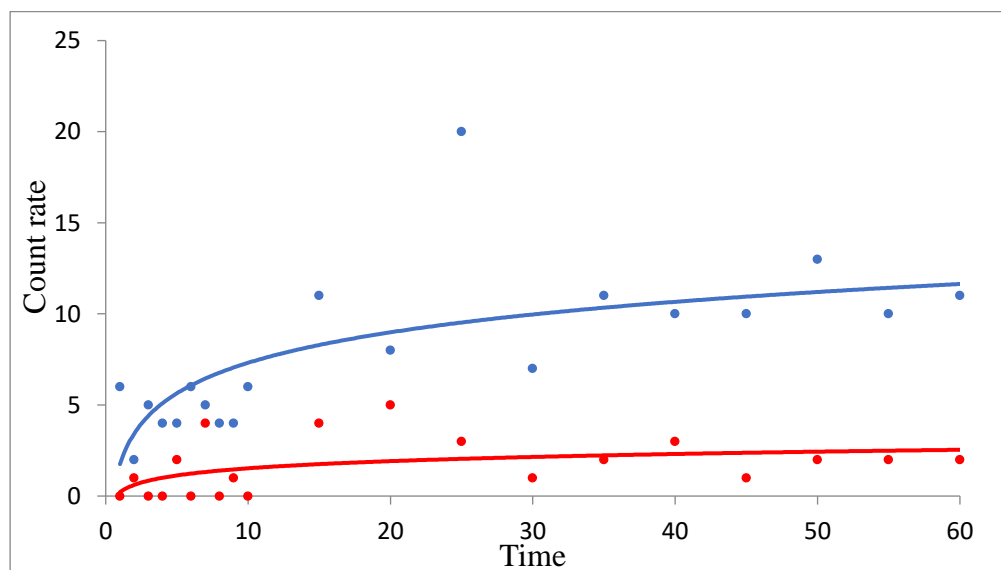
Figure 3.37 Dependence of the increase in counting rate on time when measuring sand: in the absence of voltage - red, the presence of voltage - blue.

The spectra obtained as a result of ground measurements are shown in Figures 3.38 - 3.40. In Figure 3.38, the spectrum obtained in the absence of voltage. The

spectrum obtained by applying voltage to the electrodes of the storage chamber is shown in Figure 3.39. Both spectra are combined in Figure 3.40.
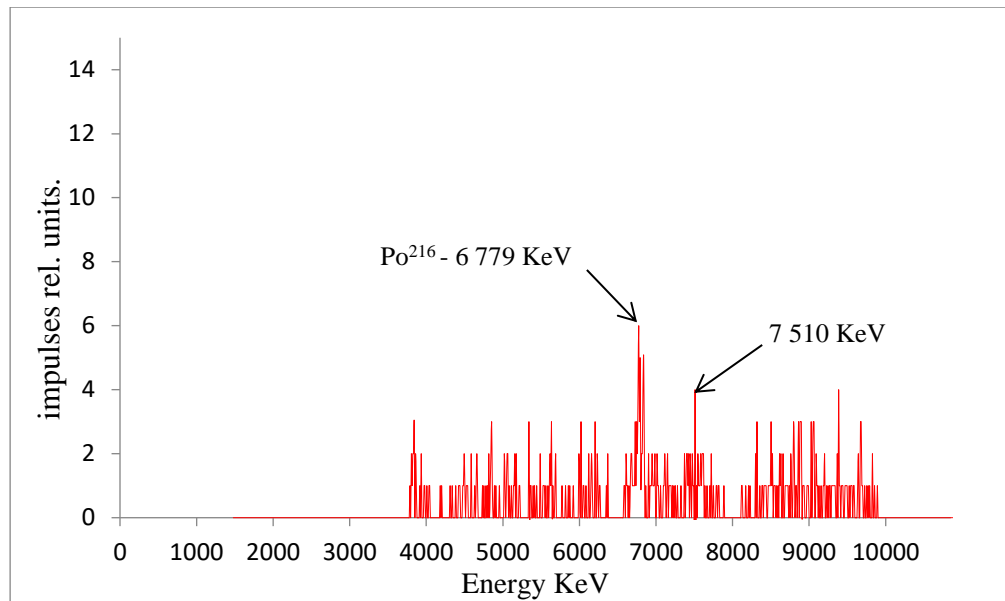
Figure 3.38 The spectrum of the earth taken in the absence of tension.

On the spectrum of the earth, taken off with no voltage, Fig. 3.38 can clearly be distinguished, 2 maxima with energies: 6,779 keV, 7,510 keV. The maximum with an energy of 6,779 keV belongs to Po^{216}. The area below it is 43 imp. at an amplitude of 6 pulses.
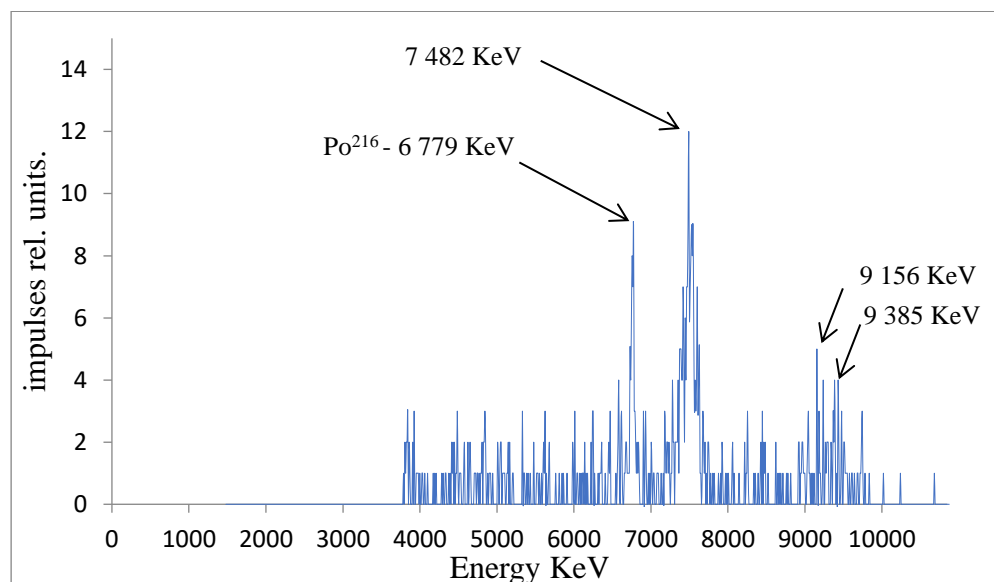
Figure 3.39 The spectrum of the earth taken at a voltage equal to U1 = + 3kV.

On the earth's spectrum taken off at a voltage equal to U1 = + 3 kV Fig. 3.39 it is possible to distinguish, 4 maxima with energies: 6,779 keV, 7,482 keV, 9,156 keV, 9,385 keV. The area under the maxima with an energy of 6,779 keV is 56 pulses. at an amplitude of 7 and belongs to Po^{216}. Just as in the measurement of sand, the spectrum obtained by measuring the ground with the supply of voltage to the electrodes of the ND changes the shape and the radionuclide peaks become more marked at the background level, the number of pulses in them falls off. The area under maxima of Po^{216} without voltage registered 43 imp. a, with a voltage of 56 imp. . The number of recorded pulses at the maximum increased 1.3 times.
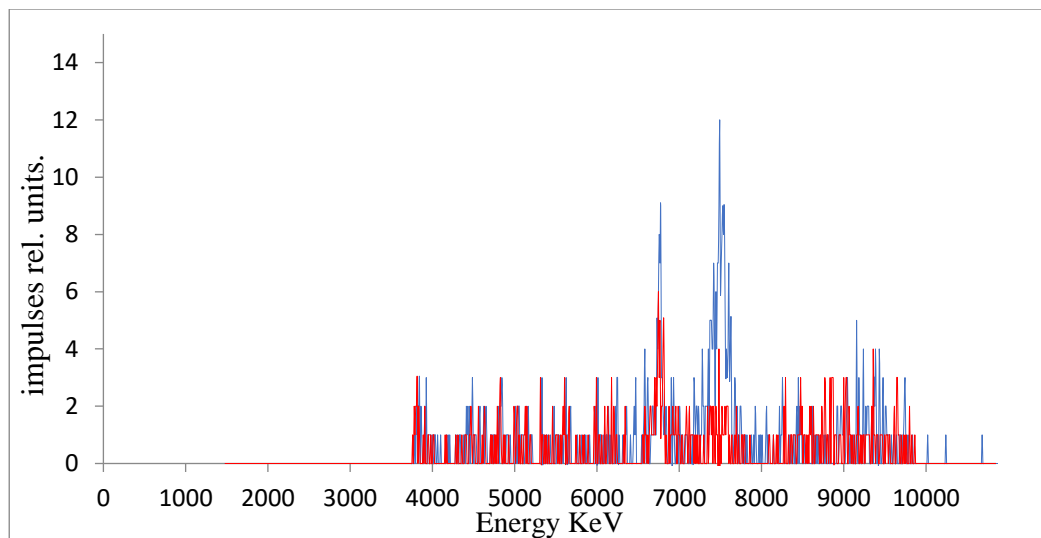
Figure 3.40 The combination of two spectra of the earth:

in the absence of - red and the presence of voltage - blue U1 = + 3 KB.

As in the study of sand and earth, the number of recorded pulses in the spectrum of Fig. 3.40 when applying voltage to the active zone of the ND. The counting speed in Fig. 3.41 also increases when the voltage is applied.

In the absence of voltage 420 pulses are registered, and in the presence of 624 pulses. 1.5 times more pulses are recorded when the voltage is applied to the active zone of the ND.
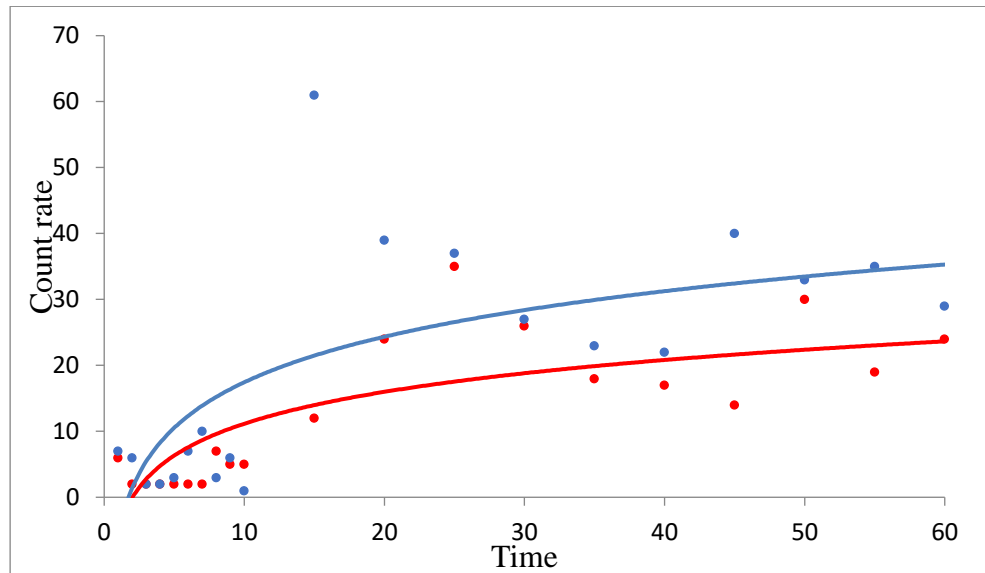
Figure 3.41 Dependence of the increase in counting speed on time when measuring the earth: in the absence of voltage - red, the presence of voltage blue.

When measuring sand, the number of pulses registered in the spectrum with applying voltage to the active zone of the ND increased by 2.9 times, and when the earth was measured 1.5 times. Also, the area under the maximum increased from 43 to 56 pulses in the Po216 maximum found.

3.16 The choice of the best design of a storage electrostatic chamber

Tables 3.12 to 3.41 summarize the results of measurements with three designs of storage electrostatic chambers. The analysis of the measurement results presented in these tables made it possible to choose the best design of a storage electrostatic chamber. The key factors that influenced the choice were the number of radionuclides identified and the increase in the amplitude of the spectral maxima upon application of the voltage. We also took into account such a factor as the degree of increase in the total number of recorded pulses with the applied voltage, but this factor was of secondary importance, since with the application of the voltage, the number of all registered pulses can increase significantly, and the amplitude of the spectral maximum does not increase.

Structures Number 1 and 2 with a circuit for applying voltage to the electrodes $U1,2 = + 3$ kV of the storage electrostatic chamber are the best for measuring the radon

and thoron flux density from the soil surface. First, using these NDs in the alpha spectrum, two peaks corresponding to the PPR of radon and thoron clearly appeared. Secondly, the maximum amplitude was obtained in the spectral maximums of radionuclides upon application of the voltage. In this case, the total number of registered pulses in both cases increased by 2 times.

Table 4.3. Analysis of research results with sand

Chamber	Applied voltage	$\Sigma_i^n N_i(U=0)$	$\Sigma_i^n N_i(U\neq0)$	$\dfrac{\Sigma_i^n N_i(U\neq0)}{\Sigma_i^n N_i(U=0)}$	Quality spectrograms
	U1=U2=+2 kV	118	295	2,5	clear
	U1=+3 kV, U2=0 kV	112	104	0,92~1	clear
	U1,2=+3 kV		251	2,3	clear
	U1=+3kV	103	287	2,8	fuzzy

where $\Sigma_i^n N_i$ is the sum of all registered pulses during the measurement time of 2 hours

Table 4.4. Analysis of research results with land

Chamber	Applied voltage	$\Sigma_i^n N_i(U=0)$	$\Sigma_i^n N_i(U\neq0)$	$\dfrac{\Sigma_i^n N_i(U\neq0)}{\Sigma_i^n N_i(U=0)}$	Quality spectrograms
	U1=U2=+2 kV	332	598	1,8	clear
	U1=+3kV, U2=0 kV	559	780	1,4	clear
	U1,2=+3 kV		1038	1,8	clear
	U1=+3 kV	420	624	1,5	clear

Comparison of the results of data processing presented in Table. 4.3 and 4.4 allow us to draw the following conclusions.

1. Good quality of the spectrogram in a study with a soil with an elevated content of radium and thorium showed three NDs No. 1, 2 and 3. However, in studies with sand in which a low content of radium and thorium is observed, clear spectrograms were obtained only with the use of two ND No. 1 and 2.

2. In the absence of electrostatic precipitation, different chambers recorded a different total number of pulses in 2 hours of measurement. In the study of sand, all cameras showed approximately the same result. When studying the ground - camera number 2 recorded the largest number of imp.

3. When creating conditions for electrostatic deposition, the total number of imp. for all ND, the average increase was 2.2 times. With sand, the best results were shown by chamber # 1 and # 3.

Table 4.5 Analysis of spectra: sand

Chamber	Applied voltage	Identity radio frequency $U = 0$	Amplify, imp..	Area under the peak, imp. $U = 0$	Identity radio frequency. $U \neq 0$	Amplify, imp.	Area under the peak. imp. $U \neq 0$
	U1=U2 =+2 kV	Po^{216}		12	Po^{214} Po^{216}		21 27
	U1=+3 kV, U2=0kV	Po^{216}		23	Po^{214} Po^{216}		16 22
	U1,2=+ 3 kV				Po^{214} Po^{216}		17 29
	U1=+3 kV	not found		-	Po^{214}		14

Table 4.6 Analysis of spectra: earth

Chamber	Applied voltage	Identity radio frequency. $U = 0$	Amplify, imp	Area under the peak, imp. $U = 0$	Identity radio frequency. $U \neq 0$	Amplify, imp.	Area under the peak. imp. $U \neq 0$
	U1=U2 =+2 kV	Po^{216}		46	Po^{214} Po^{216}	0	89 97
	U1=+3 kV, U2=0 kV	Po^{216}		39	Po^{214} Po^{216}	4 6	61 107
	U1,2=+ 3 kV				Po^{214} Po^{216}	7 9	76 121
	U1=+3 kV	Po^{216}		43	Po^{216}		56

Comparison of the results of statistical data processing presented in Table. 4.5 and 4.6 allows us to draw the following conclusions.

1. In the absence of electrostatic deposition and studies with sand, only one radionuclide ^{216}Po was identified - the decay product of thoron and only the chambers No. 1 and 2. With ground, with an increased content of thorium, all chambers allowed the determination of ^{216}Po. DDP radon did not appear in the spectra of any chamber.

2. When electrostatic precipitation conditions were created, the peaks of the ^{214}Po, the product of the decay of radon, clearly appeared in the spectra obtained in the study of sand with chambers No. 1, 2 and 3, while the peak amplitude of ^{216}Po slightly increased. The results of studies with a land with a high content of radium and thorium confirmed the previous results with sand. The best in this case were chambers No. 1 and 2. Chambers No. 3 did not show significant improvements in the quality of the spectrograms when electrostatic precipitation conditions were created in them. The

peaks in the alpha radiation spectra of the PPR did not appear in the measurements by these chambers.

3.17 Measurements with the best designs of storage electrostatic chambers

Spectrometric earths with the best variants of constructions of accumulating electrostatic chambers are carried out.

Figure 3.42 shows the spectrum obtained by measuring the earth using a storage electrostatic chamber of Design No.1 with a voltage at the electrodes U1,2 = + 2 kV. The spectrum obtained with the use of design No.2 with the circuit for applying voltage to the electrodes U1,2 = + 3 kV is shown in Figure 4.48
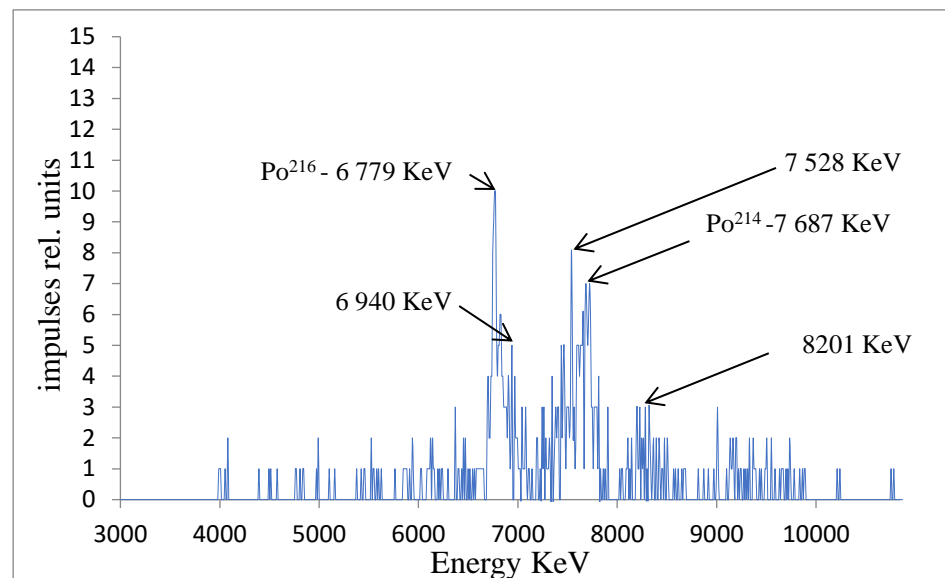
Figure 3.42 Construction No. 1. The ground spectrum, taken at a voltage equal to U1 = U2 = + 2kV

Several maxima with energies: 6779 keV, 6,940 keV, 7528 keV, 7687 keV, 8201 keV are located on the spectral distribution of the earth. The maxima with energies of 6779 keV, 7687 keV belong to Po^{216} and Po^{214}, respectively. The number of recorded pulses under these radionuclides is: Po^{216} - 118 pulses, Po214- 97 imp. The amplitude of Po^{216} is 10 pulses. , Po^{216} - 7 pulses.
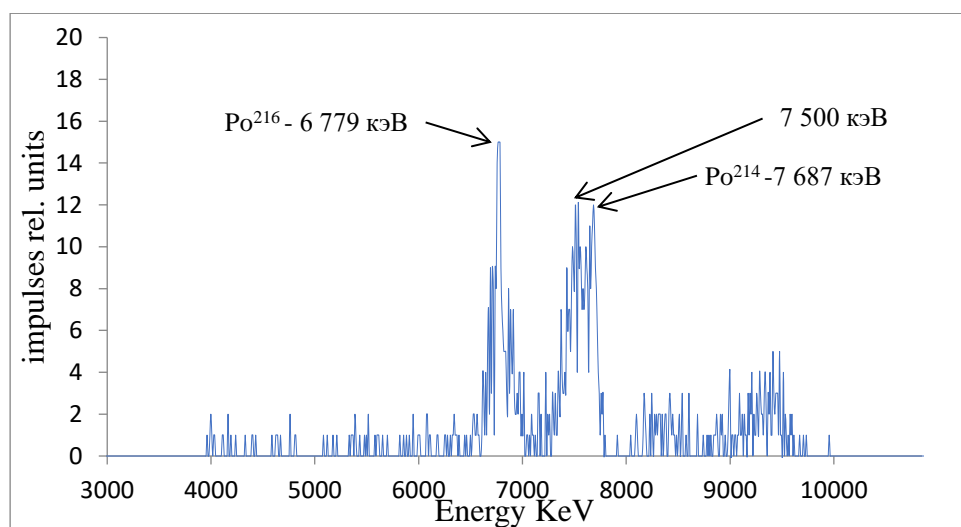
Figure 3.43 Construction No. 2 The spectrum of the earth, taken at a voltage equal to U1,2 = + 3 kV.

On the spectrum of sand removed at a voltage equal to U1,2 = + 3kV Fig. 3.29 three maxima with energies: 6779 keV, 7423 keV, 7687 keV are distinguishable on the ND electrodes. Maxima with energies: 6779 keV and 7687 keV with an area under it of 119 and 96 imp. belongs to Po^{216} and Po^{214}, respectively. Amplitude Po^{216} - 15 imp. Po^{216} - 12 pulses.

3.18 Method for determining the flux density of radon and thoron

To determine the PPD and PPT, it is necessary to make a measurement using one of the most successful designs of the storage chambers No.1 or No.2 The storage chamber must be pressed into the ground for 1-2 cm, a high voltage is applied to the electrodes of the chamber.

The voltage U1,2 = + 2 kV should be applied to the electrodes (cylinder and large metal mesh) of chamber No.1. On the electrodes of chamber number 2 (a truncated hemisphere and a small metal grid), it is also necessary to apply voltage U1,2 = + 2 kV.

Simultaneously with the supply of high voltage to the electrodes of the chamber, it is necessary to include an alpha spectrometer and a personal computer. The alpha spectrometer will begin to take readings from the PDD located in the ND of one

of the two designs to amplify the signal and transmit to the PSI board integrated into the PC motherboard. The spectrum obtained as a result of measurements is displayed on the monitor and can be saved as a text file (and further processed) with the help of a specially developed software product ACP-control v1.1.

Radionuclide analysis of spectra (processing of spectra stored in a text file) is made as a result of measurements with different designs, and the peaks of decay products of radon and thoron are determined in an area under these peaks. Knowing the area under the peaks and the correction factor, as well as the measurement time, we can generate a formula to find the PPR and PPT.

4 Financial management, resource efficiency and resource conservation.

4.1 Financial Management.

Financial Management refers to planning, organizing, directing and controlling the financial activities such as procurement and utilization of funds of the enterprise. It means applying general management principles to financial resources of the enterprise. [40]. Financial management as a discipline sprung out from economics to become a stand-alone profession. That is why we have people that call themselves financial manager and investment managers today.

4.2 Scope of Financial Management

Financial management cuts across wide range of sectors today- in fact, all sectors. Government agencies for instance make use of cost-benefit-analysis to determine the economic wisdom in certain projects.

Financial management has so advanced that many behavioural factors now play significant role in certain aspects of financial management like valuation where bankruptcy cost is factored in options price. The legal practitioners rely on time-value of money to same claims that involves financial compensation.

Importance / Significance of Financial Management

- Economic growth and development: through investing decision, financing decision, dividend decision, and risk management decision, better and more economically viable projects are undertaken by companies. The resultant effect on the economy is economic growth and development. Financial management serve as a good guide to online investing.

- Improved standard of living: growth and development in the economy that is brought about by financial management will ultimately translate into improved standard of living for all.

- Improved health: again, good economic condition and improved standard of living culminates into improved health as a lot of 'financial stress' related sicknesses will be completely eliminated or reasonably reduced.

- Allows for better financial decision

- Creates jobs – those that teach financial management and the jobs that are created as a result of flourishing economy. Better financial decisions will lead to profitability, and profitability will eventually lead to expansion which will in turn mean more jobs.

- Alleviation of poverty

- Preserve our environment

- Promotes efficiency: good financial management does not give room for wastes and inefficiencies that characterizes poor financial management and decision making.

The importance of financial management can take us a whole lot of space to finish listing. This is to say that the once listed above are just but few. [41]

4.3 Potential consumers of project results

A potential consumer of the storage chamber is Geophysicist, Geologists, Research institutions and any country that has an Environmental Protection Agencies (EPA). Thus, in the territory of the Russian Federation, both the Ministry of Natural Resources and the Environment and private entrepreneurs can act as consumers. Also, in Ghana through the EPA it is possible to enforce laws that will enable all buildings have a Radon certificate and in by so doing generate revenue for the agency and entrepreneurs.

Industries in Ghana and other countries that makes use of radiation can also be potential consumers of the designed SC.

4.4 Analysis of competitive technical solutions using QuaD technology

The Storage Chamber (SC) can solve one important task, that is, measurement of the flux density of radon and thoron on soil surfaces. At the same time, manufacturing of the chamber is provided not by only one element of the system, but by a set of organizational measures together with other engineering and technical facilities.

4.5 QuaD technology

This technology is a flexible tool for measuring the characteristics of a new development and its prospects in the market. The evaluation map of the analysis is presented in Table 4.1. Position development and competitors is estimated for each indicator expert by a five-point scale, where 1 - the weakest position, and 5 - the strongest. The weights of the indicators, determined by an expert way. Analysis of competitive technical solutions is determined by the formula:

$$C = \sum_{i=1}^{n} CW_i * P_i \,, \tag{4.1}$$

where C - the competitiveness of scientific developments or competitor;

CW_i - weight index (expressed as a decimal);

P_i - expert points. *i-th* index

Table 4.1 - Evaluation map for comparing competitive technical solutions (developments)

Evaluation criteria	Criteria Weight CW	Points (P)			Score=CW*P		
		P	P_1	P_2	S_0	S_1	S_2
1	2						
Performance resource evaluation criteria							
1. Increasing user productivity	0,1				0,5	0,4	0,4
2. Ease of operation (corresponding to the requirements of consumers)	0,1				0,5	0,4	0,3
3. Energy Efficiency	0,06				0,3	0,24	0,18
4. Reliability	0,06				0,3	0,24	0,24
5. Noise	0,01				0,05	0,05	0,05
6. Safety	0,06				0,3	0,3	0,3
7. The demand for material resources	0,03				0,12	0,12	0,12

8. Functional capacity (possibility provided)	0,06				0,3	0,24	0.18
9. Interferences	0,04				0,2	0,2	0.2
10. Ease of use	0,1				0,4	0,4	0.4
economic criteria for evaluating the 5effectiveness of							
1. The product competitiveness	0,03				0,15	0,12	0.12
2. Price	0,05				0,25	0,2	0.15
3. Estimated useful life	0,2					0,8	0,8
4. After-sales service	0,05				0,25	0,25	0,25
5. Financing scientific development	0,05				0,25	0,2	0,2
Total	**1**				**4,87**	**4,16**	**3,89**

Based on the analysis presented above, it can be concluded that the manufacturing of the storage chamber studied in this thesis is the most suitable for measurement in specified modes.

4.6 SWOT Analysis

SWOT (Strengths, Weaknesses, Opportunities and Threats) analysis is a process that identifies an organization's strengths, weaknesses, opportunities and threats. Specifically, SWOT is a basic, analytical framework that assesses what an entity (usually a business, though it can be used for a place, industry or product) can and cannot do, for factors both internal (the strengths and weaknesses) as well as external (the potential opportunities and threats). Using environmental data to evaluate the position of a company, a SWOT analysis determines what assists the firm in accomplishing its objectives, and what obstacles must be overcome or minimized to achieve desired results: where the organization is today, and where it may be positioned in the future. [42]

In this work, the designed system has a detector which is connected to an amplifier and a pulse analyzer for accurate measure of the flux density of radon and

thoron emanating from the soil surface. Also, it is safe to work with the installation and easy repairability of each individual unit of the installation. Furthermore, it is also easy to operate the installation.

Weaknesses are a shortcoming, omission or limitation of a research project that hinders the achievement of its objectives. This is something that is poorly achieved within the project or where it has insufficient capabilities or resources compared to competitors. The main weaknesses of the designed system may arise from soil with low radon gas levels or a faulty detector. Lack of funding and lack of necessary knowledge is also a major weakness to this research. Not lot of people know about this research therefore lack of awareness is also a contributing factor. Also, long term delivery of materials and components used in the conduct of this research is a factor and last but not least long processing time of final results.

Opportunities include any preferable situation in the present or future that occurs in the environment of the project, for example, a trend, change, or perceived need that supports demand for project results and allows project management to improve their competitive position.

The Environmental Protection Agencies by-laws which enables all buildings to possess a validated radon certificate makes it idle for entrepreneurs to venture into, since its market is valued over 1 million dollars in a year [43]. Also, the emergency of additional demand for a new product and the cooperation with a number of new organizations makes this research work an opportunity to look at. Using obsolete methods by competitors and decreasing the cost of competitive developments

A threat represents any undesirable situation, trend or change in the project environment that is destructive or threatening for its competitiveness in the present or future.

The main threats in the production of the storage chamber is uncertainties in the construction cost i.e. increase in construction and raw material cost as the economics of the world keeps varying. Secondly competition of other products on the market. Also lack of funding from both the university and the state contributes to the threats in this research. The complexity of supplying samples for research and

depreciation of equipment's are all factors. Below are some measures that can help to reduce the threats and weaknesses of the designed system based on comparison of the SWOT described above.

Table 4.2 presents the interactive project matrix, which shows the correspondence of strengths to capabilities, which allows for more detailed consideration of the development prospects.

Table 4.2- Interactive matrix of the project

	S1	**S2**	**S3**	**W1**	**W2**	**W3**
O1	+	+	-	+	-	-
O2	+	+	+	-	-	-
O3	-	-	+	+	-	-
T1	+	+	+	+	-	-
T2	+	+	+	+	+	+
T3	-	+	+	-	-	-

Based on the result of the SWOT analysis above, a final SWOT-analysis matrix is presented in Table 4.3.

Table 4.3-SWOT Analysis

	Strengths:	**Weak sides:**
	S1- sufficient installation reliability	W1- Lack of funding
	S2 - safety of work with installation	W2 - Lack of necessary knowledge
	S3 - Repairability of installation	W3 - Long processing time
	S4 - Easy operation of installation	W4 - Lack of awareness
		W5 - Long term delivery of materials

Capabilities:	O1S1 - Large	O2W3 - Priority of
O1 - EPA by-laws	number of research orders.	competitive organizations due to a long period of research or outstanding in time.
O2 – Using innovative infrastructure of tpu	O3S2 - The growth in demand for this type of research through distribution among various organizations and universities	
O3 - additional demand for new product		
O4 – Using obsolete methods by competitors	O4S1S2- Priority to this research in comparison with competitors due to the implementation of proper reliability and safety of the installation.	

Threats:	T4S3- Carry out the repair of the current installation without replacing the component parts.	T3W2- The lack of demand for technology due to its unsustainable competitiveness
T1 – High price of technology		
T2 – Competition	T2S1 - Resistance to the struggle with competitors due to the novelty of the idea.	T1W1. Stagnation of studies due to lack of funding
T3 – Lack of funding from both university and state		
T4 – depreciation of equipment	T4S3- Improvement	

Based on the results of the analysis of this matrix, it can be concluded that the difficulties and problems that this research project may encounter in one way or another can be solved through the strengths of the research

4.7 Evaluation of the Project Readiness for Commercialization

Table 4.3 - Assessment of the Readiness of the Research Project to Commercialization

The indicators which depicts the degree of maturity of the project from the perspective of commercialization and competence developer of a research project is considered in the table 4.4 below.

Table 4. 3 - Blank assess the readiness of a research project to commercialize

S/No	Criteria	Degree of elaboration in the research project	Level of developers existing knowledge

1	Scientific and technical potential is determined	5	5
2	Promising areas of commercialization of scientific and technological potential are identified	5	5
3	Industries and technologies (products and services) to offers on the market are identified	4	4
4	Commodity form (product form) of the scientific and technical basis for the presentation to the market is determined	4	4
5	Author is identified and protection of their rights is secured	4	4
6	Assessment of the value of Intellectual Property is done	4	4
7	Marketing research of potential markets is carried out	4	4
8	Business plan for commercialization of scientific development is developed	4	4
9	The ways of promoting scientific development to the market	5	5
10	The strategy (form) the implementation of scientific development is developed	4	5
11	International cooperation potential and access to foreign markets are studied	3	4
12	Use of infrastructure support services to receive benefits is studied	4	5
13	Funding issues commercialization of scientific development is formed	4	5

14	Team for the commercialization of scientific development is formed	4	4
15	Arrangements for the implementation of a research project are made	5	5
16	Total points (B$_{sum}$)	63	67

Readiness Assessment research project to commercialization (or the level of existing knowledge from the developer) is defined by the formula:

$$B_{sum} = \sum B_i ,$$ (4.2)

Where B$_{sum}$ - the total number of points in each direction;

B$_i$ - point on the i-th indicator.

The value of B$_{sum}$ suggests the extent of readiness of scientific development and its developer to commercialization. For example, if the value of B$_{sum}$ turned out between 75 and 60, such a development is considered promising, and developer of knowledge sufficient for successful commercialization. If 59 to 45 - that the prospect of above-average. If 44 to 30 - the average prospect. If 29 to 15 - that the prospect of lower than average. If 14 and below - the prospect is extremely low.

The evaluation concludes that the volume of investment in the ongoing development and direction of further development is considered above-average, and developer of knowledge sufficient for successful commercialization.

4.8 Planning for the management of the scientific and technical project

The organizational structure of the project is the most appropriate a temporary organizational structure that includes all its participants and is created to successfully achieve the project's objectives.

Development of the organizational structure of the project includes:

- Identification of all organizational units

- Defining the roles of project participants and their interaction,

- Definition of responsibility and authority

- Distribution of responsibility and authority between organizational units of the structure

- Development of instructions regulating interactions in the structure and working procedures.

The organizational structure of the project is a dynamic structure, which is undergoing changes in the project implementation process. These changes depend on the phases of the life cycle of the project, the types used in project contracts, and other conditions for the implementation of the project.

The Project stakeholders and Participants include:

- Research Institute (Performer: Heads, Supervisors and Students)

- Business company dealing with radiation monitoring and Nuclear fuel use activities (Head of Company, Engineers and Consultants)

- Educational Institutions (Head, Engineers and Consultants)

4.9 Structure of work under the project

In the process of creating the hierarchical structure of the project, the content of the entire project is structured and defined. The planning process group consists of the processes performed to determine the overall content of the work, clarify the objectives and develop the sequence of actions required to achieve these goals. Work breakdown Structure (WBS) - detailing of the enlarged work structure: the division of the entire volume of the planned work into small operations so that they correspond to the level at which the way of performing the planned actions would be clear, and the operations would be evaluated and planned.

Table 4.4- Morphological matrix for research implementation alternatives

Characteristics	Alternatives		
	1	2	3
Entity	University	Research Institute	Business Company
Executives	Supervisor	Head of institute	Head of Company
Materials	Free	Bought	Bought

Equipment	Free	Bought	Rented
Software	General	Special	Special
Software access	Free	Free	Free
Facilities	Classroom	Lab	Office
Facilities access	Free	Bought	Rented

4.10 Project plan

As part of the planning of the research project, a calendar schedule was constructed. In this case the Gantt chart was used to map the distribution of the work carried out. Gantt chart is a type of bar charts which is used to illustrate the planned schedule of project, in which the works can be shown the extensive length of time, characterized by the dates of beginning and end of the implementation of these works.
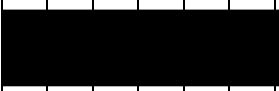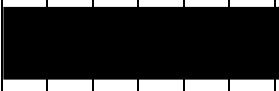
The graph is constructed and shown in table 4.5 below by month and seven-day working periods during run-time of project. The difference in the length of the distribution of each working period largely depends on the task needed for a particular work. The task performed are written and shown in appendix. The work on the topic is represented by long stretches of time, characterized by the dates of commencement and completion of work. The linear graph is presented in Table 4.6.

Table 4.5- Stages of work and executors

Main stages	Duration, days	Work content	Position performer
Development of technical specifications	3	Drafting and approval of technical specifications	Supervisor

Choice of direction research	60	Selection and study of materials on the topic	Engineer
	60	Conducting patent research	Engineer
	5	Choice of Research Directions	Supervisor Engineer
	5	Scheduling of work on the topic	Supervisor Engineer
Theoretical research	10	Consideration of similar research work	Engineer
	10	Selection of Semi-conductor	Supervisor Engineer
	10	Selection of Amplifiers and pulse analysers	Engineer
	15	Corrections on literature reviews	Engineer
Carrying out of modeling			
Development of technical documentation and design	40	Construction of the storage chambers	Supervisor Engineer
	20	Performing calculations and analysis of data received	Supervisor Engineer

Table 4.6 - Work schedule

work Number	Type of work	Performes	,al, days.	Duration of work execution				
				Feb	March	April	May	June
1	Drafting and approval of technical specifications	Supervisor		▉ (blue)				
2	Selection and study of materials on the topic	Engineer	0	██████ (black, Feb–mid March)				
3	Conducting patent research	Engineer	0	██████ (black, Feb–mid March)				
4	Choice of Research Directions	Supervisor Engineer			▉ (blue) / █ (black)			
5	Scheduling of work on the topic	Supervisor Engineer			▉ (blue) / █ (black)			
6	Consideration of similar	Engineer			█ (black)			

103

№		Role																						
	research work		0																					
7	Selection of Semi-conductor,	Supervisor Engineer	5										▓(blue)▓(black)											
8	Selection of Amplifiers and pulse analysers	Engineer												█										
9	Correction of literature reviews	Engineer													█									
10	Drawing up the plan of the object	Supervisor Engineer													▓(blue)▓(black)									
11	Performing calculations and analysis of data received	Supervisor Engineer														▓(blue)▓(black)								

▓(blue)	Supervisor

■■■■■	Engineer

4.11 Budget of scientific research

When planning the research budget, it must be ensured that full and reliable reflection of all types of costs associated with its implementation. In the process of budget formation, cost like material costs, costs for special equipment for scientific work, additional salaries among others were calculated. The scientific work was carried out under a budget allocated to a supervisor and one student of the university. The supervisor is allocated 300 Rub per hour and the engineer has 100 Rub per hour. The total cost incurred during the cost of the project was then calculated and shown below. The main costs in this research are costs for electricity and purchase of office supplies. The cost of electricity is calculated by the formula:

$$C = T_{el} \cdot P \cdot t = 6 \cdot 0.5 \cdot 600 = 1800 \qquad (4.3)$$

where T_{el} - tariff for industrial electricity (6 rubles per 1 kW · h);

P - capacity of equipment, kW;

t - time of use of equipment, h (120×5).

The cost of electricity amounted to 1440 ruble

4.12 Raw materials, purchased products and semi-finished products

This item includes the cost of all kinds of purchasing materials, components and semi-finished products necessary for the implementation of works on the subject. Number of required material values determined by the norms of consumption.

Material cost calculation is carried out according to the following formula:

$$C_m = (1 + K_{tr}) \cdot \sum_{i=1}^{m} p_i \cdot N_i \qquad , \qquad (4.4)$$

Where m – number of types of material resources consumed in carrying out scientific research;

N_i – the number of physical resources i-th species, planned to be used in carrying out scientific research (pieces, kg, m, mon.);

105

P_i– acquisition unit price i-th species consumable material resources (rubles / pc, rub / kg, rub / m, rub / m etc.....);

K_{tr}– coefficient taking into account transportation and procurement costs.

Calculating the expenses of material costs based on the current price list or negotiated prices. The expenses of material costs include transportation and procurement costs (15-25% of the price). In the same item, includes the expenses of paperwork (stationery, copying materials). The results of this term are presented in the Table 4.7 below.

Table 4.7 - Raw materials, components and semi-finished products

Title	unit	Quantity			Price per each, ruble			The sum, ruble		
		Atl 1	Alt 2	Alt 3	Atl 1	Alt 2	Alt 3	Atl 1	Alt 2	Alt 3
Electricity	-	600 kW°hr	620 kW°hr	640 kW°hr	6	6	6	1800	3100	3120
Paper	SvetoCopy	1 packet of 500 sheets	1 packet of 500 sheets	1 packet of 500 sheets	0.54	0.54	0.54	270	270	270
Printing	-	400	420	430	2	2	2	800	840	860
Pen	Stabilo	4	4	4	30	30	30	120	120	120
Access to the Internet	-	4 months	4 months	4 months	350	350	350	1400	1400	1400
Total of materials								4390	5730	5770
Transportation and procurement expenses (15%)								658.5	859.5	865.5
Total items C_M								5048.50	6589.50	6635.50

4.13 Calculation of costs for special equipment for scientific

This item includes all costs associated with the acquisition of special equipment necessary for work on specific topic. In this research work on special equipment, necessary for carrying out experimental is listed in the table 4.8

Table 4.8 - Budget cost for the purchase of special equipment for scientific paper

#	Name of equipment	Number of units of equipment			Unit price of equipment, ths. Rub.			The total cost of equipment, ths. Rub.		
		Atl 1	Alt 2	Alt 3	Atl 1	Alt 2	Alt 3	Atl 1	Alt 2	Alt 3
1	computer	1	1	1	26000	36000	40000	26000	36000	40000
2	Alpha-spectrometer MKS-01A "Multirad-AC".	1	1	1	485800	491000	501000	485800	491000	501000
3	ADC (4K-CATSPP).	1	1	1	24000	25100	26200	24000	25100	26200
4	MHV 12-2.0k 1000P	1	1	1	16605	17500	18600	16605	17500	18600
5	BNV-30-01	1	1	1	10000	11566	12500	10000	11566	12500
	Total:							562405	581166	598300

4.14 The basic salary of the performers of the topic

The article includes the basic wages of employees, directly involved in the implementation of the project (including bonuses, co-payments) and additional wages.

The item includes basic wages of workers directly involved in the implementation of the project (including premiums, bonuses) and additional wages.

Table 4.9 – Calculation of basic salary

No.	Executives	Work, person-days.	Salaries per one person-days, ths. Rub.	Total salaries at the rate (salary), ths. Rub.

		Atl 1	Alt 2	Alt 3	Atl 1	Alt 2	Alt 3	Atl 1	Alt 2	Alt 3
1	Supervisor	36	-	-	2760	-	-	99360	-	-
2	Head of Lab	-	42	-	-	3220	-	-	135240	-
3	Research Director	-	-	48	-	-	3680	-	-	176640
4	Student	120	-	-	920	-	-	110400	-	-
5	Specialist	-	50	-	-	2760	-	-	138000	-
6	Engineer	-	-	70	-	-	1840	-	-	128800
Total								**209760**	**273240**	**305440**

4.15 The main salary of the performers of the topic

The article includes the basic wages of employees, directly involved in the implementation of the project (including bonuses, co-payments) and additional wages.

The item includes basic wages of workers directly involved in the implementation of the project (including premiums, bonuses) and additional wages.

$$S_t = S_b + S_{ad},\qquad(4.5)$$

Where S_b – basic salary;

S_{ad} – additional salary.

Basic salary can be calculated, based on hourly labor rates:

$$S_b = S_h * 8,\qquad(4.6)$$

where S_h - basic salary of one employee per hour, rub/hour; Hourly labor rate may vary depending on the type of executive in the research project.

4.16 Additional salary of performers of the topic

Costs for additional pay for the performers of the topic allowance for the amount of additional payments foreseen in the Labor Code of the Russian Federation

for deviation from normal working conditions, as well as payments related to guarantees and compensation.

The additional salary is calculated on the basis of 10-15% of basic salaries of employees directly involved in implementation of the topic:

Calculation additional salary conducted according to the following formula:

$$S_{ad} = k_{ad} * S_b, \tag{4.7}$$

where kad - factor of additional salary (taken at the design stage at 0.12 - 0.15).

We take the coefficient of additional salary equal to 0.15 for the supervisors while 0.12 for an engineer, student and specialist. The results of calculating the main and additional wages of performers of scientific research are presented in Table 4.10.

4.17 Contributions to social funds (insurance contributions)

In Russian Federation, employees pay insurance payments for state social insurance fund (SIF), the Pension Fund (PF) and medical insurance fund (MIF). Employers on behalf of the employees make these payments. Contributions to these funds determined based on the following formula:

$$S_f = k_f * (S_b + S_{ad}), \tag{4.8}$$

where k_f - coefficient for payments to funds (SIF, PF, MIF).

In 2018 the size of insurance payments was set at the level of 30%. Yet for institutions engaged in educational and scientific activity the reduced rate of 27.1% is used. Social funds contributions have been calculated and tabulated in Table 4.10

Table 4.10 Contributions to social funds

Artist	basic salary, rubles.			Additional salary, rubles.		
	Alt.1	Alt.2	Alt.3	Alt.1	Alt.2	Alt.3
Supervisor	2400			360		
Head of Lab		3200			480	
Research Director			4000			600
Student	800			120		

Specialist		2400			360	
Engineer			1600			240
Ratio of contributions to social funds	27.1%	27.1%	30%	27.1%	27.1%	30%

Total amount of social fund payments	
Alternative 1	997.28
Alternative 2	1745.24
Alternative 3	1932.00

4.18 Overhead costs

This article includes the costs of management and maintenance, which can be attributed directly to a particular topic. In addition, this includes expenses for the maintenance, operation and repair of equipment, production tools and equipment, buildings, structures, etc. The calculation of overhead costs is carried out according to the following formula:

$$C_{ovh} = C_{total} * k_{ovh} ,$$
(4.9)

Where C_{total} – Total costs of the above cost items in $1 - 7$ and

k_{ovh} – Overhead coefficient, which can be taken at a rate of 16%.

Table 4.11 - Overhead Expenses

	Alt 1	Alt 2	Alt 3
C_{total}	241805.78	317574.74	354007.50
K_{ovh}	38688.92	50811.96	56641.20

The calculated value of the costs of research work is the basis for the formation of the project cost budget, which, when forming an agreement with the customer, is protected by a scientific organization as the lower limit of the cost of developing scientific and technical products.

The definition of the cost budget for a research project for each option is shown in Table 4.12.

Table 4.12 – Calculation of the expenditure budget of the research project

No	Name of the item	Amount, Rubles		
		Alt 1	Alt 2	Alt 3
1	Material costs of the study	5048.50	6589.50	6635.50
2	Expenses for special equipment	562405	581166	598300
3	Costs for the salaries of the performers of the topic	209760	273240	305440
4	Contributions to social funds	997.28	1745.24	1932.00
5	Overhead expenses	38688.92	50811.96	56641.20
6	Research Cost Budget	**280494.70**	**335986.70**	**410648.70**

4.19 The definition of resource (resource-saving), financial, budgetary, social and economic research effectiveness

The definition of efficiency is based on the calculation integral indicator of the effectiveness of the scientific research and this can be related to the definition of two weighted averages; financial efficiency and resource efficiency.

Integral component cost-effectiveness research obtained during budget cost estimates three (or more) variants of scientific studies (see Table 4.13). To do this, the most integral indicator of the implementation of the technical problem is taken for the

calculation base (the denominator), which relates to the financial value of all the embodiments.

Integral financial efficiency indicator development is defined as:

$$E_{\text{fin}}^{\text{alt.i}} = \frac{TC_i}{TC_{max}},$$

(4.10)

Where $E_{\text{fin}}^{\text{alt.i}}$ – an integral index of financial efficiency;

TC_i – Total cost of the i-th alternative;

TC_{max} – the maximum total cost of research project (including analogs).

The obtained value of the integral financial indicator of the development reflects the corresponding numerical increase in the development costs budget in times (value greater than one), or the corresponding numerical reduction in the cost of development in times (the value is less than one, but greater than zero).

Since the development has one execution, then;

$$E_{fin}^{alt.1} = \frac{TC_1}{TC_{max}} = \frac{280494.70}{410648.70} = 0.68$$

For analogues respectively:

$$E_{fin}^{alt.2} = \frac{TC_2}{TC_{max}} = \frac{335986.70}{410648.70} = 0.82$$

$$E_{fin}^{alt.2} = \frac{TC_2}{TC_{max}} = \frac{410648.70}{410648.70} = 1$$

Integral resource-efficiency indicator of research alternatives can be determined as follows:

$$E_{\text{res}}^{\text{alt.i}} = \sum a_i \cdot b_i$$

(4.11)

Where $E_{\text{res}}^{\text{alt.i}}$ – an integral indicator resource for i-th embodiment of the development;

a_i – weight factor of i-th research alternative;

b_i – a score of i-th execution of development options is set by an expert in the chosen scale of assessment;

n – number of parameters comparison. Calculation of the integral indicator resource is recommended in tabular form (Table 4.13).

Table 4.13 - Comparative evaluation of characteristics of the project alternatives

Criteria	Weighting coefficient of the parameter a_i	b_i Score		
		Alt.1	Alt.2	Alt.3
1. Convenience in operation (meets the requirements of maintenance personnel)	0,05	3	3	5
2. Reliability	0,25	5	4	4
3. Safety in operation	0,05	4	5	4
4. Possibility of improvement	0,12	4	5	5
5. Efficiency	0,22	4	5	4
6. Complexity	0,10	4	5	4
7. Ability to connect to a computer network	0,10	4	5	5
8. Repairability	0,10	3	4	4

9.Product Competitiveness	0,01	4	5	5
Total	1			

Alt.1=

0.05*3+0.25*5+0.05*4+0.12*4+0.22*4+0.1*4+0.1*4+0.1*3+0.01*4=4.50

Alt.2=

0.05*3+0.25*4+0.05*5+0.12*5+0.22*5+0.1*5+0.1*5+0.1*4+0.01*5=4.55

Alt.3   =

0.05*5+0.25*4+0.05*4+0.12*5+0.22*4+0.1*4+0.1*5+0.1*4+0.01*5=4.28

Integral total efficiency indicator of alternatives is determined based on the integral resource and financial efficiency by formula:

$$E_{total}^{alt.i} = \frac{E_{res}^{alt.i}}{E_{fin}^{alt.i}}$$

(4.12)

Hence

$$E_{total}^{alt.1} = \frac{E_{res}^{alt.1}}{E_{fin}^{alt.1}} = \frac{4.50}{0.68} = 6.62; \quad E_{total}^{alt.2} = \frac{E_{res}^{alt.2}}{E_{fin}^{alt.2}} = \frac{4.55}{0.82} = 5.5; \quad E_{total}^{alt.3} = \frac{E_{res}^{alt.3}}{E_{fin}^{alt.3}} = \frac{4.28}{1} =$$

4.28

Comparison of the integrated indicator of the effectiveness of the current project and its analogues will determine the comparative effectiveness of the project. Comparative efficiency of the project:

$$E_{comp}^{alt.i} = \frac{E_{total}^{alt.i}}{E_{total}^{min}}$$

(4.13)

The result of calculating the comparative efficiency of the project and the comparative effectiveness of the analysis are presented in Table 4.14.

Table 4.14 Comparative development effectiveness

No. p / p	Indicators	Alt.1	Alt.2	Alt.3
1	Integral financial efficiency indicator	0,68	0,82	1,00
2	Integral resource-efficiency indicator	4,50	4,55	4,28
3	Integral total efficiency indicator	6,62	5,50	4,28
4	Comparative project efficiency indicator	1,55	1,28	1,00

Comparison of the values of integral performance enables to understand and select most effective alternative for solution of the technical problem in the research taking into account financial and resource efficiency. Therefore, Alternative one is proved to be more efficient compared to the other two alternatives.

5. Production and Environmental Safety in Developing a Storage Chamber with Electrical Deposition

The concept of labor protection means a system of legislative acts, socio-economic, organizational, technical, hygienic and therapeutic and preventive measures and means that ensure the safety, health and human performance in the labor process.

Based on the requirements of the Labor Code of the Russian Federation, specific measures to create healthy and safe working conditions, prevention of accidents and occupational diseases are regulated by special Rules and Norms. According to the Labor Code of the Russian Federation, the rules on labor protection are divided into single, intersectoral and sectoral. Unified apply to all sectors of the economy. They fix the most important guarantees of safety and hygiene of work, which are the same for all industries. Cross-industry fixes the most important guarantees of occupational safety and health in several industries, either in individual types of production, or in certain types of work (for example, on certain types of equipment in all sectors).

5.1 Analysis of working conditions

In accordance with GOST 12.0.003-74 SSBT (Hazardous and harmful production factors, classification.), All hazardous and harmful factors arising in production conditions are subdivided by the nature of the action into the following groups: biological (micro- and macro-), psychophysiological, physical and chemical.

Table 7.1 The main elements of the production process that form dangerous and harmful factors

Name of work types and parameters of the production process	FACTORS GOST 12.0.003-74 SSBT		Normative documentation
	Harmful	Dangerous	
Calibration of PPD Ra^{226}	Elevated level of ionizing radiation in the work area		NRB-99

	Electricity		GOST 12.1.038-82 SSBT. electrical safety
Carrying out of measurements, calculations, the literature review with use of the high-voltage power unit and the COMPUTER.	The impact of radiation (HF, UHF, SHF, etc.)		SanPiN 2.2.2/ 2.4.1340-03 Sanitary and epidemiological rules and regulations. "Hygienic requirements for PC and organization of work"

5.2 Organizational arrangements

To prevent physical injuries, occupational diseases and property damage (personal and state), all personnel are required to know and strictly observe the safety rules. Training of personnel in occupational safety and industrial sanitation consists of an introductory briefing and instruction in the workplace by the responsible person.

The knowledge of the safety rules is checked by the qualification commission after training at the workplace. The audited person is given the qualification group corresponding to his knowledge and experience of work, and he is given a special certificate.

The diploma work was carried out in the laboratory of radiation control. This laboratory is a room with increased electrical danger due to the fact that pipes and heating batteries are open. Here in operation is expensive equipment, which requires compliance with special safety regulations, labor protection, electrical and fire safety rules.

The work was carried out using modern computer technology, which made it possible to achieve high process efficiency and reduce the time spent on it.

Persons serving electrical installations must not have injuries and illnesses that interfere with production work. The state of health is established by medical examination.

Before the beginning of the work, an introductory briefing was conducted on the rules of using the equipment and instruction in the workplace. Examinations on safety precautions were also passed, including:

1.Exam for electrical safety, for electrical systems with voltage up to 1000 V;

2.Examination on radiation safety (NRB-99);

3.Exam for fire safety (use of fire extinguishing means).

The exams were certified in the safety journal and valid for one year. The organization of the workplace contributed to the most effective implementation of each specific section of work. Technical health and safety of use, of the equipment used, were regularly checked by qualified specialists.

Working and rest modes:

The efficiency of labor activity of a person is significantly influenced by the mode of work and rest. A rational mode is a regime in which high labor productivity and sustained performance are provided without the signs of excessive fatigue for a long time.

The correctness of the work and rest regime is assessed on the basis of an examination of the state of the physiological functions of a person and the dynamics of his working capacity during the working day. The more effective the regime, the longer the period of stable working capacity, the shorter the periods of workability and decline in efficiency.

In production, the alternation of periods of work and rest is achieved by the introduction of a lunch break in the middle of the working day and short-term regulated breaks that are established taking into account the dynamics of efficiency, severity and labor intensity.

Thus, in jobs requiring great effort and attention, fast and accurate movements, frequent (but short) (5-10 minute) breaks are advisable. In works associated with significant effort and participation of large muscles, it is recommended to take more break, but long (10-12-minute) breaks. In particularly hard work (blacksmiths, metallurgists) should combine work for 15-20 minutes with rest of the same duration.

In addition to the regulated breaks, there are micro-pauses-breaks that arise spontaneously between operations. They maintain an optimal pace of work and high performance and make up 9-10% of the working time.

The working capacity and vital activity of the body depends on the daily mode of work and rest, that is, on the alternation of periods of work, rest and sleep. In accordance with the daily cycle of working capacity, the highest level is observed in the morning and afternoon: from 8 to 12 and from 14 to 17. In the evening hours, working capacity decreases, reaching its minimum at night. These patterns should be taken into account when determining the shift of work, the beginning and end of work in shifts, rest breaks and sleep. The dynamics of working capacity changes during the week: the highest working capacity is on the 2nd, 3rd and 4th day of work, in the following days it goes down. On Monday, working capacity is reduced due to workability.

Elements of a rational mode of work and rest are industrial gymnastics, psychophysiological unloading. At the heart of industrial physical education is the phenomenon of active rest, described by I.M. Sechenov: exhausted muscles are better rest when working with other muscle groups. The task of industrial physical education is the resumption of the working stereotype at the beginning of the working shift and its preservation during the working day. For this purpose, introductory gymnastics (5-7 minutes), physical-pause (5-10 minutes 1-4 times per shift) and physical training minutes (2-3 minutes) are applied.

To remove fatigue and neuro-psychological tension, specially equipped rooms are used, where the effect of psych emotional unloading is achieved due to the interior of the room, functional music and other factors.

5.3 Technical Activities

The complication of production processes and equipment changed the functions of man in modern production: the responsibility for the tasks to be solved increased; increased the amount of information perceived by the worker, and the speed of the equipment. Human work has become more difficult, the load on the nervous system has increased and the physical load has decreased. There was a problem of maintenance of reliability and safety of work of the person on manufacture. This problem is solved by ergonomics and engineering psychology.

Ergonomics (from the Greek ergon - work and nomos - the law) is a scientific discipline that studies a person in the conditions of his activity associated with the use of machines. The goal of ergonomics is the optimization of working conditions in the "man-machine" system. Ergonomics defines a person's requirements for technology and the conditions for its functioning. Ergonomics of technology is the most general indicator of properties and other indicators of technology.

Engineering psychology is a scientific discipline that studies the patterns of information interaction between man and technology for the design, creation and operation of the human-machine system. Engineering psychology examines the processes of receiving, storing, processing and selling information by a person. On the basis of the laws of psychic, psychophysiological processes and human properties, it determines the requirements for technical devices and the construction of the human-machine system, as well as the requirements for the properties of the human operator.

As generalized indicators of the operator and the "human-machine" system, engineering psychology uses efficiency, reliability, accuracy, speed.

The tasks of ergonomics as an applied discipline are:
- the design of the "man-machine" system, that is, the distribution of functions between the person and the machine;
- designing the workspace so that the physical environment corresponds to the characteristics of the person;
- Designing the environment in accordance with the requirements of the operator;
- designing of working situations (working hours, breaks for rest, etc.).

Engineering psychology, as it follows from the foregoing, is practically an integral part of ergonomics, which solves the problems of organization of the "man-machine" system by:

- distribution of functions between the person and the machine;

- analysis of the functions performed by a person in the human-machine system;

- designing the information system, selecting a sensitive channel;

- the design of controls;

- designing of workplaces;

- maintenance of convenience of maintenance of machines;

- selection of personnel and their professional training.

In Russia there are a number of standards for ergonomics GOST 16456-70 (Product quality, Ergonomic indicators, Nomenclature.), GOST 16035-70. (Product quality: General ergonomic indicators, Terms.), Etc.

Ergonomic hardware:

To work was comfortable and safe, you need to take care of the hardware of the computer. Typically, the greatest harm to the health of the user of the computer is caused by input-output devices: monitor, keyboard, mouse.

At the present time, when the problems of computer security are as acute as possible, there are many different standards for the environmental safety of personal computer equipment. A modern monitor should comply with at least three generally accepted safety standards and ergonomics:

• FCC Class B - This standard was developed by the Canadian Federal Communications Commission to provide acceptable environmental protection against the effects of radio interference in confined spaces. Equipment meeting FCC Class B requirements should not interfere with the operation of tele- and radio equipment.

• MPR-II - this standard was issued by the Swedish National Department. MPR-II imposes restrictions on emissions from computer monitors and industrial equipment used in the office.

• TCO'95 (as well as the modern TCO'99) - the recommendation developed by the Swedish Trade Union Conference and the National Council of Industrial and

technical Development of Sweden (NUTEK), regulates interaction with the environment. It requires the reduction of electric and magnetic fields to a technically possible level in order to protect the user. In order to get the TCO'95 certificate (TCO'99), the monitor must meet the standards of low radiation (Low Radiation), i.e. have a low level of electromagnetic field, provide automatic to automatically reduce energy consumption with long not use, meet European standards of fire and electrical safety.

• EPA Energy Star VESA DPMS - According to this standard, the monitor must support three power-saving modes - stand-by, suspend and "off". Such a monitor, when the computer is idle for a long time, is translated into the appropriate mode, with low power consumption.

It is also necessary that the monitor has the ability to adjust image parameters (brightness, contrast, etc.). It is recommended that when working with a computer, the frequency of the vertical scan of the monitor is not lower than 75Hz (the user ceases to notice the flickering of the image, which leads to rapid eye fatigue).

Currently, many monitor manufacturers have increased the mass production of so-called flat panel monitors (LCDs) that lack many of the environmental flaws inherent in CRT monitors, such as electromagnetic radiation, magnetic field, flicker, etc. Therefore, it is most effective to use LCD monitors.

5.4 Electrical safety

Electrical safety is a system of organizational and technical measures and means to protect people from harmful and dangerous effects of electric current, electric arc, electromagnet field and static electricity.

Safe for humans is the amount of alternating current - 10mA, constant-50mA, safety voltage 12V.

Computer studies used equipment powered by a network with a voltage of 220V. The laboratory equipment is low-voltage. By the presence of signs of electrical hazards - the room is classified as a room with a reduced risk.

To prevent the failure of computers due to inrush of the mains voltage, and also to ensure the safety of data in the event of an emergency shutdown of the network, power is supplied through the UPS-400 uninterruptible power supply. To avoid injury, follow these rules:

1. The operating instructions for the equipment must be studied. Before each inclusion, the workplace was inspected;

2. Pay special attention to the sequence of switching on and off the power of individual components;

3. All nodes of the computer complex must be grounded through the ground loop;

4. The ground loop is periodically checked for electrical resistance.

The analysis of the danger of electrical networks is practically reduced to determining the value of the current flowing through the human body under various conditions in which a person may find himself in the operation of electrical networks.

When an electric current pass through a person's body, damage to the body can occur. The effect of current on the human body can be local and general. General (reflex) damage - an electric shock, is the greatest danger for a person: the work of the central nervous and cardiovascular systems is disrupted, which leads to fibrillation and paralysis of the heart, as well as to stopping breathing.

The nature and consequences of damage depend on the magnitude, frequency and path of the current flow; duration of exposure. Timely assistance provided with electric shock allows you to save the life of the victim. Therefore, assistance must be provided immediately. When providing first aid, the injured person must be disconnected from the live part while protecting himself from the danger of contact with the current leads.

First you need to turn off the current. In case of mild lesions, the injured person should be taken to fresh air. If breathing is very sharp and convulsive, artificial respiration is necessary. When breathing is stopped and there is no pulse, artificial respiration and indirect heart massage are performed. Then hospitalization is necessary.

Measures to ensure the electrical safety of electrical installations:
Disconnecting the voltage from live parts where work is to be carried out or near which measures are taken to ensure the impossibility of applying voltage to the work place, posting posters indicating the workplace, grounding the housings of all installations through a neutral wire, covering the metal surfaces of tools with reliable insulation, inaccessibility current-carrying parts of equipment (the conclusion in the case of electro-impacting elements, the conclusion in the body of current-carrying parts).

5.5 Radiation safety

The main goal of radiation safety is to protect people's health from the harmful effects of ionizing radiation by observing the basic principles and norms of radiation safety.

The main document on radiation safety in the organization of work with sources of ionizing radiation is the "Basic Sanitary Rules for Working with Radioactive Substances and Other Sources of Ionizing Radiation NRB-99/2009".
This work was related to work with open-type radioactive substances.

Work with open sources (OI) suggests:

- Determination of the class of works on the use of OI in relation to the radionuclide group;

- Definition of requirements for accommodation and equipment of premises;

- Ensuring the protection of personnel against internal and external exposure;

- Use of the static (equipment, walls) and dynamic (ventilation, gas cleaning) barriers;

- Performing operations with radioactive substances by remote means;

- Minimization of radioactive waste generated during technological processes.

Under the influence of ionizing radiation in the body, inhibition of the function of the hematopoietic organs, disruption of normal blood clotting and an increase in the fragility of blood vessels, a decrease in the body's resistance to infectious diseases and etc. It is necessary to apply protective measures, which must prevent radioactive contamination of air, the surfaces of working premises, skin and clothing of personnel.

For this, there are acceptable levels of doses that a person can receive. Levels are divided according to the category of radiation safety standards (NRB-99). Personnel (group A) - persons working with technogenic sources, ionizing radiation, or under the conditions of work in the sphere of their impact (group B). Population - all persons, including staff outside of work.

Table 7.2. Limits of admissible doses.

The normalized quantities	Limits of doses	
	Group A staff	Population
The equivalent dose	20mSv	1mSv
Equivalent dose for the year: In the lens in the skin in hands and feet	150mSv 500mSv 500mSv	15mSv 50mSv 50mSv

Dose limits and allowable levels for personnel of group B are equal to 1/4 of group A.

Table 5.3 The equivalent dose rate used in the design of protection.

Category Irradiated persons		Purpose of the room	Duration of irradiation, h / year	Projected dose rate, μSv / h
staff	Gr A	Permanent Stay	700	6.0
		Temporary stay	850	12
	Gr B	The premises of the organization and the territory	2000	1.2
Population		Any other room and territory	8800	0.06

5.6 Fire and explosive safety

From the point of view of fire safety, special attention should be paid to the proper operation of electrical installations, as well as not to ensure compliance with

fire safety rules for organizations approved by the Main Fire Department of the Ministry of Internal Affairs of the Russian Federation, as well as industry regulations on fire safety.

The concept of fire safety means the state of an object in which the possibility of a fire is excluded, and in cases of its occurrence, prevention.

Fire hazards for people include open fire, sparks, excessive air and object temperature, toxic combustion products, smoke, reduced oxygen concentration, damage to plants, as well as explosions, etc.

At work the following rules were observed:

1. Only standard fuses were used in electrical equipment. The connecting cords have been selected taking into account the appropriate currents and voltages (standard, the lowest insulation resistance of 500 Ohm), are supplied complete with electrical equipment.

2. To eliminate the causes of short-circuits, regular

preventive inspections of equipment. The power board is closed with a fireproof casing to prevent the burning of surrounding objects from possible sparks that arise when it is switched.

3. The work was carried out in a room that meets the requirements of fire safety rules. No heating devices with open elements were used. After the end of the work, the necessary part of the equipment was de-energized.

4. The passages were not cluttered and did not smoke in the room.

5. The room was provided with fire alarm and fire extinguishing means.

In case of fire, it is necessary to immediately leave the room where the fire occurred according to the evacuation scheme using emergency exits, if evacuation cannot be carried out through the main ones. During the evacuation, notify all those in the neighboring premises of the occurrence of a fire without raising panic or raising a fire alarm by pressing the fire alarm button, if any. Call the fire service at the fire address and wait for it from outside the premises at a safe distance from it.

Conclusion

Three designs of accumulating electrostatic chambers for measuring the radon and thoron flux density from the ground surface was developed and investigated. With each of the developed designs, no less than 2-hour measurements of the alpha-spectrum were made.

Analysis of the results of measurements made the following conclusions:

1.In the absence of the electrostatic precipitation effect, only one radionuclide 216Po, the decay product of thoron, is identified in all spectra. The peaks corresponding to the PPR of radon do not appear in this case.

2. When creating conditions for electrostatic precipitation, the peaks of 214Po, the product of the decay of radon, clearly appeared in the spectra obtained by chambers No. 1 and 2, while the peak amplitude of 216Po slightly increased.

3. The total number of recorded pulses in the conditions of electrostatic precipitation increased, on average, by 2.2 times for all NDs.

However, the best quality of spectrograms in studies with different types of soils was shown by chamber No. 1 and 2 (voltage $U_{1,2} = +2\,kV$ applied to the chamber electrodes).

Based on the results of the research, the optimal variants of chamber designs (# 1 and # 2) for measuring the values of PPR and PPT from the soil surface using electrostatic precipitation of ions were chosen.

The developed accumulation chambers can be operated in laboratory and field conditions and are designed to equip monitoring stations for atmospheric radioactivity and seismic activity.

Reference

1. Sisigina TI Fluctuations of radon exhalation from the soil to the atmosphere due to changes in meteorological conditions. Proceedings of the Institute of Experimental Meteorology. Radioactivity of the atmosphere, soil and fresh water, Moscow: Moscow Department of Hydrometeorology Publishing. 5, pp. 3-15. 1970.

2. Grammakov AG, Popretinsky IF Distribution of radon in loose sediments in the presence of scattering haloes of radium. Izv. AN SSSR. Series of physical. №6. C. 789-793. 1957.

3. Miklyaev PS, Petrova TB Mechanisms for the formation of radon flux from the soil surface and approaches to assess the radon hazard of residential areas. ANRI number 2. P. 2-16. 2007.

4. Parovik RI, Firstov PP Approbation of a new technique for calculating radon flux density from a surface (based on the example of the Petropavlovsk-Kamchatka geodynamic test site). ANRI number 3. Pp. 52-57. 2009.

5. Chalmers JA Atmospheric electricity. - L .: Gidrometeoizdat, 1974. 420 p.

6. Sun K., Guo Q., Zhuo W. Feasibility for Mapping Radon Exhalation Rate from Soil in China. J. Nucl. Sci. Technol. V. 41. N.1. P. 86-90. 2004.

7. Ielsch G., Ferry C., Tymen G., Robe M.-C. Study of a predictive methodology for quantification and mapping of the radon-222 exhalation rate. J. Environ. Radioactiv. No. 63. P. 15-33. 2002.

8. Yakovleva VS, Pluzhnikova DA, Nagorsky PM, Karataev VD, Vukolov AV, Moskalev SS Model of ionization density of the atmosphere due to radon, thoron, and their decay products. Aerosols of Siberia: Materials of the XVI working group. - Tomsk, 24-27 November 2009. - Tomsk: IO SB RAS, 2009. - P. 40.

9. Chandrashekara M.S., Sannappa J., Paramesh L. Studies on atmospheric electrical conductivity related to radon and its progeny concentrations in the lower atmosphere at Mysore. Atmos. Environ. No. 40. P. 87-95. 2006.

10. Engineering and environmental surveys for construction. Code of Regulations SP 11-102-97.

11. Crozier W. Direct Measurement of Radon-220 (Thoron) Exhalation from the Ground. J. Geophys. Res. V.74. №17. P. 4199-4205. 1969.

12. Megumi K., Mamuro T. A method for measuring radon and thoron exhalation from the ground. J. Geophys. Res. V.77. P. 3052-3056. 1972.

13. Schery S.D., Whittlestone S., Hart K.P., Hill S.E. The flux of radon and thoron from Australian Soils. J. Geophys. Res. V. 94. P. 8567-8576. 1989.

14. Hosoda M., Shimo M., Sugino M., Furakawa M., Fukushi M. Effect of Soil Moisture Content on Radon and Thoron Exhalation. J Nucl Sci Technol V. 44. N.4. P. 664-672. 2007.

15. Lehmann B.E., Ihly B., Salzmann S., Conen F., Simon E. An automatic static chamber for continuous 220Rn and 222Rn flux measurements from soil. Radiation. Meas. V.38. P.43-50. 2004.

16. Yakovleva VS, Pluzhnikova DA, Nagorsky PM, Karataev VD, Vukolov AV, Moskalev SS Model of ionization density of the atmosphere due to radon, thoron, and their decay products. Aerosols of Siberia: Materials of the XVI working group. - Tomsk, 24-27 November 2009. - Tomsk: IO SB RAS, 2009. P. 40.

17. Schery S.D., Gaeddert D.H., Wilkening M.H. Factors affecting exhalation of radon from a gravelly sandy loam. J. Geophys. Res. V.89. P.7299-7309. 1984.

18. Kirichenko L.V. Evaluation of radon exhalation from large areas on the vertical distribution of its short-lived decay products in a free atmosphere. Proceedings of the Institute of Experimental Meteorology. Radioactivity of the atmosphere, soil and fresh water, Moscow: Moscow Department of Hydrometeorology Publishing. 5, pp. 15-28. 1970.

19. Yakovleva VS, Ryzhakova NK Method for estimating the radon flux density from the earth's surface from the measured radon concentration in soil air. ANRI number 4. Pp. 18-22. 2002.

20. Tsapalov AA, Kuvshinnikov SI Dependence of volumetric activity of radon in the premises from the difference in internal and external air temperatures. ANRI number 2 (53). Pp. 37-43. 2008.

21. Chau N.D., Chrusciel E., Prokolski L. 2005. Factors controlling measurements of radon mass exhalation rate. J. Environ. Radioactiv. V.82. P.363-369. 2005.

22. Szegvary T., Leuenberger M.C., Conen F. Predicting terrestrial 222Rn flux using gamma dose rate as a proxy. Atmos. Chem. Phys. V.7. P.2789-2795. 2007.

23. Chalupnik S., Wysocka M. Development of the method for measurement of radon exhalation from the ground. Extended Abstracts of ICGG7 P. 62-64 Copernicus GmbH. 2003.

24. Aldenkamp F.J., Put L.W., de Meijer R.J. Aspects of an instrument for in-situ measurements of radon exhalation rates. Environ. Int. V.14. N.4. P.341-344. 1988.

25. Method for the rapid measurement of the flux density of 222Rn from the ground surface using a radon radiometer PPA-01M. ANRI number 4 C.33-41. 1998.

26. APPLICATION NOTE AN-006_EN. Quantifying of Radon Exhalation on Surfaces. Version March 2008 (link www.sarad.de, AN-006_RadonExhalation_EN_19-03-08.doc)

27. Experimental methods of nuclear physics. Part I: A Tutorial. The author - cand. tech. Associate Professor Yu.M. Stepanov. - Tomsk: TPU Publishing House, 2008 - 368 p.

28. Porstendorfer J. and Mercer T. T. Influence of electric charge and humidity on the diffusion coefficient of polonium -218 // Science / - 1981.- №211.-3. 480 - 481.

29. Wellisch, E.M., The distribution of the active deposit of radium in an electric field, Philosophical Magazine. -1913.-No. 28-P.623-635.

30. V.S. Yakovleva Measurement of radon flux density from the earth's surface. Tomsk: Publishing house TPU, 2008 - 17 p.

31. V.S. Yakovleva Modeling of the influence of the atmosphere and lithosphere on PPR and PPT. Tomsk: TPU Publishing House, 2010 - 9 p.

32. Bormotova Elena Valerievna, Yakovleva Valentina Stanislavovna. Determination of Radon Emulation Coefficients Gamma-Method Tomsk: TPU Publishing House, 2006.

33. Saeed A. Durrani, Radomir Ilic. Radon measurements by etched track detectors: applications in radiation protection, earth sciences, and the environment / editors. Library of Congress Cataloging-in-Publication Data – 1997

40. What is Financial Management [Electronic Source], URL-https://www.managementstudyguide.com/financial-management.htm (Access date 14.04.2018)

41. Financial management meaning, importance and significance, [Electronic Source],URL-https://hubpages.com/money/financial-management-meaning-importance-and-significance (Access date 14.04.2018)